Fall 2010

Genetic analysis of Shudderer, the lithium-responsive neurological mutant of Drosophila melanogaster

Garrett Anthony Kaas
University of Iowa

GENETIC ANALYSIS OF SHUDDERER, THE LITHIUM-RESPONSIVE NEUROLOGICAL MUTANT OF DROSOPHILA MELANOGASTER

by

Garrett Anthony Kaas

An Abstract

Of a thesis submitted in partial fulfillment
of the requirements for the Doctor of
Philosophy degree in Genetics
in the Graduate College of
The University of Iowa

December 2010

Thesis Supervisor: Associate Professor Toshihiro Kitamoto

ABSTRACT

Lithium has been used for more than 50 years as a primary therapy for bipolar affective disorder (BPD) and has proven highly effective for both acute and long-term phases of the disease. Unfortunately, the molecular and cellular mechanisms underlying the mood-stabilizing action of lithium for the treatment of BPD remains largely unknown. In an effort towards understanding the complexities of lithium's action in the nervous system, I have utilized the *Drosophila* neurological mutant *Shudderer (Shu).* Previous findings have suggested that the adult *Shu* phenotypes may be improved by providing a diet containing millimolar concentrations of lithium.

Using well-established genetic techniques and behavioral paradigms I thoroughly characterized the *Shu* mutant phenotypes. I found that the mutant displays morphological and behavioral abnormalities indicative of dysregulated neuronal excitability that include: down-turning wings and indented dorsal thorax, defects in negative geotaxis, deficits in locomotion, abnormal sleep architecture and unusual patterns of leg-shaking behaviors upon recovery of ether anesthetics. Furthermore, I confirmed that lithium was able to significantly improve many aspects of *Shu* behaviors.

Recombination-based mutation mapping in *Shu* revealed that the genetic lesion lies somewhere within the gene *CG9907*, which encodes the voltage-gated sodium channel α-subunit *paralytic (para)*. Subsequent genetic experiments using *para* hypomorphic mutant alleles as well as a UAS-RNAi/GAL4 system showed that a reduction in sodium channel levels resulted in a drastic improvement of the mutant defects. Together, these data suggest that the lithium-responsive *Shu* mutant is likely a gain-of-function allele of *para.* Sequencing of the entire *para* coding region identified a missense mutation in a

highly conserved region of the para coding sequence, in transmembrane segment S2 of homology domain III ((M1350I). To date, this is the first known discovery of a sodium channel mutant allele in *Drosophila* which causes hyperactivity. These data suggest that the *Shu* phenotypes are somehow caused by an increase in sodium channel activation.

Lastly, I identified a number of genes likely to functionally interact with the *Shu* mutation. Of note, the Ca^{2+}/calmodulin-activated Ser/Thr protein phosphatase alpha subunit gene *CanA-14F* is up-regulated in *Shu* and reduction of its activity suppresses the mutant phenotypes. Furthermore, a large percentage of genes encoding anti-microbial peptides (AMP) were also significantly up-regulated in *Shu*, possibly acting downstream of *CanA-14F.* A genetic deficiency screen looking for genes that alter the *Shu* phenotypes has identified that the gene *Glutathione s-transferase S1 (Gsts1)* suppresses the morphological and behavioral defects in the lithium-responsive mutant. Overall, these genes will help decipher how the gain-of-function sodium channel *Shu* mutation alters nervous system function. In addition, they will shed light on those mechanisms responsible for lithium's mood-stabilizing effects in the brain.

Abstract Approved: _____
Thesis Supervisor

_____
Title and Department

_____
Date

GENETIC ANALYSIS OF SHUDDERER, THE LITHIUM-RESPONSIVE NEUROLOGICAL MUTANT OF DROSOPHILA MELANOGASTER

by

Garrett Anthony Kaas

A thesis submitted in partial fulfillment
of the requirements for the Doctor of
Philosophy degree in Genetics
in the Graduate College of
The University of Iowa

December 2010

Thesis Supervisor: Associate Professor Toshihiro Kitamoto

Graduate College
The University of Iowa
Iowa City, Iowa

CERTIFICATE OF APPROVAL

_____

PH.D. THESIS

_____

This is to certify that the Ph.D. thesis of

Garrett Anthony Kaas

has been approved by the Examining Committee
for the thesis requirement for the Doctor of Philosophy
degree in Genetics at the December 2010 graduation.

Thesis Committee: _____
Toshihiro Kitamoto, Thesis Supervisor

_____
Pedro Gonzalez-Alegre

_____
Wayne A. Johnson

_____
Robert Philibert

_____
Chun-Fang Wu

To Michelle, Owen and Lorelei

ACKNOWLEDGMENTS

First and foremost, I would like to express thanks to my thesis advisor Toshi Kitamoto for his unremitting guidance during my graduate career. Throughout my many years in your lab I have benefited greatly from your ability to mentor me in a way that has allowed for independence, yet firm enough to train me properly in the multifaceted skills necessary to become a successful scientist. As your first graduate student, I can confidently say that all those that come after me will be fortunate to have you as their mentor.

I would also like to acknowledge my outstanding thesis committee members, Dr. Pedro Gonzalez-Alegre, Dr. Wayne A. Johnson, Dr. Robert Philibert, and Dr. Chun-Fang Wu. It is my belief that each member has gone above and beyond what is expected of a committee member in helping guide me towards completion of my thesis project. Furthermore, they have offered me constructive criticism and novel ways of thinking about my experiments that have ultimately led to an overall improvement in the quality of my research.

I would like to thank all current and past members of the Kitamoto laboratory and Genetics program students for the wonderful times we had both in and outside of the lab. I have made some lasting friendships that will stay with me always.

Most importantly, I would like to bestow the utmost gratitude to my wonderful wife Michelle. She has been a constant companion and supporter of mine through the ups and downs of the scientific process. Also, to my children Owen and Lorelei who were born to us during our time here at Iowa.

ABSTRACT

Lithium has been used for more than 50 years as a primary therapy for bipolar affective disorder (BPD) and has proven highly effective for both acute and long-term phases of the disease. Unfortunately, the molecular and cellular mechanisms underlying the mood-stabilizing action of lithium for the treatment of BPD remains largely unknown. In an effort towards understanding the complexities of lithium's action in the nervous system, I have utilized the *Drosophila* neurological mutant *Shudderer (Shu).* Previous findings have suggested that the adult *Shu* phenotypes may be improved by providing a diet containing millimolar concentrations of lithium.

Using well-established genetic techniques and behavioral paradigms I thoroughly characterized the *Shu* mutant phenotypes. I found that the mutant displays morphological and behavioral abnormalities indicative of dysregulated neuronal excitability that include: down-turning wings and indented dorsal thorax, defects in negative geotaxis, deficits in locomotion, abnormal sleep architecture and unusual patterns of leg-shaking behaviors upon recovery of ether anesthetics. Furthermore, I confirmed that lithium was able to significantly improve many aspects of *Shu* behaviors.

Recombination-based mutation mapping in *Shu* revealed that the genetic lesion lies somewhere within the gene *CG9907* or *paralytic (para)*, which encodes for a voltage-gated sodium channel α-subunit. Subsequent genetic experiments using *para* hypomorphic mutant alleles as well as a UAS-RNAi/GAL4 system showed that a reduction in sodium channel levels resulted in a significant improvement of the mutant defects. Together, these data suggest that the lithium-responsive *Shu* mutant is likely a gain-of-function allele of *para.* Sequencing of the entire *para* coding region identified a missense mutation in a highly conserved region of the *para* coding sequence, in transmembrane

segment S2 of homology domain III (M1350I). To date, this is the first known discovery of a sodium channel mutant allele in *Drosophila* which causes hyperactivity. These data suggest that the *Shu* phenotypes are somehow caused by an increase in sodium channel activity.

Lastly, I identified a number of genes likely to functionally interact with the *Shu* mutation. Of note, the Ca^{2+}/calmodulin-activated Ser/Thr protein phosphatase α subunit gene *CanA-14F* is up-regulated in *Shu* and a reduction of its activity suppresses the mutant phenotypes. Furthermore, a large percentage of genes encoding anti-microbial peptides (AMP) were also significantly up-regulated in *Shu*, possibly acting downstream of *CanA-14F.* A genetic deficiency screen looking for genes that alter the *Shu* phenotypes has identified that the gene *Glutathione S-transferase S1 (GstS1)* suppresses the morphological and behavioral defects in the lithium-responsive mutant. Overall, these genes will help decipher how the gain-of-function sodium channel *Shu* mutation alters nervous system function. In addition, they will shed light on those mechanisms responsible for lithium's mood-stabilizing effects in the brain.

TABLE OF CONTENTS

LIST OF TABLES ix

LIST OF FIGURES x

LIST OF ABBREVIATIONS xii

CHAPTER I PHENOTYPIC CHARACTERIZATION OF THE LITHIUM-RESPONSIVE *DROSOPHILA* MUTANT, *SHUDDERER* 1

Introduction 1
History of the therapeutic use of lithium in medicine 1
Lithium effects on developmental and physiological processes 3
Lithium effects on nervous system functions 3
Lithium and relevant neurotransmitter systems 4
Lithium and Glycogen synthase kinase 3β (GSK-3β) 6
Lithium and inositol phosphate, PKC signaling 8
Lithium and neuroprotection 16
Using *Drosophila* as a model organism to study the lithium-responsive neurological processes 17
Advantages and disadvantages of using *Drosophila* as a model organism for psychiatric disease 19
Shudderer 20
Materials and Methods 20
Fly stocks and culture conditions 20
Behavioral analyses 21
Reactive climbing assay 21
Shuddering assay 22
Video-tracking locomotor analysis 22
Analysis of ether-induced leg shaking behavior 23
Sleep anlayses 24
Analysis of “wing-down and indented thorax” 25
Muscle staining 25
Drug treatment 25
Measurement of internal lithium 26
Statistical analysis 26
Results 27
Shu mutants exhibit morphological defects 27
The *Shu* mutant displays abnormalities in locomotion 28
The anesthesia-induced leg-shaking behavior in *Shu* 40
Shu mutants display abnormalities in day and night sleep architecture 46
Shu mutants display reduced lifespan 47
Lithium improves several of the behavioral abnormalities observed in *Shu* mutants 52
Shu mutants accumulate higher levels of lithium 54
Discussion 55

CHAPTER II *SHUDDERER* IS A GAIN-OF-FUNCTION ALLELE OF THE VOLTAGE-GATED SODIUM CHANNEL GENE, *PARALYTIC* 60

Introduction 60
Structure and function of sodium channels 60
Neuronal sodium channels and disease 65
Sodium Channels and *Drosophila* 66
Materials and Methods 69
Fly stocks and culture conditions 69
Mapping Procedure 70
Behavioral analyses 71
Reactive climbing assay 71
Video-tracking locomotor analysis 71
Analysis of ether-induced leg shaking behavior 72
Analysis of “wing-down and indented thorax” 73
DNA sequencing 73
Statistical analysis 74
Results 75
The *Shu* mutation maps to the gene *CG9907,* encoding the voltage-gated sodium channel gene *paralytic* 75
Shu behavioral and morphological defects are suppressed when in a transheterozygous combination with *para* hypomorphic alleles 81
RNAi knockdown of *para* transcripts in neurons rescues the *Shu* mutant phenotypes. 82
Shu mutants carry a missense mutation in a highly conserved region of *para* 83
Discussion 84

CHAPTER III IDENTIFICATION OF GENES FUNCTIONALLY INTERACTING WITH *SHUDDERER* 94

Introduction 94
Microarray analyses and lithium 94
Drosophila genetic screens 95
Materials and Methods 97
Fly stocks and culture conditions 97
Reactive climbing assay 98
Analysis of "wing-down and indented thorax" 98
Microarray and RT-PCR analyses 99
Whole-mount RNA *in situ* hybridization 100
Deficiency screen for suppressors of *Shu* 101
Statistical analsyis 102
Results 102
Microarray analysis of *Shu* mutant gene expression reveals the upregulation of CanA-14F and immune response genes 102
Overexpression of an inhibitor of calcineurin reduces the severity of the *Shu* phenotypes 107
Hypomorphic mutant alleles of *CanA-14F* improve the *Shu* phenotypes 108
Genes involved in innate immune responses are up-regulated in 115
An unbiased forward genetic screen reveals several regions on the second and third chromosomes that suppress the *Shu* mutant phenotypes 116

RNAi knockdown of genes covered by the deletion *Df(2R)BSC433* reveals that *GstS1* is the gene responsible for suppression of the *Shu* phenotypes 121
Discussion 122

CHAPTER IV SUMMARY AND FUTURE DIRECTIONS 130

REFERENCES 135

LIST OF TABLES

Table

1. Recombination rates between *Shu* and P-element markers..... 78

2. Genes differentially* expressed in *Shu* compared to *CS*..... 105

3. Expression levels of calcineurin subunit genes in *Shu*..... 106

4. Deficiencies that significantly improve the *Shu* phenotypes..... 120

LIST OF FIGURES

Figure

1. Lithium inhibition of GSK-3β mimics Wnt signaling 9

2. Lithium inhibits IMPase and IPPase, blocking inositol phosphate turnover and its down-stream signaling cascades..... 13

3. *Shu* displays morphological defects 29

4. *Shu* exhibits locomotor defects that are improved by lithium treatment..... 32

5. Representative 1 minute traces of *CS* and *Shu* flies 35

6. Video tracking analysis to quantify the abnormal locomotion behaviors of the *Shu* mutant 37

7. *Shu* displays unique behaviors under recovery from ether anesthesia..... 41

8. *Shu* mutants display abnormalities in sleep architecture 44

9. *Shu* mutants have reduced lifespan 48

10. Lithium has contrasting effects on video tracking locomotor parameters in *Shu* and *CS* flies..... 50

11. Structure of the voltage-gated sodium channel alpha and beta subunits .. 63

12. Schematic diagram of predicted mutation sites after meiotic mapping of the *Shu* locus..... 76

13. *Shu* mutant phenotypes are improved when placed in a *para* hypomorphic mutant background..... 79

14. RNAi knockdown of *para* in neurons rescues all aspects of *Shu* mutant phenotypes..... 85

15. Identification of a novel mutation in a highly conserved residue in *Shu* mutants..... 87

16. *CanA-14F* is expressed in both larval and adult CNS..... 109

17. Overexpression of *nebula* suppresses *Shu* mutant morphological defects..... 111

18. P-element insertion mutants near the 5' start site of *CanA-14F*, improve *Shu* phenotypes..... 113

19. Lithium suppresses the increased expression of innate immune response genes in *Shu* mutants..... 117

20. Downregulation of *GstS1* strongly suppresses the *Shu* phenotypes 123

LIST OF ABBREVIATIONS

ADAR	adenosine deaminase acting on RNA
AMP	antimicrobial peptides
APC	adenomatous polyposis coli
Akt	protein kinase B
ALS	amyotrophic lateral sclerosis
Ank3	ankyrin 3
Axs	abnormal X segregation
Bax	bcl-2-associated protein X
Bcl-2	b-cell lymphoma 2
BPD	bipolar affective disorder
CanA-14F	calcineurin A at 14F
CI	climbing Index
CNS	central nervous system
CS	canton-S
DAG	diacylglycerol
DAM	drosophila activity monitor
DAT	dopamine transporter
dfmr1	drosophila fragile X mental retardation
DIG	digoxigenin
DLM	dorsal longitudinal flight muscles
eag	ether-a-go-go
eas	easily shocked
EtOH	ethanol
FDA	U.S. Food and Drug Administration
FM6	first chromosome balancer 6

FM7	first chromosome balancer 7
GAL4	galactose 4
GEFS+	generalized epilepsy with febrile seizures plus
GPCRs	G-protein-coupled receptors
GS	GeneSwitch
GSK-3	glycogen synthase kinase-3
GSK-3β	glycogen synthase kinase-3 beta
GWAS	genome wide association study
Hk	Hyperkinetic
IFM	isoleucine, phenylalanine, methionine
IMPase	inositol monophosphatase
IMPA1	inositol monophosphatase A1
ine	inebriated
IPPase	inositol 1-polyphosphate phosphatase
IP3	inositol-1,4,5 triphosphate
K^+	potassium
KD	knockdown
KO	knockout
LEF	lymphoid enhancer factor
Li^+	lithium
List	lithium-inducible SLC6 transporter
MARCKS	myristoylated alanine-rich C kinase substrate
Mg^{2+}	magnesium
Na^+	sodium
NMJ	neuromuscular junction
NMDA	N-methyl-D-aspartic Acid
Ocd	out cold

p53	protein 53
PCR	polymerase chain reaction
para	paralytic
PI3K	phosphatidylinositol 3-kinase
Pink1	P-TEN induced putative kinase 1
PIP2	4,5 phosphatidylinositol bisphosphate
PKA	protein kinase A
PKC	protein kinase C
PNS	peripheral nervous system
PP2A	protein phosphatase 2A
qvr	quiver
rbp2	ribosomal binding protein 2
RNAi	ribonucleic acid interference
r	rudimentary
Sh	shaker
Shu	shudderer
sgg	shaggy
SMEI	severe myoclonic epilepsy of infancy
SMIT1	sodium myo-inositol transporter 1
SNC1A	sodium channel, voltage-gated, type I, alpha subunit
SNC2A	sodium channel, voltage-gated, type 2, alpha subunit
SNC1B	sodium channel, voltage-gated, type I, beta subunit
SNC8A	sodium channel, voltage-gated, type 8, alpha subunit

SNC9A	sodium channel, voltage-gated, type 9, alpha subunit
SNP	single nucleotide polymorphism
TCF	T-cell factor
TipE	temperature-induced paralysis E
RTK	receptor tyrosine kinase
ts	temperature-sensitive
UAS	upstream activating sequence
VDRC	Vienna *D*rosophila RNAi center
Wnt	wingless/int

CHAPTER I

PHENOTYPIC CHARACTERIZATION OF THE LITHIUM-RESPONSIVE *DROSOPHILA* MUTANT, *SHUDDERER*

Introduction

Lithium has been utilized for over 50 years as a first line therapy for bipolar affective disorder (BPD), a severe, disabling illness most simply characterized by cycling between periods of extreme elation (mania) and depression. Although lithium has proven to be one of the more effective drugs available, it is not the ideal drug for the treatment of BPD because of its narrow therapeutic window (Okusa and Crystal, 1994), extensive list of side-effects and a significant amount of non-responders to its treatment (Baraban, 1994). In addition, despite decades of intensive scientific examination, the mechanisms underlying lithium's mood altering properties remain largely unknown. This gap in the knowledge base is a major obstacle to the development of improved therapies for BPD. It is thus clinically important to elucidate the molecular and cellular processes responsible for lithium's effect on nervous system function. Understanding the mechanisms behind lithium's action is also of great scientific interest, because it should provide important insights into the neurobiological basis of mood regulation as well as the etiology and pathophysiology responsible for the manifestation of BPD.

History of the therapeutic use of lithium in medicine

Lithium has been employed as a therapeutic agent by members of the medical community as early as the mid-1800s where it was used to relieve the

symptoms of gout, a painful condition resulting from a buildup of uric acid in the joints (Lenox et al., 1998). Later, in the 1880s evidence surfaced that the alkali metal could be used to treat patients suffering from depression-like symptoms (Lange, 1886). However, lithium's therapeutic potential was soon overshadowed by its toxic side-effects and its use was soon discontinued. In 1949, a novel discovery by the Australian psychiatrist, Dr. John Cade, led to its reemergence as a treatment for mania in patients suffering from BPD (Cade, 1949). At this time, mental illness was thought to be the cause of a toxic build up of unknown compounds in the body. Cade believed this unidentified compound to be uric acid. To test his hypothesis he injected guinea pigs with lithium urate, the only soluble salt available for uric acid at the time (Cade, 1949). Surprisingly, the animals began exhibiting lethargic behavior and became docile. Thereafter, Cade began treating his psychiatric patients with the drug and found that lithium had no noticeable effect on individuals suffering from either depression or schizophrenia. However, the symptoms of those diagnosed with manic depression were largely muted. Over the next two decades, lithium was subjected to a number of carefully controlled studies (Baastrup and Schou, 1967, Coppen et al., 1971, Cundall et al., 1972, Stallone et al., 1973) that established its use as an effective prophylactic treatment for BPD, leading to its approval by the FDA in 1974 (Schou, 2001). At present, lithium continues to be used as an effective therapeutic tool for the treatment of BPD (Bowden et al., 1994, Miklowitz and Johnson, 2006, Sysko and Walsh, 2007).

Lithium effects on developmental and physiological processes

Lithium has a profound impact on the embryonic development of numerous organisms, ranging from the slime mold *Dictyostelium* to humans (Van Lookeren Campagne et al., 1988, Jacobson et al., 1992, Stachel et al., 1993). For example, in sea urchins, zebrafish and the frog *Xenopus,* lithium causes an expansion of dorsal tissues, resulting in a duplication of the dorsal axis to an extent that some embryos may lack any identifiable ventral structures (Klein and Melton, 1996). In humans, lithium treatment during pregnancy is known to increase the incidence of Ebstein's anomaly in newborns, a congenital heart condition characterized by malformation of the tricuspid valve, which requires surgical correction (Cohen et al., 1994). In addition, lithium is known to exert its effect on a number of other physiological processes independent of development such as glucose metabolism, hematopoiesis, endocrine regulation and heart function (Boggs and Joyce, 1983, Choi and Sung, 2000, Mamiya et al., 2005).

Lithium effects on nervous system functions

Recent evidence from both *in vitro* and *in vivo* studies have demonstrated that lithium elicits multiple effects on the nervous system, including neurotransmitter/receptor-mediated signaling, signal transduction cascades, ion transport, gene expression patterns and regulation of circadian rhythms. For further information please refer to the following reviews (Manji and Lenox, 1998, Phiel and Klein, 2001, Lenox and Wang, 2003). Most of the effects of the drug listed above are thought to be mediated either directly or indirectly through the

ability of lithium to inhibit several key enzymes at therapeutically-relevant concentrations by competition for magnesium-binding sites. The ion's most notable targets include, inositol monophosphatase (IMPase) (Berridge et al., 1989), inositol 1-polyphosphate phosphatase (IPPase), the family of phosophomonoesterases (York et al., 1995) and glycogen synthase kinase-3β (GSK-3β) (Klein and Melton, 1996). These targets and there relevance as a mechanism of lithium action in the nervous system are discussed below in further detail.

Lithium and relevant neurotransmitter systems

In the early 1970's, the effects of lithium on the monoaminergic neurotransmitter signaling pathways were extensively studied because of their known roles in the pathophysiology of depression and other manic behaviors, the two major phenotypic characteristics of patients with BPD (Perez-Cruet et al., 1971, Friedman and Gershon, 1973). Studies exploring the effects caused by lithium treatment have shown both increases and decreases in the levels of monoamine neurotransmitter concentrations in the central nervous systems (CNS) (Hesketh et al., 1978, Ferrie et al., 2008). However, the interconnected nature of neurotransmitter systems and the existence of multiple lithium targets localized both pre- and post-synaptically in these systems, complicate the definitive meaning of the abnormalities observed (Marmol, 2008).

A handful of studies have indicated that dopamine plays a role in the pathophysiology of mood disorders. Lithium appears to be able to attenuate the effects of dopamine receptor-mediated neurotransmission. Specifically, in a

pharmacologically-induced rat model of manic activity, lithium could attenuate D1-receptor mediated increases in acetylcholine release in the frontal cortex (Acquas and Fibiger, 1996). However, during normal tactile stimulation of the rat, this inhibitory effect of lithium was not observed. These findings provide an intriguing hypothesis for why lithium reveals its effect in BPD patients and not in healthy controls. The mood-stabilizing ion has also been shown to inhibit hyperactivity in a Dopamine transporter (DAT) knockout (KO) mouse model for mania (Beaulieu et al., 2004). In addition, lithium has been shown to block D2-receptor interactions with beta-adrenergic G-protein coupled receptors and affect the subsequent release of cAMP second-messengers (Montezinho et al., 2006). Furthermore, it has been reported that several single nucleotide polymorphisms (SNPs) in the dopamine transporter and D1-receptor are associated with BPD (Chiaroni et al., 2000, Dmitrzak-Weglarz et al., 2006). Despite the convincing findings listed above, in certain cases dopamine agonists have been show to actually act as effective antidepressants in BPD patients, while precipitating manic episodes in others (Manji and Potter, 1997). Thus, a straightforward explanation for the role of the dopaminergic system in lithium's effect on BPD patients remains elusive.

The serotonergic neurotransmitter system has long been implicated in mood disorders because of the antidepressive effects observed after increasing serotonin levels. Many studies have found alterations in serotonin (5-HT) levels and signaling in patients suffering from depression, a major feature of BPD (Price et al., 1990, Grahame-Smith, 1992). Yet, the exact role of the serotonergic

neurotransmission system in the mood disorder remains unclear. Several reports have shown that lithium can induce or increase serotonin levels at the synapse (Baumann et al., 1996) and biochemical studies have shown its interaction with $5HT_{1B}$ receptors, which are know to be the major controller of the serotonergic system(Massot et al., 1999).

All in all, lithium likely exerts its mood-stabilizing effects through modulation of neurotransmitter signaling in many different regions of the brain. Much like the evidence reported with the dopaminergic system, the intricate, collaborative nature of these systems makes pin pointing the exact change or changes resulting from lithium administration challenging.

Lithium and Glycogen synthase kinase 3β (GSK-3β)

One of the most thoroughly studied targets of lithium has been the serine/threonine kinase GSK-3β, aptly named for its ability to phosphorylate and deactivate glycogen synthase (Embi et al., 1980). Lithium inhibits GSK-3β directly by competing with Mg^{2+} for access to its binding sites, which is independent and noncompetitive with respect to its substrates (Klein and Melton, 1996). Binding of lithium to the GSK-3β catalytic site is possible because Li^{+} and Mg^{2+} have very similarly sized ionic radii (Hart, 1979), where as other group I ions like Na^{+} and K^{+} cannot compete for Mg^{2+} sites due to their larger ionic radii (Pasquali et al., 2010).

Lithium can also inhibit GSK-3β indirectly through the phosphorylation of the serine 9 residue on the kinase, which subsequently inactivates the enzyme. This phosphorylation can be achieved through a couple of interactions, which

include a reduction in the levels of Protein phosphatase-2A (PP2A) (Mora et al., 2002) and through an increase in PKC-α or Akt activity levels (Chalecka-Franaszek and Chuang, 1999, De Sarno et al., 2002, Beaulieu et al., 2004). Increased Akt activation by lithium is known to be at least partially mediated by the Phosphoinositide 3-kinase (PI3K) and its signaling cascades.

The extensive interest in GSK-3β inhibition as the mechanism of lithium action is due to the fact that the kinase is a component of many influential signaling pathways leading to an even larger number of potential biological targets. Most notably, the insulin/insulin-like growth factor signaling, neurotrophic factor signaling and the Wnt signaling pathways are the best established pathways of GSK-3β action (Gould and Manji, 2005).

Activation of the Wnt signaling pathway is initiated by the binding of Wnt glycoproteins to members of the frizzled family of receptors, which in turn causes Disheveled-mediated inhibition of a destruction complex composed of Axin, Adenomatous polyposis coli (APC) and GSK-3β. Under normal, non-Wnt activating conditions, GSK-3β phosphorylates β-catenin leading to its ubquitin dependent degradation (Aberle et al., 1997). On the other hand, when GSK-3β is inhibited by Wnt signaling, β-catenin is not degraded, allowing it to enter the nucleus and interact with its transcriptional activation partners, T-cell factor (TCF) or Lymphoid enhancer factor (LEF) to activate Wnt-dependent target genes (Cadigan and Nusse, 1997) (Figure 1). Thus, by inhibiting GSK-3β, lithium administration mimics the effects of Wnt signaling (Klein and Melton, 1996).

Several lines of evidence from animal models have supported the idea

that GSK-3β inhibition mediates the behavioral effects of lithium. First, lithium inhibits GSK-3β *in vivo* in murine models (Gurvich and Klein, 2002) and alternative, specific pharmacological inhibitors of GSK-3β mimic the effects of lithium treatment on behavior (Gould et al., 2004, Kaidanovich-Beilin et al., 2004). Second, the effect of lithium in attenuating hyperactivity caused by pharmacological or genetic activation of dopaminergic transmission (Beaulieu et al., 2004) was also mimicked by the GSK-3β inhibitors alsterpaullone, SB216763, 6BIO and TDZD. Third, *Gsk-3β* heterozygous mutant mice exhibit behaviors similarly to lithium-fed mice in the forced swim-test, exploratory behaviors and the tail suspension test (O'Brien et al., 2004, Beaulieu et al., 2008). Lastly, several genome wide association studies (GWAS) have shown SNPs in *Gsk-3β* to be associated with BPD (Szczepankiewicz et al., 2006, Luykx et al., 2010).

Lithium and inositol phosphate, PKC signaling

Lithium is a powerful inhibitor of both inositol monophosphatase (IMPase) (Ki =0.8mM) and inositol 1-polyphosphate phosphatase (IPPase) (Ki = 0.3mM) at therapeutically relevant concentrations (Allison and Stewart, 1971, Berridge et al., 1982, Inhorn and Majerus, 1988, Phiel and Klein, 2001). Similar to its effect on GSK-3β, lithium achieves its inhibition of these enzymes by competing for Mg^{2+} binding sites. Biochemical studies have shown that IMPase contains at least two Mg^{2+}-binding sites designated M1 and M2. Mg^{2+} first binds to the M1 site on the free IMPase enzyme and is required before the enzyme can bind its substrate, Inositol-1-monophosphate (Ins(1)P) (Greasley and Gore, 1993). Lithium binding occurs at the allosteric M2 site, after the enzyme-substrate

Figure 1. Lithium inhibition of GSK-3β mimics Wnt signaling. Under non-activating conditions, a destruction complex comprised of GSK-3β, Axin and APC phosphorylates β-catenin, leading to its degradation by the proteosome. However, in the presence of Wnt ligands, the destruction complex is inactivated through a Disheveled-mediated process. This mechanism allows β-catenin levels to increase in the cytoplasm. The intact β-catenin then translocates into the nucleus and interacts with its binding partners LEF or TCF to activate downstream target genes. Lithium blocks GSK-3β activity by competing for Mg^{2+} sites, leading to non-competitive inhibition of the enzyme and accumulation of β-catenin. Thus, administration of lithium mimics Wnt signaling.

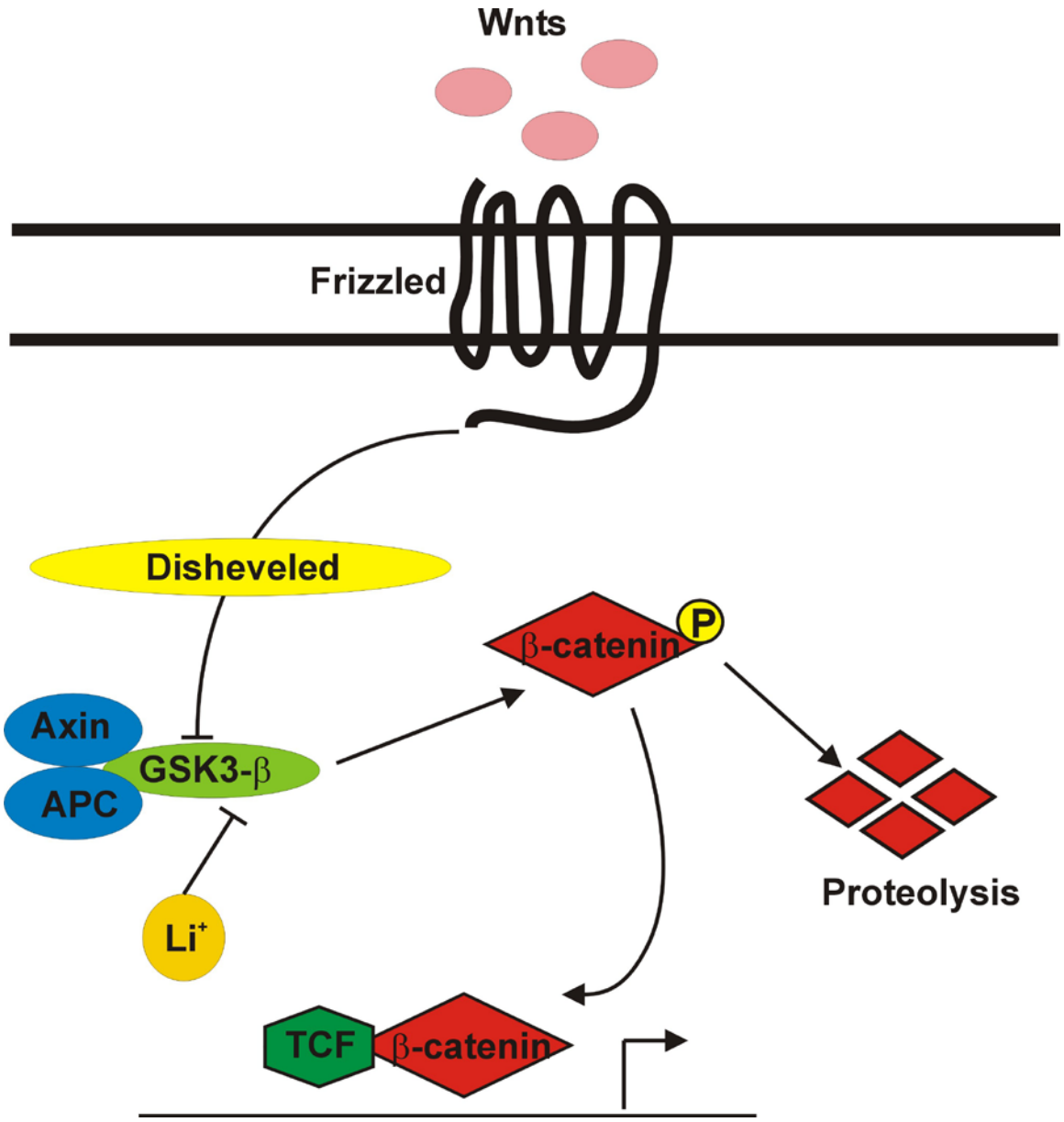
Wnts
Frizzled
Disheveled
β-catenin
P
Axin
GSK3-β
APC
Li+
Proteolysis
TCF
β-catenin

complex has already formed leading to a noncompetitive inhibition. Studies have provided evidence that lithium binding leads to the formation of either an inhibitory IMPase-M1(Mg^{2+})-Ins(1)P-M2(Li^{+}) complex (Attwood et al., 1988, Ganzhorn and Chanal, 1990) or a IMPase-M1(Mg^{2+})-Pi-M2(Li^{+}) complex resulting from an inability to release the phosphate after cleavage from Ins(1)P (Leech et al., 1993). Likewise, lithium blocks IPPase from processing its substrates, 1,4 bisphosphate and 1,3,4-triphosphate through a similar noncompetitive inhibitory mechanism. This inhibition results in the accumulation of Ins(1)P in the cell, the substrate of IMPase, which in turn is itself inhibited by lithium.

The inhibitory effect of lithium on both IMPase and IPPase has led to a long-held hypothesis to explain lithium's therapeutic effect, called the "inositol depletion hypothesis" (Silverstone et al., 2005). This hypothesis postulates that inhibition of IMPase and to a lesser extent IPPase by lithium, will lead to a depletion of inositol in the cell (Berridge et al., 1989). This depletion is achievable because of the low inositol permeability of the blood-brain barrier, which causes the brain to rely exclusively on the inositol polyphosphate recycling system for access to inositol (Pasquali et al., 2010). Lack of inositol in the cell leads to a severe reduction in 4,5 phosphatidylinositol bisphosphate (PIP_2), a necessary precursor of the two essential second messengers, inositol-1,4,5 trisphosphate (IP_3) and diacylglycerol, both of which activate the release of Ca^{2+} from intracellular stores, leading to activation of Protein kinase C (PKC), in response to extracellular signaling (Phiel and Klein, 2001) (Figure 2).

The subject of intense research interest, PKC represents a family of at

least 12 known isozymes, all with very similar molecular structures but differ in regards to their intracellular and anatomical distribution in the brain, second messenger activators and substrate affinities (Marmol, 2008). Members of the PKC family are known to regulate neuronal excitability, neurotransmitter release, neuronal plasticity and long-term changes in gene expression (Lenox, 1987, Manji and Lenox, 1994). Several studies have shown that lithium administration can inhibit the effects of PKC isozymes and the subsequent suppression of its down-stream signaling cascades. For instance, PKCα and PKCε reductions have been observed in the rat subiculum and in CA1 regions of the hippocampus after chronic treatment with 1 mM lithium and validated further *in vitro* using a hippocampal cell line (Manji et al., 1993, Manji et al., 1996). Furthermore, the PKC-regulated actin-binding protein myristoylated alanine-rich C kinase substrate (MARCKS), which is involved in reorganizing the cytoskeleton in neurites, is down-regulated by chronic lithium treatment (Lenox et al., 1998). In line with this finding, lithium and two other mood-stabilizing compounds have been shown to inhibit the collapse of neurite growth cones (Williams et al., 2002). This suppression could be reversed by addition of *myo*-inositol. Intriguingly, the administration of the PKC inhibitor drug tamoxifen has shown early promise as an effective treatment for acutely manic patients with BPD (Wang and Friedman, 2001). Further evidence to bolster tamoxifen's potential as a mood-stabilizing drug comes from a recent study showing that the drug can also antagonize manic-like behaviors in rats (Einat et al., 2007).

Despite several decades of investigation regarding the "inositol depletion

Figure 2. Lithium inhibits IMPase and IPPase, blocking inositol phosphate turnover and its down-stream signaling cascades. Lithium directly inhibits the enzymes inositol monophosphate phosphatase (IMPase; $K_i \approx 0.8$ mM) and inositol 1-polyphosphate phosphatase (IPPase; $K_i \approx 0.3$ mM). Binding of ligands to G-protein-coupled receptors (GPCRs) activates PLC and causes hydrolysis of PIP_2 to IP_3 and DAG. IP_3 stimulates Ca^{2+} release from cellular stores, and DAG IMPase and IPPase results in a depletion of *myo*-inositol (and an accumulation of DAG followed by a downregulation of PKC isozymes *α* and *ε*. PKC can activate MARCKS, an actin binding protein involved in reorganization of the cytoskeleton in neurites. PKC is involved in many biological processes including glucose transport, secretion, exocytosis and cell proliferation.

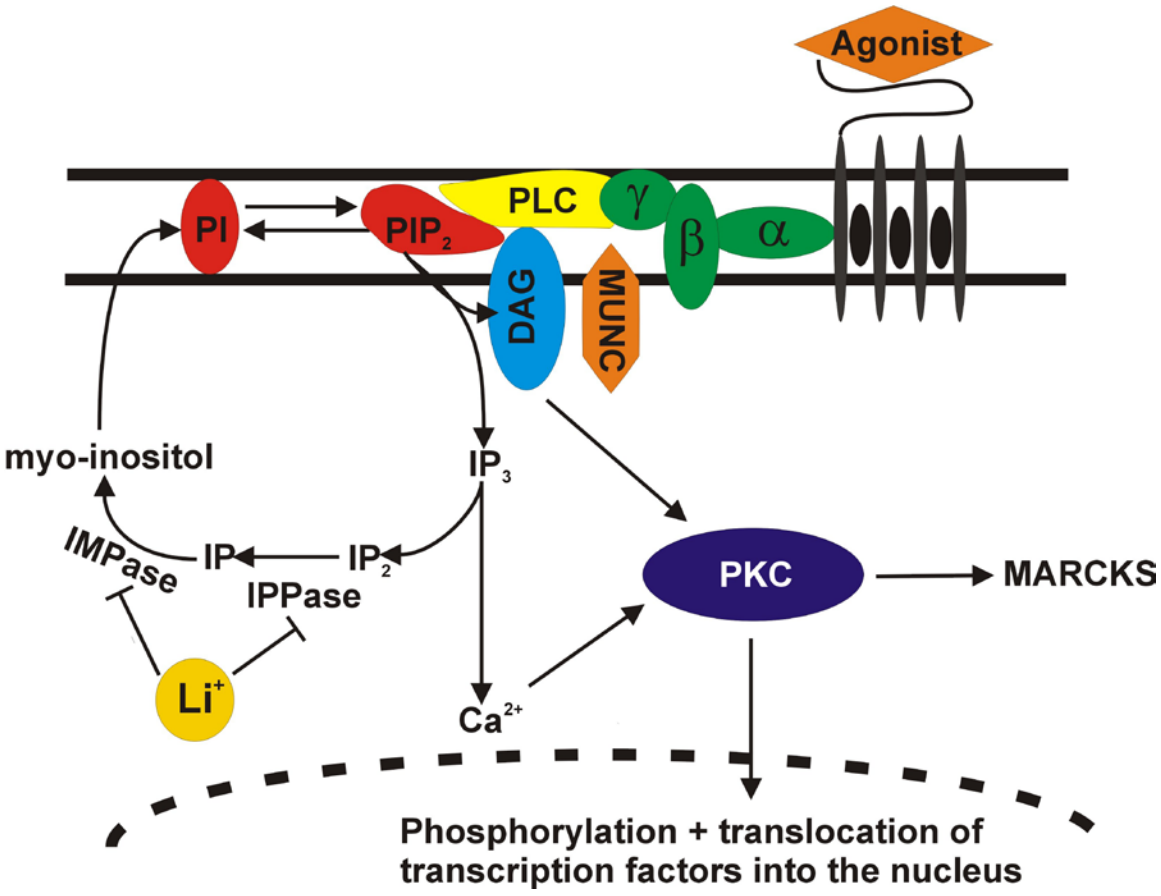
Agonist
PI
PIP2
PLC
γ
β
α
DAG
MUNC
myo-inositol
IP3
IMPase
IP
IP2
IPPase
Li+
PKC
MARCKS
Ca2+
Phosphorylation + translocation of
transcription factors into the nucleus

hypothesis", a great many conclusions from studies both *in vitro* and *in vivo,* examining the effect of the mood-stabilizing drug on inositol phosphate metabolism, have been ambiguous or inconsistent. For example, post-mortem studies examining IMPase activity in the frontal and occipital cortical samples from bipolar, unipolar and schizophrenic patients was the same as controls (Shaltiel et al., 2001). In addition, a study of cholinergically stimulated cortical slices from guinea pigs, mice and rats found lithium to actually increase IP_3 levels (Lee et al., 1992). Finally, changes in the brain PIP_2 response in experimental animal models have often been small and inconsistent, providing conflicting evidence that lithium treatment actually results in a reduction in PIP_2 recycling due to inositol depletion (Manji et al., 1995).

Nevertheless, several murine knockout mutants have been generated in genes involved in the inositol phosphate signaling pathway in an attempt to recapitulate the effect of lithium. Again, these genetic models have continued to provide little consistent evidence to solidify the importance of inositol phosphate metabolism in lithium action. For example, knockout mouse models for the IMPase encoding gene, *Impa1,* reduces IMPase activity by 65% and the mutant exhibits some behavioral phenotypes that mimic lithium administration such as increased sensitivity to pilocarpine-induced seizures as well as increased mobility in the forced swim test (Cryns et al., 2008). However, the mutant also exhibits hyperactive locomotion in the open field test, thought to be a measure of a mouse's baseline state. Thus, the hyperactivity of the *Impa1 -/-* mouse makes

any interpretation of the forced swim test as well as a definitive assessment of lithium's effect on its depressive behavior difficult.

Similarly, a homozygous knockout of the sodium-myo-inositol transporter 1 *(Smit1)* gene reduces inositol levels in the fetal mouse brain by more than 90% and yet has no effect on global phosphoinositide levels, indicating that the more modest inositol reduction observed with lithium is unlikely to reduce phosphoinositide production (Berry et al., 2003). Furthermore, mice heterozygous for the *Smit1* gene still exhibit a robust 33-37% decrease in inositol levels, substantially larger than that observed after lithium treatment, yet display no differing results in the forced swim test, amphetamine-induced hyperactivity or sensitivity to pilocarpine-induced seizures compared to controls (Shaldubina et al., 2006). In agreement with these findings, lithium has never been shown to decrease PI or PIP_2 levels *in vivo* (Baraban, 1994, Jope and Williams, 1994).

In summary, evidence both for and against the "inositol depletion hypothesis" has been generated over the past 20 years using both *in vitro* and *in vivo* experimental models. Unfortunately, the inconsistency of the experimental data in combination with the difficulty in developing drugs that target the inositol phosphatases has hampered the progress of this area of investigation.

Lithium and neuroprotection

Growing support now indicates that lithium possesses an intrinsic neuroprotective ability in both cultured cells and animal models of disease (Manji et al., 1999, Grimes and Jope, 2001). Lithium is thought to provide this protective effect mostly through its ability to up-regulate the expression of the

anti-apoptotic factor gene, B-cell lymphoma 2 (Bcl-2) (Manji et al., 2000, Rowe and Chuang, 2004), while at the same time down-regulating pro-apoptotic genes such as p53 and Bcl-2-associated protein X (Bax). Lithium accomplishes these alterations in expression by acting upstream to attenuate the phosphorylation of N-methyl-D-aspartic acid (NMDA) receptors, which also leads to protection against glutamate-induced excitotoxicity (Wada et al., 2005). Interestingly, in mice models for brain ischemia, chronic pretreatment with low doses of lithium reduces the severity of apoptosis in the surrounding tissue and improves neurological function (Xu et al., 2003). Remarkably, even when administered post-insult, lithium has been shown to lessen ischemia-induced brain damage, while facilitating cognitive recovery (Ren et al., 2003). Due to its neuroprotective potential, lithium is now considered a possible, and potentially effective treatment for chronic neurodegenerative disorders such as Huntington's disease, Parkinson's disease, Alzheimer's disease and amyotrophic lateral sclerosis (ALS) (Fornai et al., 2008, Camins et al., 2009).

Using *Drosophila* as a model organism to study the lithium-responsive neurological processes

Many genes are evolutionarily conserved between fruit flies and humans. Among these, a large portion of genes known to be involved in human disease have *Drosophila* homologues (Fortini et al., 2000). In addition, there are numerous similarities in the basic molecular components, cellular structures, inter- and intracellular signaling pathways, developmental patterning (Miklos and Rubin, 1996), learning and memory formation (Davis, 2005), circadian rhythm

regulation as well as tumor formation and metastasis (Brumby and Richardson, 2005). The fruit fly *Drosophila melanogaster*, which offers versatile genetic tools and information, has great potential for the study of evolutionarily conserved biological processes. The following studies strongly indicate that *Drosophila* is an excellent model system to study the effects of the mood-stabilizing drug lithium and its role in modulating neural function. First, similarly to what has been reported in mammalian studies (Padiath et al., 2004, Dokucu et al., 2005), lithium modifies the circadian rhythms in *Drosophila* by lengthening the period of the cycle through inhibition of GSK-3β. Second, in *Drosophila* lithium has been demonstrated to protect against polyglutamine-mediated neuronal toxicity for neuronal death (Berger et al., 2005) as is observed in mammalian cell culture models of Huntington's disease (Carmichael et al., 2002). In *Drosophila* Alzheimer's disease models, lithium also provides beneficial effects by inhibiting GSK-3β-mediated hyperphosphorylation of tau (Yeh et al., 2010) as well as ameliorating amyloid beta pathology (Sofola et al., 2010). Third, McBride et al. have found that cognitive deficits displayed by mutants for *Drosophila fragile X mental retardation 1 (dfmr1)*, a *Drosophila* model for Fragile X syndrome, are restored by lithium (McBride et al., 2005). Lastly, microarray gene expression data from adult fly heads treated with a brief dose of lithium revealed a number of genes whose expression levels were significantly altered (Kasuya et al., 2009a). In particular, a potentially novel target of lithium action, the lithium-inducible SLC6 transporter (List), was found to be an essential component in glial cells required for resistance to lithium toxicity (Kasuya et al., 2009b).

Advantages and disadvantages of using *Drosophila* as a model organism for psychiatric disease

Drosophila offers many advantages over other well-established organisms for identification and exploration of the underlying mechanisms responsible for the manifestation of psychiatric illnesses. First, many of the genes in the fly genome share a high degree of evolutionary conservation with humans as mentioned above. Recently, researchers have found that greater than 60% of rare genes linked to familial neurological disorders like Alzheimer's disease, Parkinson's disease, ALS, epilepsy, and others, are evolutionary conserved in the *Drosophila* genome (Celniker, 2000, Schneider, 2000, Bernards and Hariharan, 2001, Koh et al., 2004, Bier, 2005, Bilen and Bonini, 2005). Second, the development of the UAS/GAL4 system (Brand and Perrimon, 1993) together with recent modifications (McGuire et al., 2004) now allow for the manipulation of gene expression both temporally and spatially in the fly. At present, this level of experimental sophistication is not available in any other model organism. Third, due to their short generation time, visible mutation markers and mutagenesis techniques, large genetic screens for novel genes involved in neural processes can be easily undertaken.

However, one glaring disadvantage of using *Drosophila* as a model organism is that many psychiatric illnesses including schizophrenia and BPD involve alterations in mood. Clearly, *Drosophila* does not possess a nervous system complex enough to harbor the higher-order brain functions needed to generate emotion. Although this disadvantage exists, other model systems such

as mice, rats and non-human primates are also not exempt from this limitation. So, although the fly is not the ideal system to study psychiatric disorders, ethical limitations do not allow for a rigorous molecular, cellular and behavioral examination of these illnesses in humans. Therefore, the overall advantages afforded by *Drosophila* appear to outweigh the obvious disadvantages and should be a useful tool to try to unravel the underlying mechanisms in the nervous system responsible for the manifestation of mood disorders like BPD, schizophrenia and others.

Shudderer

The *Shudderer (Shu)* mutant was originally discovered over three decades ago (Williamson, 1982). It was reported that the adult mutant flies exhibit several behavioral phenotypes such as sporadic seizure-like jerks, ether-induced leg shaking and a defect in reactive climbing. Interestingly, many of the behavioral phenotypes of *Shu* mutants are suppressed by administration of lithium to adult mutants at therapeutic treatment levels (Williamson, 1982). These data suggest that the *Shu* gene plays a role in the lithium-responsive neurological pathway(s). In spite of this mutant's great potential as a tool for studying lithium-responsive neurological processes, only one paper was published regarding this mutant (Williamson, 1982) and no research has followed the original findings.

Materials and Methods

Fly stocks and culture conditions

Flies were reared at 25°C in a 12 hr light: 12 hr dark cycle, on a conventional cornmeal/glucose/yeast/agar medium supplemented with the mold

inhibitor methyl 4-hydroxybenzoate (0.05 %). The *Canton-S*^{2202U} (*CS*^{2202U}) strain was used as the wild-type control and hereafter will be referred to as *CS* in the text. *Shu* (Williamson, 1982) was obtained as *Shu*/FM6 from Rodney Williamson (Beckman Research Institute of the City of Hope, Duarte, CA). *Shu* mutants were outcrossed to the *CS* line at least 26 times, and balanced with FM7-Actin-GFP. *Shu*/FM7-Actin-GFP females were crossed to *CS* and the resultant *Shu*/+ flies were used for experiments in this study. Due to their severe behavioral defects and very short lifespan, *Shu* males were not used in any of the behavioral experiments presented here. *Shaker*^{5} *(Sh*^{5}*), ether-a-go-go*^{1} *(eag*^{1} and *Hyperkinetic*^{1} *(Hk*^{1}*)* were received from the lab of Dr. Chun-Fang Wu (University of Iowa, Iowa City, IA).

Behavioral analyses

Reactive climbing assay

The reactive climbing assay was performed as previously described (Greene et al., 2003) using a countercurrent apparatus that was originally invented for phototaxis behaviors (Benzer, 1967). Briefly virgin female flies of each genotype were collected shortly after eclosion and wings cut with a micro dissecting scissor (LADD Research, Williston, VT) and housed in groups of 20 flies. After being aged appropriately, groups of 20 flies were placed into one tube (tube #0), tapped to the bottom and allowed 15 sec to climb, at which point the flies that had climbed were transferred to the next tube. This process was repeated a total of 5 times. After the fifth trial, the flies in each tube (#0 ~ #5) were counted. The climbing index (CI) was calculated using the following

formula: $CI = \Sigma(Ni \times i)/(5 \times \Sigma Ni)$, where i and Ni represent the tube number (0-5) and the number of flies in the tube, respectively. At least 5 groups were tested for each genotype or treatment unless otherwise noted in the text.

Shuddering assay

Newly eclosed virgin *Shu* and *CS* females were collected and wings cut with a micro dissecting scissor (LADD Research, Williston, VT). Flies were then kept and tested in an environmental chamber at 24.5^{o}C $\pm$ 0.5 ^{o}C and 60-70% humidity. Flies were individually placed into standard mating chambers (15mm diameter X 3mm depth) using a manual aspirator and allowed to acclimate for 5 min. At the end of 5 min fly behavior was video recorded (DCR-PC300; Sony, Tokyo, Japan) for 2 min. *Shu* and wild-type flies were scored for the number of times a strong convulsive episode flipped the fly onto its backside. The experimental treatments given to the flies were performed blind to the investigator. At least 30 flies were used for each treatment, genotype and time point tested.

Video-tracking locomotor analysis

Newly eclosed virgin *Shu* and *CS* females were collected and wings cut with a micro dissecting scissor (LADD Research, Williston, VT). Flies were then kept and tested in an environmental chamber at 24.5^{o}C $\pm$ 0.5 ^{o}C and 60-70% humidity. After being aged for 5 days, flies were individually placed into standard mating chambers (15mm diameter X 3mm depth) 8 at a time, using a manual aspirator and allowed to acclimate for 5 min. At the end of 5 min fly behavior was recorded using a web camera (Logicool Quickcam IM, Logitech, Fremont, CA).

The camera was attached with a telephoto lens (HLM35V8E, Honeywell, Morristown, NJ) and was mounted 20 cm above the mating chambers. Images were captured at 15 frames/sec for 10 min and analyzed using pySolo, a multiplatform for the analysis of *Drosophila* sleep (Gilestro and Cirelli 2009) to track fly locomotion and compute x, y coordinates of individual flies during every frame for a total of 9,000 frames. Locomotor parameters were calculated using Microsoft Excel and the following formula =ATAN2 $((X_1-X_2)*(X_3-X_2)+(Y_1-Y_2)*(Y_3-Y_2),(X_1-X_2)*(Y_3-Y_2)-(Y_1-Y_2)*(X_3-X_2))$ for turning angle, arctangent for three consecutive frames resulting in an angle presented in radians. Radians were converted to degrees and the resulting angle was subtracted from 180 degrees to give the outside angle of that the turning flies. For total distance, Pythagoras's theorem was used with the following formula, $=SQRT((X_2-X_1)^2+(Y_2-Y_1)^2)$ and was summed for all 9000 frames. For velocity, $=SQRT((X_2-X_1)^2+(Y_2-Y_1)^2)/(1/15)$. Pixels were converted to millimeters (mm) after calculating distance in pixels with Image J compared to actual mm distance of the mating chambers.

Analysis of ether-induced leg shaking behavior

5 day old flies were introduced into a *Drosophila* etherizer (Science Kit & Boreal Laboratories, Tonawanda, New York). Flies were exposed to a saturated dose of diethyl ether for 10 seconds. A drop of adhesive was then applied to the posterior dorsal thorax of each fly and fixed to a piece of plain white paper in a 35mm X 10mm petridish. Flies were then allowed to recover for 2-3min before video recording using a Quickcam connect camera (Logitech) mounted on a

Leica MZFLIII stereoscope (Leica Microsystems, Bannockburn, IL). Images were captured at 15 frames/second for 1 min and analyzed using pySolo to generate x,y data. Head movement was tracked by generating a mask (i.e cropping out the rest of the image around the selected area) focusing on the anterior lateral region of the eye and the background. This area was selected based on initial trials indicating it to be the most consistent region to track head movement without picking up antennal motion. In addition, leg movement was tracked by producing a mask selection encompassing the joint between the tibia and tarsus of the hind leg. Special care was taken to only use video where no other appendages or body parts entered the tracking mask during the 1 min recording. As a positive control for diethyl ether effectiveness, *Shu* flies were used in every anesthesia experiment performed. Velocity of both head and leg movements were calculated using Microsoft Excel and the formula $=SQRT((X_2-X_1)^2+(Y_2-Y_1)^2)/(1/15)$.

Sleep analysis

Three to four day old adult females were individually housed in a glass tube (5 [W] x 65 [L] mm) with regular fly food, and monitored while subjected to 12 hr light and 12 hr dark cycles at 25˚C. Locomotor activity of individual female flies was analyzed using the *Drosophila* Activity Monitoring (DAM) system (Trikinetics, Waltham, MA, USA). Flies were acclimated to the experimental conditions for one day before sleep was analyzed. Locomotor activity data were collected at 1 min intervals for 3 days, and analyzed with a Microsoft (Redmond, WA, USA) Excel-based program as described previously (Hendricks et al., 2003,

Kume et al., 2005). A sleep bout was defined as 5 or more min of behavioral immobility. The waking activity was calculated by dividing the total activity counts during the observation period by the length of the wake period.

Analysis of "wing-down and indented thorax"

Male and female *Shu* mutants were collected shortly after eclosion and scored 24 hr later as either *defective* (i.e. wing down and/or indented thorax) or *normal* (wild-type wing posture/thorax).

Muscle staining

Mutant and wild-type flies were decapitated and wings removed prior to being freshly frozen in Tissue–Tek II O.C.T. Compound and sectioned at a depth of 10 µm. Longitudinally sectioned samples were stained in borax/toluidine blue as previously described (Kim et al., 2004). Briefly, fly sections were stained for 2hr, and fixed and destained in Bodian's No. 2 fixative (37% Formaldehyde: acetic acid : 80% EtOH D 1:1:18) with repeated changes of fixative until a satisfactory contrast was observed. The samples were then dipped briefly in 95% EtOH 10 times, two consecutive dips in 100% EtOH 10 times each and cleared with xylene. Samples were mounted with Permount and imaged on a Leica MZFLIII stereoscope (Leica Microsystems, Bannockburn, IL).

Drug Treatment

Lithium was diluted to generate 1 M, 0.5 M, and 0.25 M lithium stock solutions, which were added to our standard fly food in a 1:10 dilution to produce the final concentrations used in these studies.

Measurement of internal lithium

Twenty virgin female flies (0-24 hr-old) were placed in a vial with food containing 25, 50 or 100 mM LiCl for 5 days, and were then homogenized in 350 μl of 1 XPBS (pH 7.4). The homogenate was centrifuged at 15,000 rpm for 15 min, and filtered through a nanosep spin filter cartridge (Pal Cooperation, East Hills, NY) (0.2 μm pore size). The supernatant was subjected to lithium analysis by spectrophotometry, using the Infinity™ lithium single liquid stable reagent (Thermo Fisher Scientific, Waltham, MA) in collaboration with the University of Iowa Hospitals and Clinics Pathology Department.

Statistical analysis

For behavioral experiments, statistical comparisons between two groups were performed using a two-tailed Student's t-test assuming unequal variance or for non-normally distributed data the Mann-Whitney *U* test. Statistical significance between multiple groups displaying a normal-distribution was determined using One Way ANOVA with Bonferroni t-test comparisons between control and treatment groups *post hoc.* For those data exhibiting non-normal distributions, Kruskal–Wallis One Way ANOVA on Ranks was performed. Comparisons between groups or groups versus a control were calculated using Dunn's method *post hoc*. Data not conforming to a normal distribution are represented as box plots. Statistical analyses were performed using SigmaStat for Windows Version 3.11 (Systat Software, Inc., Point Richmond, CA).

Results

Shu mutants exhibit morphological defects

In the previous study by Williamson (1982), the phenotype of *Shu* was examined using *Shu*/FM6 female flies. FM6 is an X-chromosome balancer with multiple inversions and marker mutations. Therefore, it was possible that genetic aberrations on the balancer chromosome contributed to the reported dominant phenotypes of *Shu* (e.g., sporadic tremors and defects in locomotor behavior). To rule out this possibility, I carried out a phenotypic analysis of *Shu* mutants using only *Shu*/+ flies (here after in the text referred to as *Shu).* To minimize potential effects of the unknown genetic background of the original *Shu* mutant, I used a *Shu* stock that had been outcrossed to a wild-type *CS* strain 26 times.

The outcrossed *Shu* females and *Shu* males exhibited a “down-turned wings and indented thorax” phenotype that became apparent shortly after eclosion (Figure 3A, B versus. 3C, D). These phenotypes were highly penetrant, as greater than 90% of females displayed some form of morphological defect, where as all males examined showed defective wings and or thorax (Figure 3C). These phenotypes do not appear to be mutually exclusive as some mutants will show one or the other, or both defects.

A similar morphological phenotype has been previously observed in mutants with increased neuronal excitability, including *Shaker* (*Sh*) in combination with either *ether a go-go (eag), inebriated (ine)* or a *paralytic* duplication (Loughney et al., 1989, Stern et al., 1990, Stern and Ganetzky, 1992). Likewise, double mutants carrying the Ly-6/neurotoxin family member *quiver*

(qvr) with *eag* or *Hyperkinetic (Hk)* (Wang et al., 2000) show similar defects. More recently, it was found that mutants for *parkin* and *PTEN-induced putative kinase 1* (*Pink1*), *Drosophila* orthologs of the human genes involved in the pathophysiology of a familial form of Parkinson's disease, display a similar wing and thorax phenotype (Greene et al., 2003, Park et al., 2006). These morphological abnormalities of the dorsal thorax are thought to be the cause of an increase in neuronal excitability resulting in hypercontraction of the dorsal longitudinal flight muscles (DLMs), which serve as wing depressors during flight and underlie the area of indented cuticle (Huang and Stern, 2002).

However, in the case of *parkin* and *Pink1* mutants, a degeneration of the gross anatomy of the muscle can be observed at the light microscope level several days after eclosion due to abnormal mitochondrial morphology and defective function in both muscle cells and dopaminergic neurons. Unlike *parkin* and *Pink1* mutants, a survey of the indirect flight muscle in *Shu* males and females showed no obvious degeneration of the musculature compared to controls (Figures 3E-H), although more subtle defects visualized using higher magnification (e.g. transmission electron microscope, TEM) cannot be ruled out.

The *Shu* mutant displays abnormalities in locomotion

As reported by Williamson (1982), the mutant flies exhibit defects in reactive climbing ability, a well-established experimental paradigm to assess the general motor activity in mutant and wild-type flies (Greene et al., 2003). Newly eclosed, outcrossed *Shu* flies showed a defect in climbing ability compared to controls, which became more severe in a time-dependent manner (Figure 4A).

Figure 3. *Shu* displays morphological defects. (A) *CS* male (B) *CS* female (C) *Shu* male (D) *Shu* female. Arrows indicate the indented dorsal thoraces in *Shu* mutants. Representative longitudinal thoracic sections of (E) *CS* male (F) *CS* female (G) *Shu* male (D) *Shu* female adult flies. Scale bar, 200μm. Arrow heads, indented thorax.

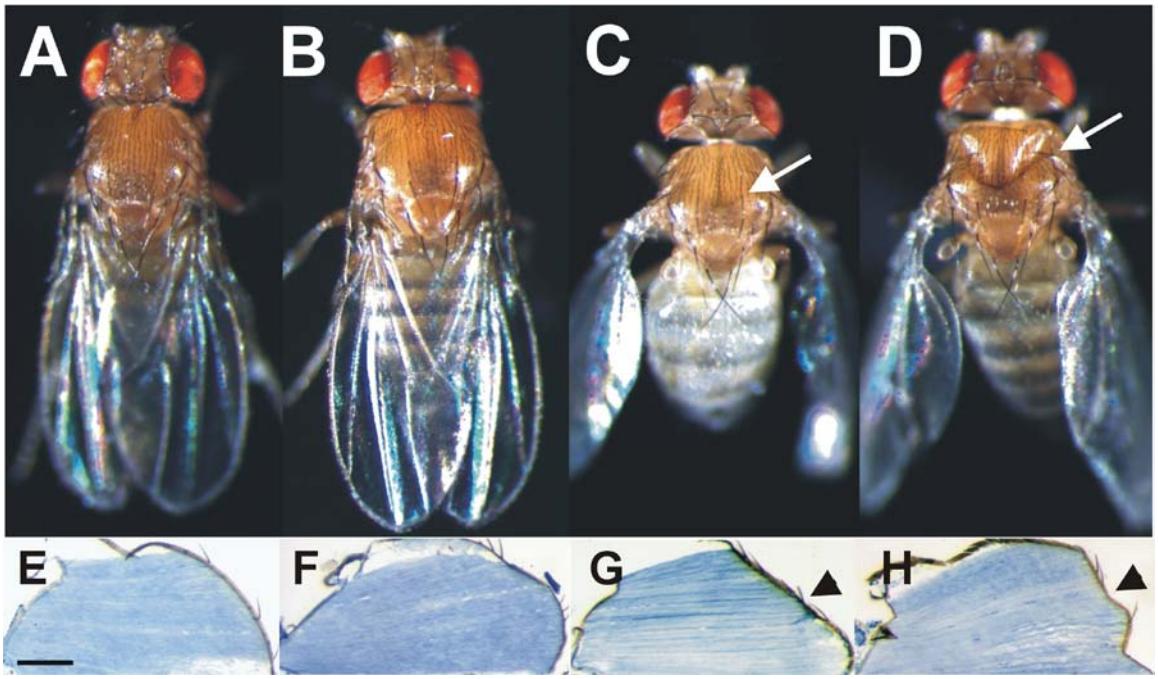
A
B
C
D
E
F
G
H

By 5 days post-eclosion, *Shu* mutants were extremely impaired in their ability to climb, whereas *CS* climbing indices through 10 days of observation remained unchanged. Our findings confirm those of the seminal report on the *Shu* mutant (Williamson, 1982). A careful analysis of the mutant's "shuddering" behaviors revealed that shortly after eclosion *Shu* mutant flies exhibit very little jerking and twitching (Figure 4B). However, this behavior appears to reach a maximum 5 days after eclosion and remains steady through 10 days of observation.

Next, I sought to analyze the behavior of *Shu* and *CS* using a more thorough, automated method in an effort to highlight the striking differences in their locomotion patterns. For this purpose, I employed a video-tracking system. originally developed to analyze sleep behaviors in *Drosophila* (Gilestro and Cirelli, 2009) (see Materials and Methods). Using the video tracking system allowed me to gather x, y positional coordinates from each individual fly per frame of video, at a recording speed of 15 frames per second. Using this data I was able to calculate instantaneous locomotor parameters for both the mutant and *CS* controls which included: total distance traveled (millimeters, mm), velocity (mm per second), acceleration (mm per second^2) and the turning angle when a fly changes directions. When placed in a circular arena, wild-type *Drosophila* flies often travel along the edge of the chamber (Besson and Martin, 2005), making smooth, repetitive circular paths with intermittent bouts of inactivity. These aspects of wild-type locomotion result in a tracking pattern represented as a circular path many times around the chamber. In contrast, the spontaneous jerking and twitching of the *Shu* mutants results in an extreme number of

Figure 4. *Shu* exhibits locomotor defects that are improved by lithium treatment. (A) Shuddering behavior of 0-10 day old *CS* and *Shu* female flies. n ≥ 30. Data are average ± SEM. $p<0.001$, One Way ANOVA; ***$p<0.001$, Bonferroni t-test *post hoc* versus wild-type. (B) Reactive climbing ability of *CS* and mutant females over the same time period. Data are ± SEM of 5 groups of 20 flies. $p<0.001$, One Way ANOVA; ***$p<0.001$, Bonferroni t-test *post hoc* versus wild-type. (C) (Left) Shuddering behavior of *CS* females after treatment with food containing 0, 25, 50 or 100 mM LiCl. This behavior was unaffected by LiCl treatment. (Right) All mutant groups receiving LiCl treatment showed a significant reduction in shuddering behavior. n ≥ 30 flies. $p<0.001$, One Way ANOVA; *$p<0.05$, Bonferroni t-test *post hoc* versus vehicle control. (D) (Left) *CS* female flies reactive climbing after 5 days of treatment with food containing 0, 25, 50 or 100 mM LiCl. *CS* climbing was significantly reduced by 100 mM LiCl treatment compared to those receiving no lithium. (Right) Reactive climbing of *Shu* females under the same conditions as controls. Data are mean ± SEM of 10 groups of 20 flies. $p = 0.005$, One Way ANOVA; **$p<0.01$, ***$p<0.001$, Bonferroni t-test *post hoc* versus vehicle control.

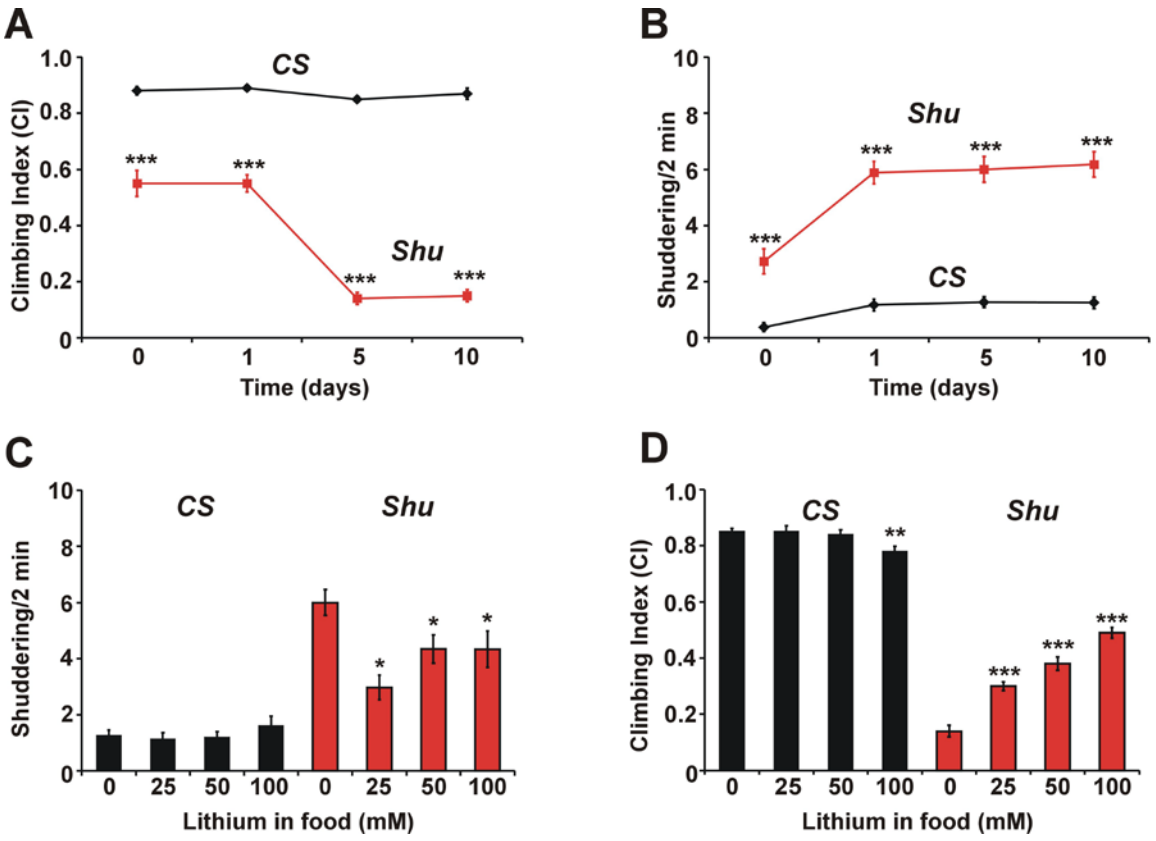
A
CS
Shu
Climbing Index (CI)
1.0
0.8
0.6
0.4
0.2
0
***
***
***
***
0
1
5
10
Time (days)
B
Shu
CS
Shuddering/2 min
10
8
6
4
2
0
***
***
***
***
0
1
5
10
Time (days)
C
CS
Shu
Shuddering/2 min
10
8
6
4
2
0
*
*
*
0
25
50
100
0
25
50
100
Lithium in food (mM)
D
CS
Shu
Climbing Index (CI)
1.0
0.8
0.6
0.4
0.2
0
**
***
***
***
0
25
50
100
0
25
50
100
Lithium in food (mM)

changes in direction and an increased presence in the center of the chambers as represented by the tracking trace (Figure 5). Because the locomotion of *Shu* mutants is constantly interrupted by jerking and twitching it was feasible to hypothesize that the mutant would travel a shorter distance, given a particular duration of time, compared to the *CS* strain. However, the mean total distance traveled during a 10 min recording period was actually longer in *Shu* (2523 ± 165 mm) when compared to *CS* (1891 ± 363 mm) controls (Figure 6A). Upon visual observation, *Shu* mutants appear to increase their velocity of movement dramatically when jerking and twitching compared to times when they are not "shuddering". Therefore, I examined the velocity of both *CS* and *Shu* female movement when the flies were in motion. In other words, I wanted to observe how fast the flies were moving, when excluding those frames when the fly was immobile (Figure 6B). As expected, there was a significant increase in the median velocity of *Shu* (15.5 mm/s) compared to *CS* (11.8 mm/s) (Figure 6D). A closer examination of velocity in these genotypes revealed that the increased median velocity in *Shu* mutants is due to a large increase in the percentage of speeds >20 mm/sec as well as a prominent decrease in the percentage of those speeds <10 mm/sec (Figure 6C).

Likewise, the mutant's locomotion is constantly interrupted by the spontaneous jerks and twitches. This continuous process leads to large changes in the velocity (acceleration) of *Shu*, where as the *CS* display a smooth, continuous locomotion which should result in less drastic fluctuations in velocity. Indeed this is the case, as the mutant has a significant increase in its median

Figure 5. Representative 1 min traces of *CS* and *Shu* flies. Traces were reconstructed using x, y coordinate data together with the x, y scatter plot chart option of Microsoft Excel. Scale Bar = 3mm

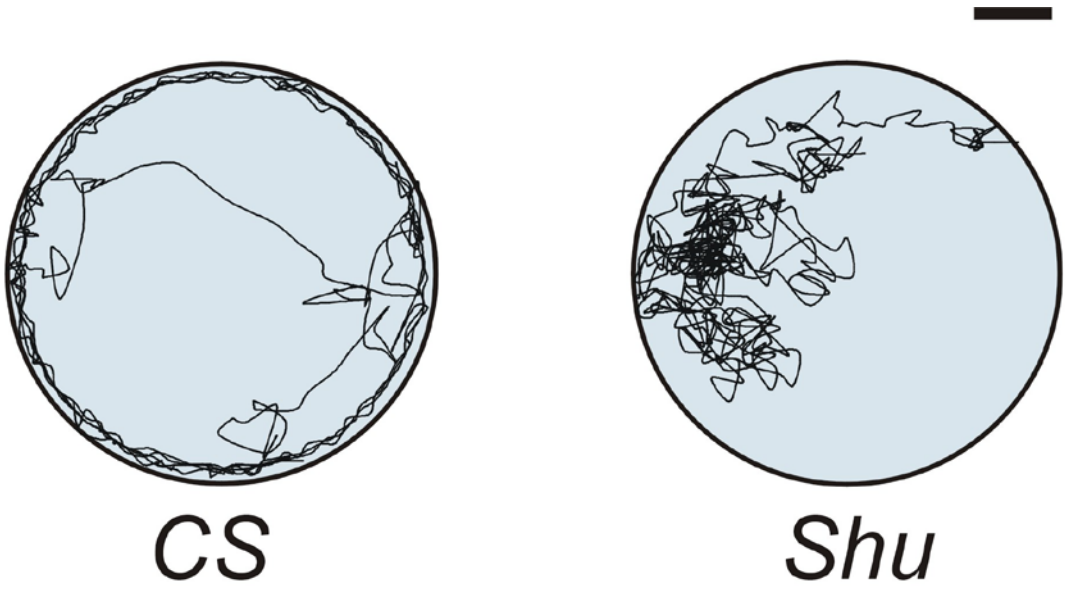
CS
Shu

Figure 6. Video tracking analysis to quantify the abnormal locomotion behaviors of the *Shu* mutant. (A) Total distance traveled in millimeters for *CS* and *Shu* flies after 10 min of video recording, n = 24. NS, p>0.05, Student's t-test. (B) Percentage of frames in 10 min where flies were immobile. (C) Percent distribution of velocity values (mm/s) for both genotypes per frame, when in motion (i.e. values > 0). ***p<0.001, Student's t-test. (D) Median velocity of *CS* and *Shu* per frame, when in motion (i.e. values > 0), ***p<0.001, Wilcox-Mann-Whitney *U* test. (E) Percent distribution of Δ in velocity (i.e. acceleration in mm/sec^2) values for both genotypes per frame, when in motion (i.e. values > 0). ***p<0.001, Student's t-test. (F) Median acceleration of *CS* and *Shu* per frame, ***p<0.001, Wilcox-Mann-Whitney *U* test. (G) Measurement of turning angles. The θ values were calculated using x, y coordinates in three consecutive frames (each frame is a time point = 1/15 second. The initial linear movement was the vector connecting Frame 1 and Frame 2. The θ change was calculated using the initial linear movement and the vector connecting Frame 2 and Frame 3. (H) Percent distribution of turning angles per frame. ***p<0.001, Student's t-test. (I) Median turning angle of the two groups per frame. ***p<0.001, Wilcox-Mann-Whitney *U* test.

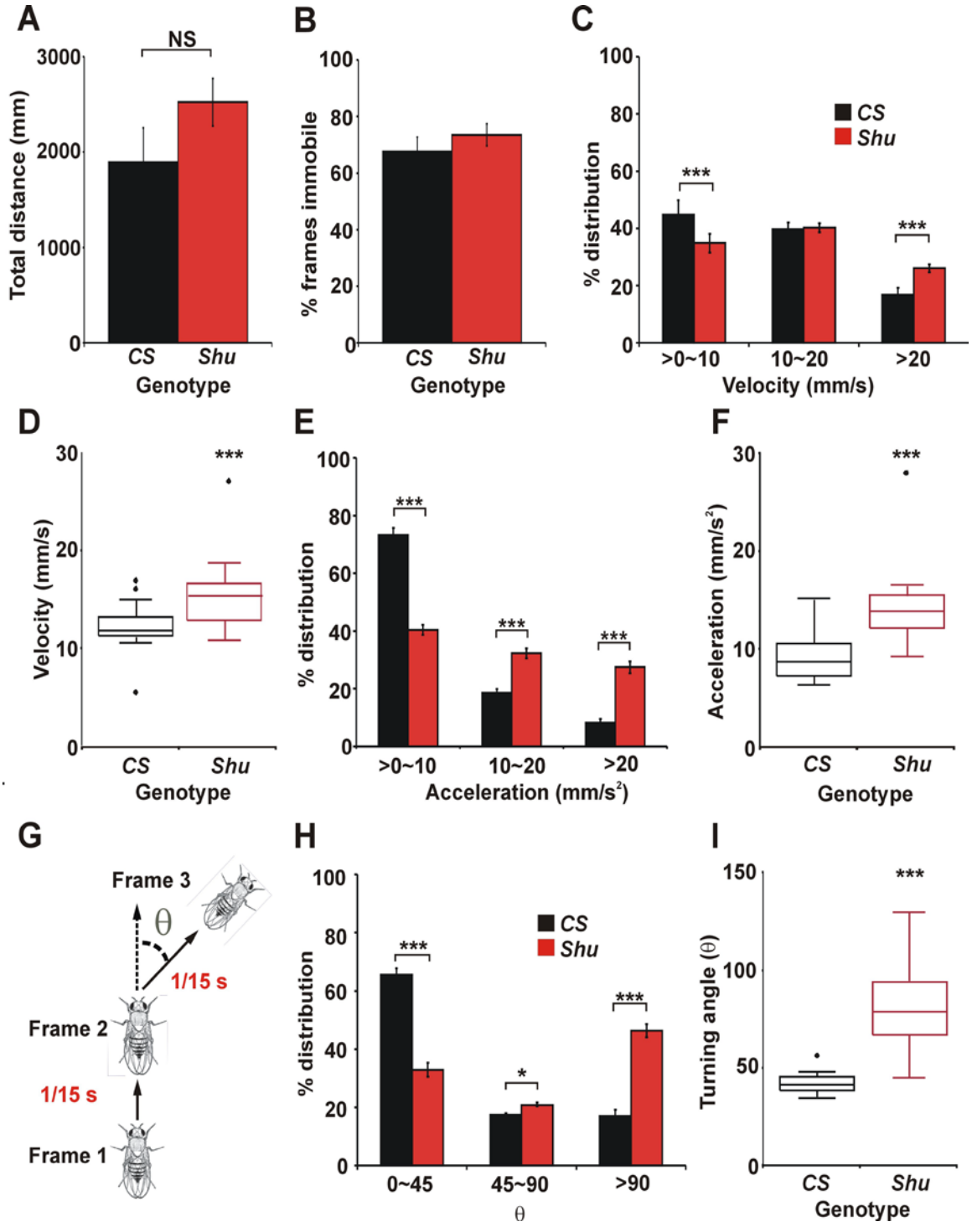
A
NS
Total distance (mm)
3000
2000
1000
0
CS
Shu
Genotype
B
% frames immobile
100
80
60
40
20
0
CS
Shu
Genotype
C
% distribution
CS
Shu
***
***
>0~10
10~20
>20
Velocity (mm/s)
D
Velocity (mm/s)
30
20
10
0
***
CS
Shu
Genotype
E
% distribution
***
***
***
>0~10
10~20
>20
Acceleration (mm/s²)
F
Acceleration (mm/s²)
***
CS
Shu
Genotype
G
Frame 3
θ
1/15 s
Frame 2
1/15 s
Frame 1
H
% distribution
CS
Shu
***
*
***
0~45
45~90
>90
θ
I
Turning angle (θ)
150
100
50
0
***
CS
Shu
Genotype

acceleration (13.8 versus 8.7 mm/s^2) (Figure 6F) due to an increased percentage of acceleration events >10 mm/s^2 and a subsequent reduction in the percentage of smaller variations in speed (i.e. <10 mm/s^2) (Figure 6E). As expected, because of its locomotion phenotype, *CS* mainly exhibits mainly small variations in its velocity (Figures 6E, F).

Finally, one of the most striking qualitative differences between the mutant and controls is the extreme number of changes in direction exhibited by *Shu* due to their spastic movements. To explore this difference further, in a quantitative manner, I calculated the angle of direction change per frame using the x, y data from three consecutive frames along with the formula for arctangent, which can be used to determine the angle size opposite the hypotenuse of a right triangle (Figure 6G). A similar method has been employed recently to calculate the turning angle in a larval study on cool temperature preference (Kwon et al., 2010). Calculation of the turning angle of both groups of flies revealed that the median turning angle for wild-type *CS* was 41.3^o. In contrast, the mutant turning angle was 78.8^o validating the qualitative differences previously observed (Figure 5). As with the other parameters examined, this large increase in the turning angle of *Shu* flies is the result of a significant increase in the percentage of total turns in the mutant greater than 90^o.

In summary, these data correlate well with the results of my visual observations of the *Shu* mutant. The mutant displays hyperactivity and spontaneous, uncoordinated movements characterized by high-speed movements. Furthermore, *Shu* displays large fluctuations in the velocity of their

movements resulting in an increase in its median value of their acceleration. Finally, the spontaneous nature of the jerking and twitching phenotype forces the mutant fly to make unusual, involuntary changes in direction as evidenced by the drastic increases in its turning angles. Taken together, this analysis system can now be employed as a powerful objective tool to study *Shu* and possibly other hyperactive mutants.

The anesthesia-induced shaking behavior in *Shu*

Consistent with the report by Williamson (1982), outcrossed *Shu* flies also exhibit vigorous leg-shaking under ether-induced anesthesia. Previous reports on other ether-induced leg-shaking mutants, including *Sh, eag, Hk* and *quiver (qvr),* (Kaplan and Trout, 1969, Wang et al., 2000), have only qualitatively explained this behavior with vague descriptions that do not fully illustrate the intricate differences of each mutant's response to the anesthetic. Therefore, I have sought to develop a system that could be used to extract quantitative parameters of ether-induced leg-shaking. I was able to accomplish this using the video-tracking analysis system described earlier. Qualitative observation of ether-induced leg shaking in *Shu* revealed that the mutant exhibited forceful bobbing of the head and halters as well as vigorous and rhythmic clenching of the legs. These characteristics of leg shaking behavior in *Shu* were not shared with either *CS*, or the mutant alleles, Sh^5 (K^+ channel, α subunit), eag^1 (K^+ channel, α subunit), and Hk^1 (K^+ channel, β subunit). After careful observation, I determined that tracking of both head and hind leg movement would provide the clearest difference between *Shu* and the other mutants. Video tracking of head

Figure 7. *Shu* displays unique behaviors under recovery from ether anesthesia. (A) Representative velocity plots of head movement (pixels/s) in *CS*, *Shu, eag*^{1}*, Hk*^{1} and *Sh*^{5} after a 1 min video recording. Head movement was tracked using the anterior lateral part of the eye. (B) Representative velocity plots of hind leg movement (pixels/s) in *CS*, *Shu, eag*^{1}*, Hk*^{1} and *Sh*^{5} after a 1 min video recording. Hind leg movement tracking was captured by focusing on the hind leg joint between the tibia and tarsus. (C and D) Median velocity (pixels/s) of head and hind leg movement in leg-shaking mutants. Asterisks indicate significant differences between *Shu* and other genotypes, $p<0.001$, Kruskal–Wallis one Way ANOVA on Ranks; *$p<0.05$, vs *Shu*, Dunn's method *post hoc.*

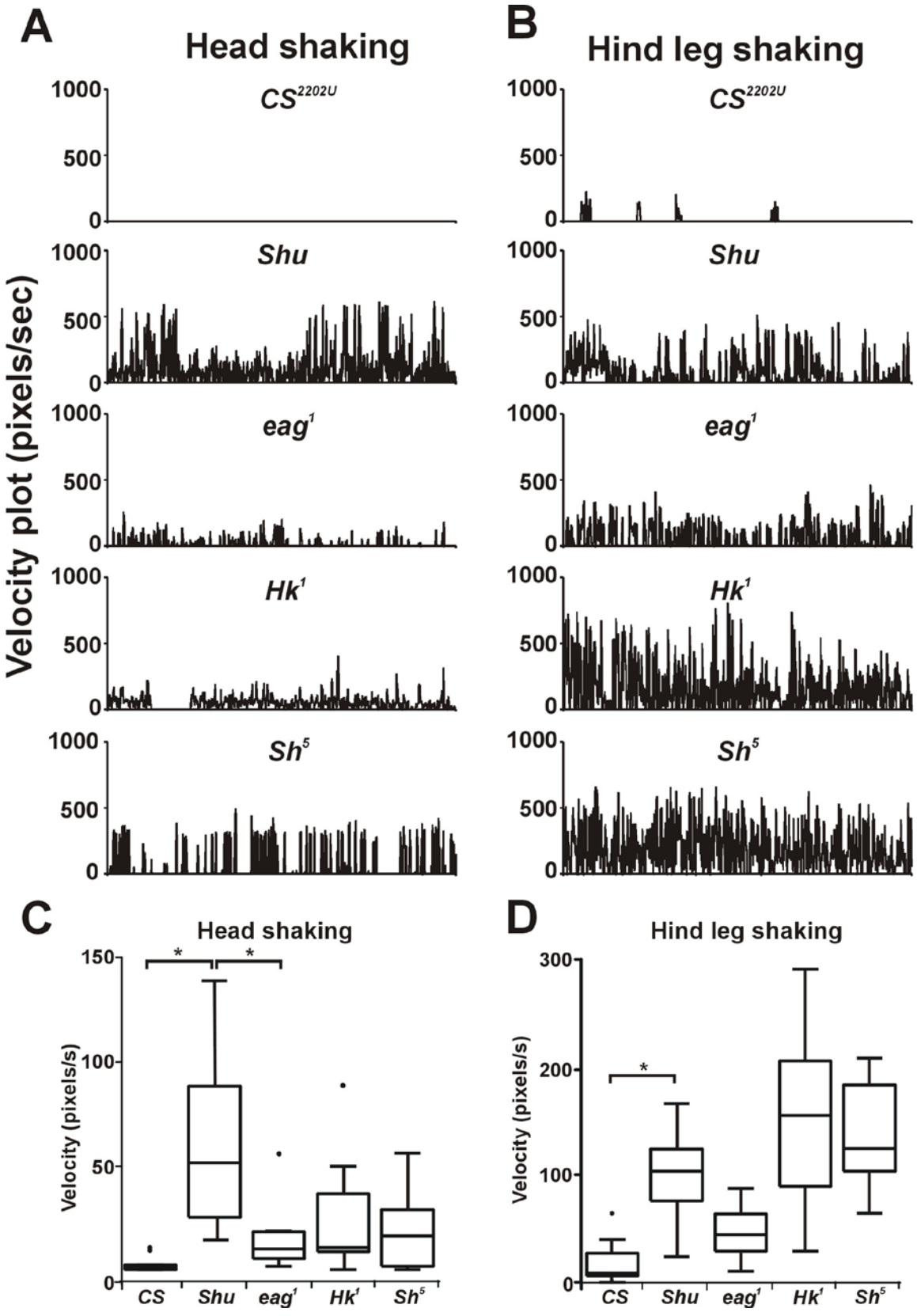
A
Head shaking
B
Hind leg shaking
Velocity plot (pixels/sec)
CS2202U
Shu
eag1
Hk1
Sh5
1000
500
0
C
Head shaking
D
Hind leg shaking
Velocity (pixels/s)
150
100
50
300
200
*
CS
Shu
eag1
Hk1
Sh5

movement in these flies confirmed my qualitative observations that *Shu* exhibited the most robust head movement upon recovery from ether as shown in velocity plots (Figure 7A). The median velocity of *Shu* head movement was 51.5 pixels/s, whereas Sh^5 (16.4 pixels/s), eag^1 (9.9pixels/s) and Hk^1 (10.8 pixels/s) showed only mild head tics (Figure 7C). The wild-type strain, *CS* was almost completely devoid of any head movement (1.17 pixels/s), as expected based on qualitative observations. However, the hind leg movement in *Shu* was only intermediate (Figure 7B, D) in velocity (107.5 pixels/s) compared to the other flies examined, Sh^5 (129.4 pixels/s), eag^1 (45.9 pixels/s) and Hk^1 (161.6 pixel/s). Again, as expected, the hind leg velocity in *CS* was very mild (9.1pixels/s). Several reports have demonstrated that the legs of *Sh* mutants will continue to shake after they are severed from the body upon recovery from ether anesthesia (Ganetzky and Wu, 1985). This observation suggests that defects present in the *Sh* peripheral nervous system or muscle is sufficient to drive this behavior. We were able to confirm this peculiar behavior in the Sh^5 allele. In contrast, severing of *Shu* legs during recovery from ether anesthesia suppressed its movement (data not shown). Our observations suggest that the defect(s) causing the leg shaking behavior in *Shu* are generated upstream of the muscle, and at least the peripheral nerves in the appendage.

In summary, we can order the severity of head movement of these flies during recovery from ether anesthesia as follows: $Shu > Hk^1 > Sh^5 > eag^1 > CS.$ Interestingly, when comparing hind leg velocity the order of severity is as follows: $Sh^5 > Hk^1 > Shu > eag^1 > CS.$ Furthermore, the experiment with severed legs

Figure 8. *Shu* mutants display abnormalities in sleep architecture. (A) *CS* and *Shu* sleep amounts (min sleeping/30 min bins) recording using the DAM system (see Materials and Methods). Data are average ± SEM of three consecutive days for all parameters analyzed. Similar results were obtained from independent experiments. *CS*, n = 31; *Shu*, n = 26. (B) Amount of time sleeping (hr) per 12 hour light period (day). (C) Waking activity index (infrared beam breaks/min) of both genotypes during the day. (D) Number of activity-rest bouts during the day. (E) Average length of time of one rest bout during the day. (E) Amount of time resting (hr) per 12 hour light period (day). (F) Waking activity index (infrared beam breaks/min when active) of both genotypes during the night. (G) Number of activity-rest bouts during the night. (H) Average length of time of one rest bout during the night. *p<0.05, **p<0.005, ***p<0.001, Student's t-test.

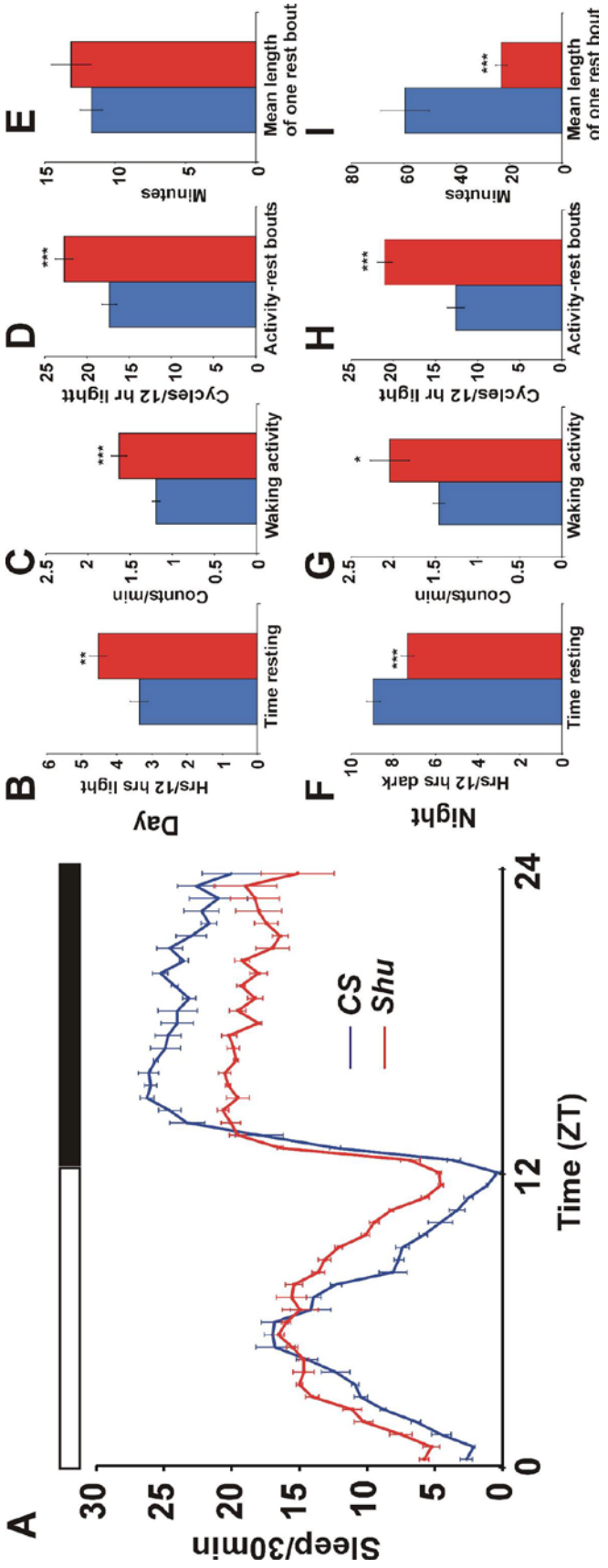
A
Sleep/30min
30
25
20
15
10
5
0
0
12
24
Time (ZT)
CS
Shu
Day
B
Hrs/12 hrs light
Time resting
C
Counts/min
Waking activity
D
Cycles/12 hr light
Activity-rest bouts
E
Minutes
Mean length of one rest bout
Night
F
Hrs/12 hrs dark
Time resting
G
Counts/min
Waking activity
H
Cycles/12 hr light
Activity-rest bouts
I
Minutes
Mean length of one rest bout

suggests that the defects driving the leg shaking behaviors in *Shu* are different from those in *Sh* in that they are localized upstream of the peripheral nerves and muscle in the mutant's limbs.

Shu mutants display abnormalities in day and night sleep architecture

All ether-induced leg-shaking mutants in *Drosophila* whose sleep has been analyzed to date have shown a severe reduction in sleep amount both during the day and at night (Cirelli et al., 2005, Bushey et al., 2007, Koh et al., 2008). As observed in previous leg-shaking mutants, *Shu* females display a significant reduction in their sleep amount during the 12 hour dark period (7.3 ± 0.3 hr) compared to wild-type controls (8.9 ± 0.3 hr) (Figure. 8A, F). This difference equates to an 18% reduction in nighttime rest. At night, *Shu* mutants cycled between episodes of sleep and activity 21.4 ± 0.9 times in 12 hr (ZT12-ZT24), whereas *CS* only had on average, 12.6 ± 1.0 cycles over the same duration (Figure 8H). Consequently, a severe reduction in the mean length of time per sleep episode (Figure 8I) was also observed in the mutant (23.0 ± 2.2 min) versus *CS* (59.6 ± 9.2 min). An analysis of the waking activity showed that the mutant's waking activity index was 2.0 ± 0.2 counts per min in contrast to *CS* We next investigated sleep crossing only 1.5 ± 0.1 counts per min (Figure 8G). These findings in waking activity are consistent with the hyperactive phenotype of the *Shu* mutant as shown using the video tracking system. The mutant travels a further distance during a given time period and when its mobile it is traveling faster then *CS* (velocity) (Figure 6C, E). Thus, *Shu* mutants exhibit less rest at

night due to hyperactivity which likely results in a fragmented sleep pattern as evidenced by the significant increases in the number of activity/rest bouts and the drastic decrease in the average length of one rest bout.

In contrast to nighttime rest, *Shu* mutants show an increase in daily rest amount (4.5 ± 0.2 hr) compared to *CS* (3.4 ± 0.3 hr), equating to a 26% increase (Figure 8A, B). In line with the observed increase in daytime rest, the average length of one activity bout in the mutant was only 21.5 min while the average in *CS* was 34.3 min. Despite its increased daytime rest, when *Shu* is mobile it displays an increase in waking activity (1.6 ± 0.1 versus 1.2 ± 0.1 counts per min (Figure 8C). As observed at night, the number of activity/rest cycles is again elevated in the mutant flies (17.4 ± 0.9 versus 22.7 ± 1.0 cycles) (Figure 8D)

In summary, the increased sleep amount during the day in *Shu* appears to be a result of fragmented sleep observed as an increase in the number of activity/rest bouts combined with a reduction in the length of time the mutant is active. My overall examination of sleep architecture in the *Shu* mutant reveals for the first time, a leg-shaking, hyperactive mutant that displays an increase in daytime sleep and a decrease in nighttime sleep.

<u>*Shu* mutants display reduced lifespan</u>

Another common feature of the *Drosophila* neurological mutants with leg-shaking and short-sleeping phenotypes is a decrease in lifespan (Trout and Kaplan, 1981, Koh et al., 2008, Bushey et al., 2010). Therefore, I examined the lifespan of *Shu* mutant females and the *CS* strain. As seen with other short-

Figure 9. *Shu* mutants have reduced lifespan. Survival of *Shu* and *CS* female flies on a diet of standard fly food. Mean survival, *CS* = 73 days, *Shu* = 40 days. p = 0.0127, n = 100**.**

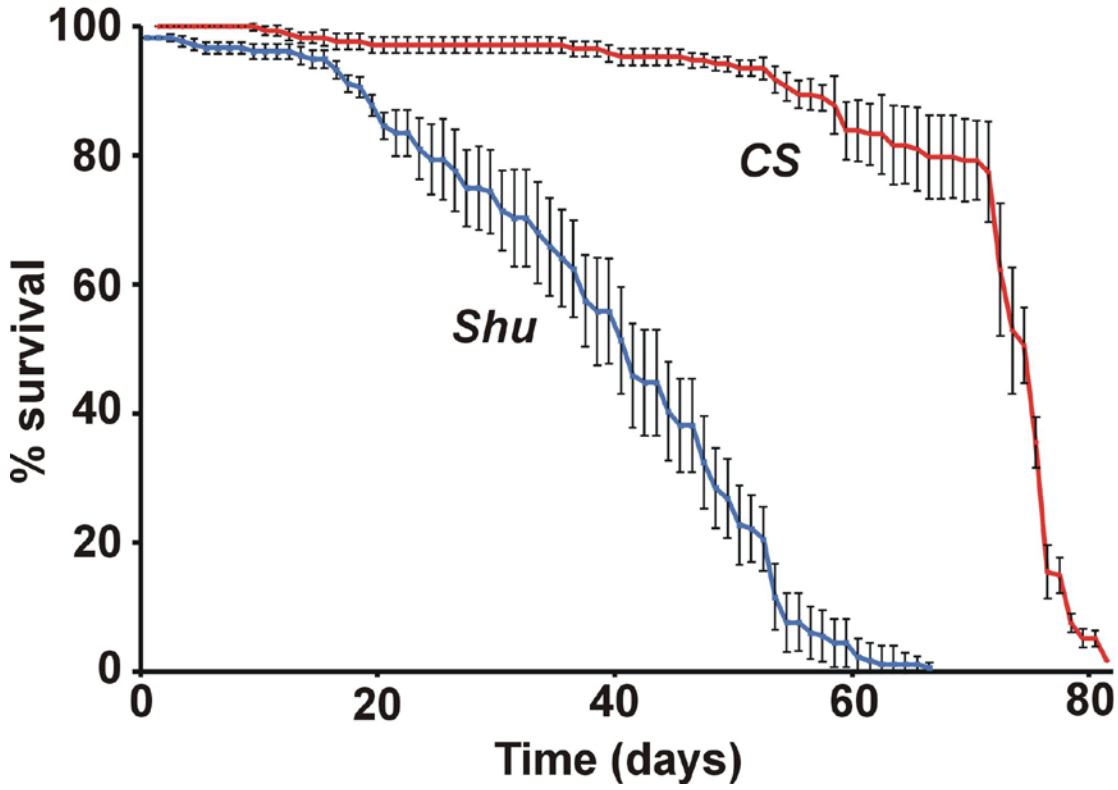
100
80
60
40
20
0
% survival
0
20
40
60
80
Time (days)
CS
Shu

Figure 10. Lithium has contrasting effects on video tracking locomotor parameters in *Shu* and *CS* flies. (A) Median turning angle was analyzed for *Shu* and *CS* flies received diets containing lithium doses of 0, 25, 50 and 100 mM LiCl, respectively. Flies were treated for 5 days. n = 40 flies. $p<0.001$, Kruskal-Wallis One Way ANOVA; *$p<0.05$, Dunn's method *post hoc.* (B) Average velocity of the same flies was analyzed. n = 40 flies. $p<0.001$, Kruskal-Wallis One Way ANOVA; *$p<0.05$, Dunn's method *post hoc.* (C) Lithium levels in female flies after 5 days of treatment with 25, 50 and 100 mM LiCl. Data are mean ± SEM of 3 independent experimental groups of 20 flies. *$p<0.05$, Student's t-test.

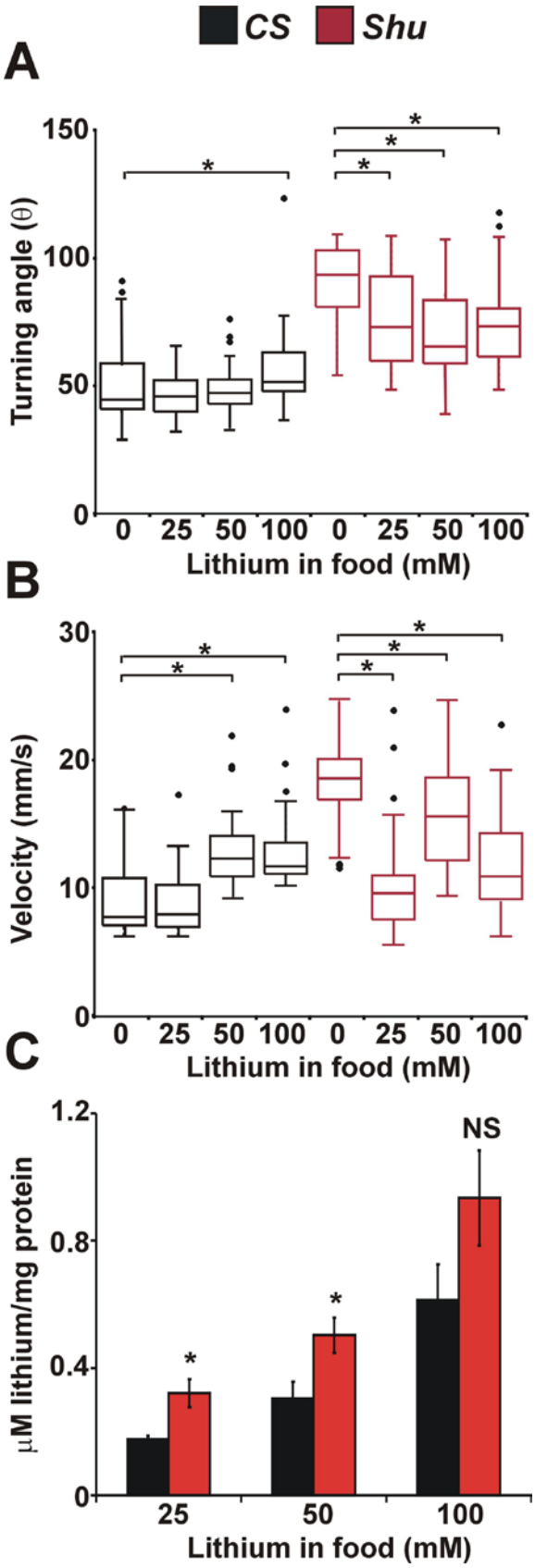
CS
Shu
A
Turning angle (θ)
150
100
50
0
0 25 50 100 0 25 50 100
Lithium in food (mM)
B
Velocity (mm/s)
30
20
10
0
0 25 50 100 0 25 50 100
Lithium in food (mM)
C
μM lithium/mg protein
1.2
0.8
0.4
0
NS
25 50 100
Lithium in food (mM)

sleeping mutants, *Shu* females mean lifespan is significantly reduced (41 days) compared to the wild-type (73 days) (Figure 9).

Lithium improves several of the behavioral abnormalities observed in *Shu* mutants

I initially examined the effect of lithium on the behavioral phenotypes of the outcrossed *Shu* flies for its effect on climbing ability and the mutant's shuddering behaviors. As reported in the seminal paper, lithium treatment was sufficient to both improve reactive climbing ability and reduce the severity of the jerking and twitching in *Shu* (Figure 4C, D right). It should be noted that even at lower concentrations of the drug (i.e. 25 and 50 mM) than those used in the original experiments, a significant improvement was observed in the behavioral phenotypes of *Shu*. In contrast, the drug had no significant impact on *CS* except that at 100 mM lithium treatment the controls began to show a reduction in the ability to climb (Figure 4C, D left)

Next, using the video tracking system I sought to examine the effect of the mood-stabilizing drug on the locomotor parameters in both genotypes. As observed in my initial locomotor assessment, *Shu* flies exhibited a median turning angle of 92.8^{o} compared to only 43.7^{o} for wild-type. Again, the large turning angles of *Shu* flies are likely due to the spontaneous jerking and twitching of the mutant. Therefore, these data can be used as an indirect readout of the shuddering behaviors in *Shu*. I tested the effects of 25, 50 or 100 mM LiCl on *Shu* and *CS* turning angles. I found that administration of all three concentrations of lithium were sufficient to reduce the median turning angles of

the mutant (25mM, 72.3^{o}; 50 mM, 64.5^{o}; 100 mM, 72.5^{o}), compared to vehicle controls (Figure 10A, red boxes). These data are in agreement with the previous subjective report by Williamson (1982), on the mood stabilizing drug's effect on *Shu* flies. Interestingly, the 25 and 50 mM doses of lithium had no statistically significant effect on the turning angles of the *CS* controls. However, a dose of 100 mM lithium was sufficient to increase the median turning angle 50.3^{o} compared to *CS* (Figure 10A, black boxes).

Another parameter indicative of hyperactive locomotion is an increase in velocity, which was shown to be significantly elevated in *Shu* compared to *CS.* This finding is likely due to an increase in high velocity bursts characteristic of the mutant when it is jerking and twitching. Therefore, I examined both genotypes to see what effect lithium would have on velocity. It turns out that the mood-stabilizing drug generally reduced the median velocity in *Shu* (25 mM, 9.8 mm/s; 50 mM 15.8mm/s; 100 mM, 11.1mm/s) compared to those flies receiving the vehicle (18.8mm/s),(Figure 10B, red boxes). In sharp contrast, the higher doses of 50 mM and 100 mM lithium increased the median velocity in *CS* (50 mM, 12.5mm/s, 100 mM, 11.9mm/s) compared to the control (8.0mm/s) (Figure 10B, black boxes),

One obvious explanation for the reduction observed in the frequency of shuddering events and the decreased median turning angle and velocity is that lithium may be eliciting a toxic effect on the mutant, resulting in an overall suppression in locomotion. This explanation is reasonable when considering the toxic side-effects often associated with the mood stabilizing drug (el-Mallakh,

1986). However, it is not likely because the ability of *Shu* to climb is actually improved by treatment with 25, 50 or 100 mM lithium (Figure 4D). Unlike lithium's effect on the video tracking locomotor parameters, the drug appeared to improve the mutant's ability to climb in a dose-dependent manner. When *CS* flies received food containing 25 or 50mM lithium there was no significant difference in their climbing ability compared to vehicle controls. Yet, when *CS* flies were administered food containing 100mM lithium there was a significant reduction in climbing ability compared to those flies receiving only the vehicle (Figure 4B). Together with the observed increases in velocity and turning angle, these data suggest that higher doses of lithium are eliciting a deleterious effect on the *CS* flies. At the same concentrations of lithium, these effects are not observed in the mutant.

A closer investigation of leg-shaking behaviors in *Shu* and *CS* flies after 5 days of treatment with 100 mM lithium revealed no significant differences between treated and control groups for either genotype (data not shown). These findings are in agreement with the observations reported by Williamson.

<u>*Shu* mutants accumulate higher levels of lithium</u>

The behavioral responses to lithium treatment were different between *CS* and *Shu* mutant flies. To examine whether physiological responses to the drug are different between the two genotypes, the internal lithium concentrations in the *CS* and *Shu* mutant flies were analyzed after they were subjected to lithium-containing food for 5 days. I found that *Shu* mutants accumulated significantly higher levels of lithium than *CS* flies when they were fed with food containing

either 25 or 50 mM lithium (Figure 10C). The same tendency was observed when food containing 100 mM LiCl was used, although the difference between the two genotypes did not reach statistical significance (Figure 10C). Lithium levels were normalized using protein concentrations from each corresponding sample. My *CS* data were comparable to internal lithium concentrations determined in previous studies under similar conditions (Padiath et al., 2004, Dokucu et al., 2005). These results further demonstrate that there is an effect of the *Shu* mutation on physiological responses to the mood-stabilizing drug, lithium

Discussion

My thorough morphological and behavioral assessment of the *Shu* mutant resulted in a number of interesting findings. Furthermore, I was able to validate the original report by Williamson that *Shu* behaviors are improved by lithium treatments. Importantly, extensive backcrossing to isogenize the mutant background did not compromise the original findings.

As reported in previous investigations, several double mutant combinations using flies that exhibit increased neuronal excitability can cause the manifestation of down-turned wings and an indented-dorsal thorax (Loughney et al., 1989, Stern et al., 1990, Stern and Ganetzky, 1992, Wang et al., 2000). Yet, in each instance the synergistic effects of two mutants with hyper neuronal excitability are required to elicit this phenotype. In contrast, the *Shu* mutant displays this phenotype even though it is likely the result of a single mutated locus based on previous mapping experiments (Williamson, 1982). Thus, these findings suggest that the *Shu* mutant displays a very severe level of increased

neuronal activity. Preliminary electrophysiological recordings from the larval neuromuscular junction (NMJ) support this idea (Atsushi Ueda and Chun-Fang Wu, Department of Biology, University of Iowa, personal communication). Interestingly, examination of the musculature of the mutant, when compared to *CS*, revealed no obvious degeneration (Figure 3 E-H), even after aging the flies for 30 days (data not shown). However, less obvious defects at higher magnifications cannot be ruled out. These data suggest that the mutant does not experience a severe degeneration of the muscle as a result of its extreme neuronal activity.

We were also able to recapitulate Williamson's findings that the mutant displayed defects in climbing ability (Figure 4A) in our isogenized strain. The inability of *Shu* to climb is likely due in part to the jerking and twitching behavior (Figure 4B) which interrupts the fly in its attempts to climb. To ensure that this climbing defect was not simply due to the down-turned wing phenotypes of the fly, all wings of the mutant and *CS* flies were removed shortly after eclosion in all locomotor experiments performed. The time-dependent loss of *Shu* climbing correlates well with the increased frequency and severity of the shuddering behaviors. However, it could be caused by general muscle fatigue of the mutant from constant stimulation coming from the nervous system or represent some sort of neuronal degeneration as seen in other neuronal excitability mutants (Fergestad et al., 2006). The latter has not been explored in *Shu* and is an important experiment going forward in this project, although it should be noted that in Fergestad et.al. (2006) no neuropathology was observed in the Sh^{5} eag^{1}

double mutant flies even though it presents the most severe morphological defects and neuronal excitability of the mutants observed in the study. Finally, unlike the Parkinson's disease model mutants *parkin* and *Pink1* whose inability to climb is due to the massive degeneration of the musculature and loss of dopaminergic neuronal clusters (Park et al., 2006), no loss of dopaminergic cell bodies (data not shown) or degenerative muscle tissue has been observed in *Shu* flies.

My initial investigations looking at the jerking and twitching behaviors of *Shu* involved visual scoring of the violent convulsions strong enough to flip the mutant unto its backside (Figure 4B). Although this method was adequate, it became evident that it was too laborious and did not accurately capture the striking differences in *Shu* locomotion compared to *CS* flies. Using the video tracking system, I was able to show that *Shu* locomotion is markedly different when comparing instantaneous velocity, acceleration and turning angles to that of controls (Figure 6). I also found that the total distance *Shu* traveled during the 10 min recording was farther than that observed in *CS,* although it did not reach statistical significance. This correlates well with the increased median velocity observed in *Shu* mutants. It is my belief that this novel technique to track adult fly movement will aid our lab and others in future investigations to answer similar questions in the fly.

The investigation of *Shu* sleep has revealed that this leg-shaking mutant sleeps more during the daytime, yet less at night compared to controls. This is a novel phenotype that is not shared with the other ether-induced leg shaking

mutants previously investigated. As mentioned above, this behavior was also not due to inhibition of locomotor activity by the down-turned wing phenotype as removal of the wings did not alter the abnormal sleep patterns of *Shu* (data not shown). To date all leg-shaking mutants have some sort of defect in ion channel function. Therefore, it is likely that the mutated locus responsible for the *Shu* mutant phenotypes is either a mutated ion channel itself or a gene whose product is necessary for proper maintenance or function of ion channels. This hypothesis has been supported by the results of my experiments that will be described next in Chapter II (see below).

I was able to show using the countercurrent apparatus, general observation and video tracking analysis of the mutant to confirm that lithium improves *Shu* locomotor behaviors (see Figures 4A, B and 10A, B). As extensively covered in the introduction, lithium is thought to elicit its mood-stabilizing effect through inhibition of GSK-3β, IMPase or IPPase. To date, my experiments to try and connect these pathways to lithium's effect on the mutant have yielded only negative results. For instance, ubiquitously reducing mRNA levels of *shaggy (sgg)*, the *Drosophila* homologue of GSK-3β in *Shu* adults using RNAi and the inducible GeneSwitch (GS) GAL4 system (Osterwalder et al., 2001) resulted in no noticeable improvement in any of the mutant's behavioral phenotypes (data not shown). Furthermore, pharmacological experiments using the specific GSK-3β inhibitor AR-A014418 at several concentrations did not mimic the effects of lithium (data not shown). AR-A014418 has been employed in a study looking at tau disease pathology in *Drosophila* larvae. The compound

was shown to reduce tau-induced pathology through inhibition of GSK-3β (Mudher et al., 2004). This effect was also observed in lithium treated larvae. Lastly, introduction of a *sgg* mutant allele into the *Shu* background had no positive influence on the mutant morphology or behaviors (data not shown). Likewise, the generation of *Shu* flies with mutant alleles of *ipp,* the gene encoding for IPPase, showed no apparent epistatic relationship. Attempts to achieve pharmacological inhibition of either IMPase or IPPase were severally hampered by the fact that the only inhibitory compounds available are highly hydrophobic (Atack, 1995). In summary, my data suggests that lithium may be acting independently of either the Wnt signaling pathway or downstream of the inositol second messenger system. However, to prove the compounds tested (i.e. AR-A014418) are working, western blots of down-stream players mediated by GSK-3β, like β-catenin, would need to be examined.

As a whole, I have re-evaluated the *Shu* mutant using more relevant behavioral analyses and found that the mutant displays both morphological and behavioral phenotypes indicative of extreme hyperactivity. When compared with the ether-induced leg-shaking phenotypes, it suggests that *Shu* harbors a robust increase in neuronal excitability. Lithium improves many of the locomotor defects observed in the mutant. However, this improvement is not the result of a general suppression of locomotion caused by a toxic effect of the drug because the ability of *Shu* flies to climb is drastically improved. It remains to be seen whether lithium elicits its effect on *Shu* through one of its previously established signaling pathway targets or through a yet-to-be-determined, novel mechanism.

CHAPTER II

SHUDDERER IS A GAIN-OF-FUNCTION ALLELE OF THE VOLTAGE-GATED SODIUM CHANNEL *PARALYTIC*

Introduction

Structure and function of sodium channels

An action potential is a transient event that causes the electrical membrane potential of a cell to rise and fall in a very stereotyped manner. Voltage-gated sodium channels play an essential role in this process by both initiating and propagating these action potentials in electrically excitable cells such as myocytes, glia and neurons. During an action potential sodium channels imbedded in the plasma membrane open allowing an influx of sodium ions into the cell resulting in a depolarization. This course of action is extended down the length of the axon to the synapse, a small gap between neurons. This depolarization of the "pre-synaptic neuron" causes a release of neurotransmitter-filled vesicles that traverse the synaptic space and bind to their post-synaptic receptors, further resulting in the opening of sodium channels on the "post-synaptic neuron". Thus, sodium channels, together with other ion-permeable channels, are essential for maintenance of the neuronal signal. It is this fundamental process that allows neurons to communicate with one another.

Sodium channels are comprised of a large (~260 kD) transmembrane α subunit formed by four highly homologous domains (I-IV), each consisting of six α-helix transmembrane segments (S1-S6) (Figure 11). The S4 segment of each

homology domain contains highly conserved repeated motifs made up of a positively charged residue followed by two hydrophobic amino acids (Catterall, 2000) that form an α-helix in the shape of a cylinder. These positive residues are held in place through ionic interactions with the surrounding, negatively charged residues and internal transmembrane electrical field. Upon depolarization of the membrane, the S4 segment is released, where it moves outward (toward the extracellular side of the cell membrane) along a spiral path. This conformational change allows an opening to form through which Na^+ influx can occur.

Ion affinity of the sodium channel is achieved by intrasegmental loops between S5 and S6 of every homology domain. These loops extend into the channel and contain the amino acids motifs DEKA and EEDD, which line the outside edge of the pore. Mutagenesis studies of these residues have strongly established them as the necessary components of the selectivity filter domain for sodium ions (Schlief et al., 1996, Sun et al., 1997).

Inactivation of sodium channels occurs in a matter of milliseconds. This inactivation occurs through a "hinged-lid" mechanism mediated by the intracellular loop connecting homology domains III and IV, respectively. An amino acid triplet motif present on the III-IV loop consisting of an isoleucine, phenylalanine and methionine (IFM) has been shown to be absolutely essential for proper inactivation of the channel (West et al., 1992).

Other features of the protein include large N-terminal and C-terminal domains as well as large intracellular loops between domain I and II and another connecting II and III. The large intracellular loop connecting domains I and II

contains many phosphorylation target sites of Protein kinase A (PKA) and PKC, respectively. Phosphorylation by both kinases results in a reduction in sodium current (Dascal and Lotan, 1991, Numann et al., 1991, Li et al., 1992). The intracellular loop between domains II and III contains a conserved motif necessary for sodium channel interactions with Ankryin G (Lemaillet et al., 2003). Ankryin G is an adaptor protein that mediates the attachment of sodium channels to their locations along the extracellular membrane of neurons. These concentrated sodium channel aggregates and their correct localization are essential for proper information processing and transmission in the nervous system (Catterall, 2000). Interestingly, GWAS indicates that ANK3 (encoding Ankyrin G) variants are potential risk factors for bipolar disorder (Ferreira et al., 2008).

Although the α-subunit is sufficient to generate sodium current, the sodium channel auxiliary proteins β1 (36 kDa) and β2 (33k Da) are necessary for the generation of electrophysiological properties similar to those observed *in vivo* (Isom et al., 1992, Schreibmayer et al., 1994, Isom et al., 1995). Besides regulating activation and inactivation of sodium channels, they also play a role in cell-cell adhesion. In particular, the β2 subunit has been shown, together with the α-subunit, to bind to the extracellular matrix proteins tenascin-R and tenascin-C, respectively (Srinivasan et al., 1998). Like Ankryin G, the β-subunits proteins regulate the localization of the sodium channel to areas that require high channel densities for proper neuronal transmission.

Figure 11. Structure of the voltage-gated sodium channel alpha and beta subunits. The 262 kDa α subunit forms the ion permeable pore of the sodium channel. It consists of four homology domains (I-IV), each made up of six transmembrane segments designated S1-S6. Transmembrane segment S4 of each homology domain contains positively charged amino acid (+) residues every third position that acts as a voltage sensor for changes in membrane potential. The selectivity filter is formed by two rings of amino acids located in the intrasegmental loop between S5 and S6 of each homology domain (green circles) that lines the pore of the sodium channel. Fast inactivation of the channel is regulated by the inactivation gate loop connecting homology domains III and IV. The highly conserved ankryin G binding domain is present in the intracellular loop between domains II and III, important for proper localization in neurons. Sodium channel activity is regulated by phosphorylation by PKA (red squares) and PKC (red circles). Several *para* mutations in *Drosophila* have been identified molecularly (grey diamonds). The β subunit (TipE*)* is an accessory protein necessary to generate physiologically correct gating kinetics of sodium channel activation and inactivation. In *Drosophila*, *TipE* is important for expression of *para* in the *Xenopus* heterologous expression system (Warmke et al., 1997). A mutation of a highly conserved methionine residue in the S2 segment of homology domain III is identified in *Shu* mutants (yellow star).

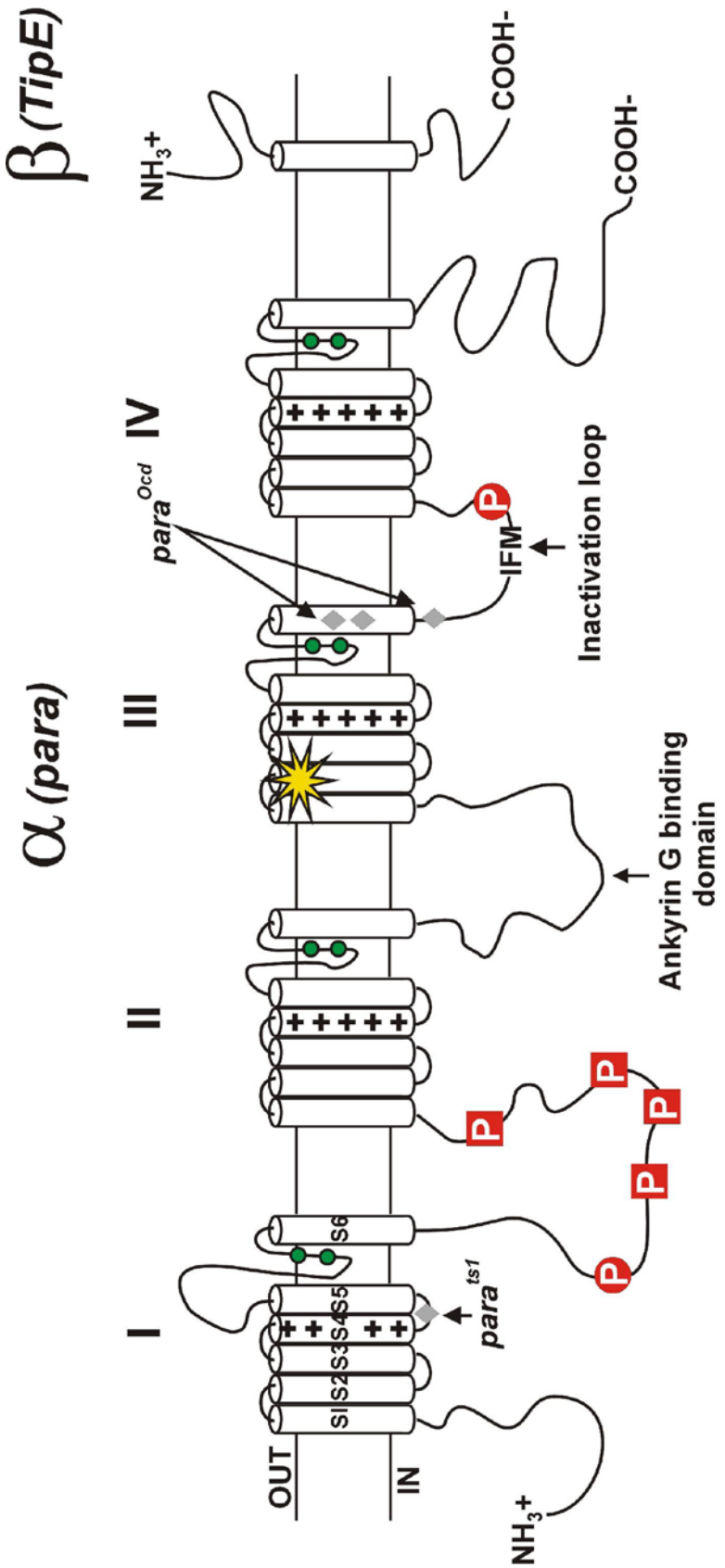
α (para)
β (TipE)
I
II
III
IV
OUT
IN
S1
S2
S3
S4
S5
S6
para ts1
para Ocd
IFM
Inactivation loop
Ankyrin G binding domain
NH3+
COOH-
COOH-
P

Neuronal sodium channels and disease

The mammal genome contains nine individual genes which encode for the sodium channel α-subunit as well as four encoding for the auxiliary β-subunits. Many of these genes are expressed either in the CNS, peripheral nervous system (PNS) or both (George, 2005). Mutations in the sodium channel α-subunit genes *SCN1A* and *SCN2A* and the β-subunit gene *SCN1B* cause a classification of epilepsy syndromes called generalized epilepsy with febrile seizures plus (GEFS+). These disorders are characterized by repeated occurrences of febrile seizures during childhood that can persist beyond six years of age. (Kamiya et al., 2004, Pineda-Trujillo et al., 2005, Scheffer et al., 2007). A more severe epileptic syndrome called severe myoclonic epilepsy of infancy (SMEI) has also been found to be caused by mutations in *SCN1A.*

Over 100 mutations have been identified in the gene *SCN1A*. As one might expect, missense mutations in this gene are mostly associated with the less severe GEFS+ syndromes (Escayg et al., 2000, Abou-Khalil et al., 2001, Wallace et al., 2001). Where as more harmful mutations found in human sodium channel genes (i.e. nonsense or frame- shifts) have been most associated with patients diagnosed with SMEI (Ohmori et al., 2002, Sugawara et al., 2002).

Several other sodium channel α-subunit genes have been implicated in more mild disorders. For instance, mutations in the α-subunit gene *SCN9A* have been linked to patients with peripheral primary erythermylgia, a rare autosomal dominant disorder characterized by episodes of severe pain, redness and warmth in the extremities (Yang et al., 2004). *Sodium channel, voltage-gated,*

type 9, alpha subunit (SCN9A) causes this disorder by affecting both sensory and sympathetic neurons in the PNS. In addition, mutations in *Sodium channel, voltage-gated, type 8, alpha subunit (SCN8A)* in the mouse result in movement disorders which include: tremors, dystonia and ataxia (Meisler et al., 2001). A genetic screen in patients with inherited or sporadic ataxia identified a truncation mutation that may cause a loss of *SCN8A* function, bolstering the evidence from the murine system (Trudeau et al., 2004). Furthermore, *SCN8A* has been associated with BPD patients in the Han Chinese population (Wang et al., 2008) as well as causing sleep abnormalities in mice carrying mutations in this gene (Papale et al., 2010). These data suggest that mutations affecting sodium channel function may play a role in the pathophysiology of several psychiatric and neurological disorders including epileptic syndromes.

Sodium Channels and *Drosophila*

As mentioned above, mammalian genomes contain nine genes that encode sodium channel α-subunit isoforms. These sodium channel genes all have unique expression patterns, developmental timing and gating properties in different cell types and tissues. Furthermore, mammals also have four individual genes that express the sodium channel β1 or β2 subunits, respectively. These combinations allow for the expression of a myriad of channels, each with unique electrophysiological functions in an effort to cater to the needs of the many neuronal subtypes present in the CNS of higher organisms (Catterall, 2000, Goldin et al., 2000, Yu and Catterall, 2003). However, insects appear to only carry a single gene encoding for the large α-subunit. In *Drosophila*, this gene is

annotated as *CG9907* and commonly referred to as *paralytic (para)* due to the phenotypes first identified in mutant alleles of the sodium channel (Fahmy and Fahmy, 1960, Grigliatti and Suzuki, 1970). This α-subunit gene is located on the X-chromosome of the fly, at cytological region 14D. The β-subunits in *Drosophila* are likely encoded by the gene *temperature-induced paralytic E (TipE)* at cytological region 64A10 on the third chromosome, which has been shown to be essential for the appropriate sodium channel expression levels in the heterologous *Xenopus* oocyte system (Feng et al., 1995, Warmke et al., 1997). A number of other genes in the fly genome have been identified which encode proteins harboring structural properties indicative of a sodium channel β-subunit. These genes are likely to encode other *TipE*-like isoforms in the fly, which would aid the organism by increasing the amount of possible α/β combinations with unique functional properties (Derst et al., 2006).

To compensate for the lack of individual sodium channel isoform genes found in mammals, *Drosophila* employs several strategies in an effort to overcome this genomic limitation. First, evidence from several studies using the adult fly and late-stage embryos has provided concrete evidence that the *para* transcript undergoes extensive alternative-splicing (Olson et al., 2008, Lin et al., 2009). In the adult fly 29 distinct splice types were identified, many with unique gating properties. Likewise, in late-stage embryos 27 individual splice types were discovered. Interestingly, only three splice-forms were found to overlap between the two developmental stages, suggesting the presence of at least 53 unique alternatively-spliced isoforms from the same sodium channel gene.

Second, functional diversity of *para* channels is achieved by adenosine (A)-to-inosine (I) editing which alters the code resulting in changes at the amino acid level (Palladino et al., 2000b). These nucleotide changes are mediated by the editase protein Adenosine deaminase acting on RNA (ADAR) (Palladino et al., 2000a). Importantly, A to I editing of sodium channels can alter their electrophysiological properties (Song et al., 2004). Finally, a number of post-translational modifications including sialyl and other types of glycosylation are important for proper sodium channel function and may also generate channels with unique gating kinetics depending on the modifications present on the channel (Loughney et al., 1989, Repnikova et al., 2010).

Many of the mutations identified in the *para* locus to date have been shown to cause temperature-sensitive paralysis such as $para^{ts1}$, $para^{ts115}$, $para^{ST76}$ and display abnormal electrophysiological properties depending on the temperature conditions (Suzuki, 1970, Siddiqi and Benzer, 1976, Wu and Ganetzky, 1980). These alleles are just some of the dozens of *para* alleles discovered which exhibit paralysis after exposure to increased temperatures (30-38^{o}C). Most of these temperature-sensitive mutant alleles are thought to be the result of hypomorphic sodium channel function. Indeed, several of the temperature-sensitive alleles have been shown to be functionally and genetically hypomorphic (Ganetzky, 1984, Stern et al., 1990). Likewise, many other mutant alleles identified are recessive lethal, owing to the essential nature of the *para* gene for *Drosophila* development and survival (Song and Tanouye, 2007). The only dominant *para* mutant allele ever reported in *Drosophila* is *Out-Cold* (Ocd),

which causes cold-induced paralysis and exhibit reduced-sodium currents (Lindsay et al., 2008). Electropysiologically, this mutant displays reduced sodium current, which worsens when exposed to low temperatures. In humans, many mutations have been identified in sodium channel genes (*e.g. SCN1A* and *SCN2A*) that result in increased neuronal excitability. However, to date, no mutations have been identified in the *para* gene that results in an increase in sodium current or increased neuronal excitability.

Here I sought to identify the primary cause (i.e. the mutated gene) responsible for the manifestations of the *Shu* mutant phenotypes. I took advantage of the powerful genetic tools available in *Drosophila* to aid me in my experiments contained in this chapter. My results presented here including extensive classical meiotic mapping of the *Shu* locus, genetic-interaction studies and implementation of the GAL4/UAS-RNAi system all strongly suggest that the *Shu* mutant is a gain-of-function allele of the voltage-gated sodium channel *para.* Furthermore, sequencing of all *para* coding exons in *Shu* has revealed a novel mutation at a highly conserved residue, which points to the likely cause of the *Shu* mutant phenotypes observed in my studies.

Materials and Methods

Fly stocks and culture conditions

Flies were reared at 25°C in a 12 hr light: 12 hr dark cycle, on a conventional cornmeal/glucose/yeast/agar medium supplemented with the mold inhibitor methyl 4-hydroxybenzoate (0.05 %). The RNAi lines w^{1118}; P{*UAS-para-RNAi*} (GD6131) and w^{1118}; P{*UAS-para-RNAi*} (GD6132) and w^{1118} control

(VDRC stock number 60000) were a gift from Dr. Daniel Eberl. The following EY lines used for P-element mapping were obtained from the Bloomington Stock Center, $y^1\ w^{67c23}\ P\{EPgy2\}EY15418$; $y^1\ w^{67c23}\ P\{EPgy2\}Axs^{EY00887}$; $y^1\ w^{67c23}\ P\{EPgy2\}CanA\text{-}14F^{EY08594}$; ($y^1\ w^{67c23}\ P\{EPgy2\}CG9902^{EY05861}$); $y^1\ w^{67c23}\ P\{EPgy2\}Rbp2^{EY00852}$; $y^1\ w^{67c23}\ P\{EPgy2\}CG4239^{EY01983}$ and $y^1\ w^{67c23}\ P\{EPgy2\}eas^{EY01463}$.

Mapping procedure

Meiotic recombination mapping of the *Shu* mutation was conducted using molecularly defined P-element insertion lines essentially as described in (Zhai et al., 2003). First, a *white* (*w*) mutation was introduced into the *Shu* chromosome, which was balanced with *w FM7*. *w Shu*/ *w* FM7 female flies were crossed to males with a P-element insertion at 15B1 ($y^1\ w^{67c23}\ P\{EPgy2\}EY15418$); 15A1, ($y^1\ w^{67c23}\ P\{EPgy2\}Axs^{EY00887}$); 14F1 ($y^1\ w^{67c23}\ P\{EPgy2\}CanA\text{-}14F^{EY08594}$); 14E1 ($y^1\ w^{67c23}\ P\{EPgy2\}CG9902^{EY05861}$); 14C6, ($y^1\ w^{67c23}\ P\{EPgy2\}Rbp2^{EY00852}$), 14C2; ($y^1\ w^{67c23}\ P\{EPgy2\}CG4239^{EY01983}$) and 14B7 ($y^1\ w^{67c23}\ P\{EPgy2\}eas^{EY01463}$). In the F1 generation, virgin female flies trans-heterozygous for *w Shu* and the P-insertion (*w Shu*/*w P*) were crossed to *w* males. In the F2 generation, recombinants were identified as *Shu* mutants with orange eyes (*w Shu P*/*w*) or Shu^+ flies with white eyes (*w*/*w*). The projected molecular position was calculated from the percentages of recombinants and the molecular insertion sites of P-elements in base pairs between each combination of P-element pairs flanking either side of the projected lesion site established from earlier mapping.

Behavioral analyses

Reactive climbing assay

The reactive climbing assay was performed as previously described (Greene et al., 2003) using a countercurrent apparatus that was originally invented for phototaxis behaviors (Benzer, 1967). Briefly virgin female flies of each genotype were collected shortly after eclosion and wings cut with a micro dissecting scissor (LADD Research, Williston, VT) and housed in groups of 20 flies. After being aged appropriately 5 days, groups of 20 flies were placed into one tube (tube #0), tapped to the bottom and allowed 15 sec to climb, at which point the flies that had climbed were transferred to the next tube. This process was repeated a total of 5 times. After the fifth trial, the flies in each tube (#0 ~ #5) were counted. The climbing index (CI) was calculated using the following formula: $CI = \Sigma(Ni \times i)/(5 \times \Sigma Ni)$, where i and Ni represent the tube number (0-5) and the number of flies in the tube, respectively. At least 5 groups were tested for each genotype or treatment unless otherwise noted in the text.

Video-tracking locomotor analysis

Newly eclosed virgin *Shu* and *CS* females were collected and wings cut with a micro dissecting scissor (LADD Research, Williston, VT). Flies were then kept and tested in an environmental chamber at $24.5^{o}C \pm 0.5\ ^{o}C$ and 60-70% humidity. After being aged for 5 days, flies were individually placed into standard mating chambers (15mm diameter X 3mm depth) 8 at a time, using a manual aspirator and allowed to acclimate for 5 min. At the end of 5 min fly behavior was recorded using a web camera (Logicool Quickcam IM, Logitech, Fremont, CA).

The camera was attached with a telephoto lens (HLM35V8E, Honeywell, Morristown, NJ) and was mounted 20 cm above the mating chambers. Images were captured at 15 frames/sec for 10 min and analyzed using pySolo, a multiplatform for the analysis of *Drosophila* sleep (Gilestro and Cirelli 2009) to track fly locomotion and compute x, y coordinates of individual flies during every frame for a total of 9,000 frames. Locomotor parameters were calculated using Microsoft Excel and the following formula =ATAN2 $((X_1-X_2)*(X_3-X_2)+(Y_1-Y_2)*(Y_3-Y_2),(X_1-X_2)*(Y_3-Y_2)-(Y_1-Y_2)*(X_3-X_2))$ for turning angle, arctangent for three consecutive frames resulting in an angle presented in radians. Radians were converted to degrees and the resulting angle was subtracted from 180 degrees to give the outside angle of that the turning flies. For total distance, Pythagoras's theorem was used with the following formula, $=SQRT((X_2-X_1)^2+(Y_2-Y_1)^2)$ and was summed for all 9000 frames. For velocity, $=SQRT((X_2-X_1)^2+(Y_2-Y_1)^2)/(1/15)$. Pixels were converted to millimeters (mm) after calculating distance in pixels with Image J compared to actual mm distance of the mating chambers.

Analysis of ether-induced leg shaking behavior

5 day old flies were introduced into a *Drosophila* etherizer (Science Kit & Boreal Laboratories, Tonawanda, New York). Flies were exposed to a saturated dose of diethyl ether for 10 seconds. A drop of adhesive was then applied to the posterior dorsal thorax of each fly and fixed to a piece of plain white paper in a 35 mm X 10 mm petri dish. Flies were then allowed to recover for 2-3 min before video recording using a Quickcam connect camera (Logitech) mounted on a

Leica MZFLIII stereoscope (Leica Microsystems, Bannockburn, IL). Images were captured at 15 frames/second for 1 min and analyzed using pySolo to generate x,y data. Head movement was tracked by generating a mask (i.e cropping out the rest of the image around the selected area) focusing on the anterior lateral region of the eye and the background. This area was selected based on initial trials indicating it to be the most consistent region to track head movement without picking up antennal motion. In addition, leg movement was tracked by producing a mask selection encompassing the joint between the tibia and tarsus of the hind leg. Special care was taken to only use video where no other appendages or body parts entered the tracking mask during the 1 min recording. As a positive control for diethyl ether effectiveness, *Shu*/+ flies were used in every anesthesia experiment performed. Velocity of both head and leg movements were calculated using Microsoft Excel and the formula =SQRT ((X_2-X_1)^2+(Y_2-Y_1)^2)/(1/15)

Analysis of "wing-down and indented thorax"

Male and female *Shu* mutants were collected shortly after eclosion and scored 24 hr later as either *defective* (i.e. wing down and/or indented thorax) or *normal* (wild-type wing posture/thorax).

DNA sequencing

Genomic DNA was extracted from *Shu/Y* (iso40) and *CS* males. DNA was amplified by Polymerase Chain Reaction (PCR) in a Robocycler® Gradient 40 Temperature Cycler (Stratagene, La Jolla, California) using primer pairs specific for all 31 coding exons of *para.* PCR products were cloned using the

StrataClone™ PCR Cloning Kit (Agilent technologies). Clones positive for the PCR product insert were submitted to the University of Iowa DNA facility for sequencing on either an Applied Biosystems Model 3730 or 3730xl DNA sequencer. Chromatograms were analyzed using FinchTV Version 1.4.0 (Geospiza Inc.). DNA reads were aligned using ClustalW (European Bioinformatics Institute).

Statistical Analysis

For behavioral experiments, statistical comparisons between two groups were performed using a two-tailed Student's t-test assuming unequal variance or for non-normally distributed data the Mann-Whitney *U* test. Statistical significance between multiple groups displaying a normal-distribution was determined using One Way ANOVA with Bonferroni t-test comparisons between control and treatment groups *post hoc.* For those data exhibiting non-normal distributions, Kruskal–Wallis One Way ANOVA on Ranks was performed. Comparisons between groups or groups versus a control were calculated using Dunn's method *post hoc*. Data not conforming to a normal distribution are represented as box plots. Statistical analyses were performed using SigmaStat for Windows Version 3.11 (Systat Software, Inc., Point Richmond, CA).

Results

The *Shu* mutation maps to the gene *CG9907*, encoding the voltage-gated sodium channel gene *paralytic*.

Shu previously mapped at 55.1 with respect to *vermilion* and *forked* loci (Williamson, 1982). The position is on the X chromosome distal to the voltage-gated sodium channel gene *paralytic* (*para*; map position 52.1 corresponding to the cytological region 14D1-14E1) and proximal to the aspartate carbamoyltransferase gene *rudimentary* (*r*; map position 55.3 ~ 55.6 corresponding to the cytological region 14F5-15A1).

To further narrow down the chromosomal position of the *Shu* mutation, I undertook a recombination-based mapping approach involving molecularly defined P-element insertions (Zhai et al., 2003). I first recombined an eye color marker, the *white* mutation (*w*) with *Shu*, and then scored the recombination events between the *Shu* mutation and seven nearby P-element insertions containing the *w*+ minigene. Calculation of the resulting recombination rates revealed that the P-element insertions *EY05861* and *EY00852,* nearest the gene *CG9907* provided the lowest recombination rates, 0.18 and 0.22%, respectively (Table 1). Furthermore, insertions more molecularly distant in either direction from 14E resulted in larger rates of recombination, as expected. Because the molecular distance between the P-element markers were known it was possible to identify the exact nucleotide localization of the potential mutation site between any combination of two P-elements used in our screen

Figure 12. Schematic diagram of predicted mutation sites after meiotic mapping of the *Shu* locus. Pairs of molecularly defined P-element insertions were used to calculate the proposed mutations site. P-element insertion sites indicated by red triangles. Brackets indicate the transgene insertion pairs used to calculate the mutation site equation derived from Zhai *et. al*. Dashed bracket indicates a pairing with *EY15418*, whose insertion site is outside the field of view for this diagram. Red Xs indicate calculations between P-element pairs that resulted in an estimation of the mutation site within the *para* genomic locus, a blue X indicates those combinations that resulted in estimation outside of the *para* genomic locus.

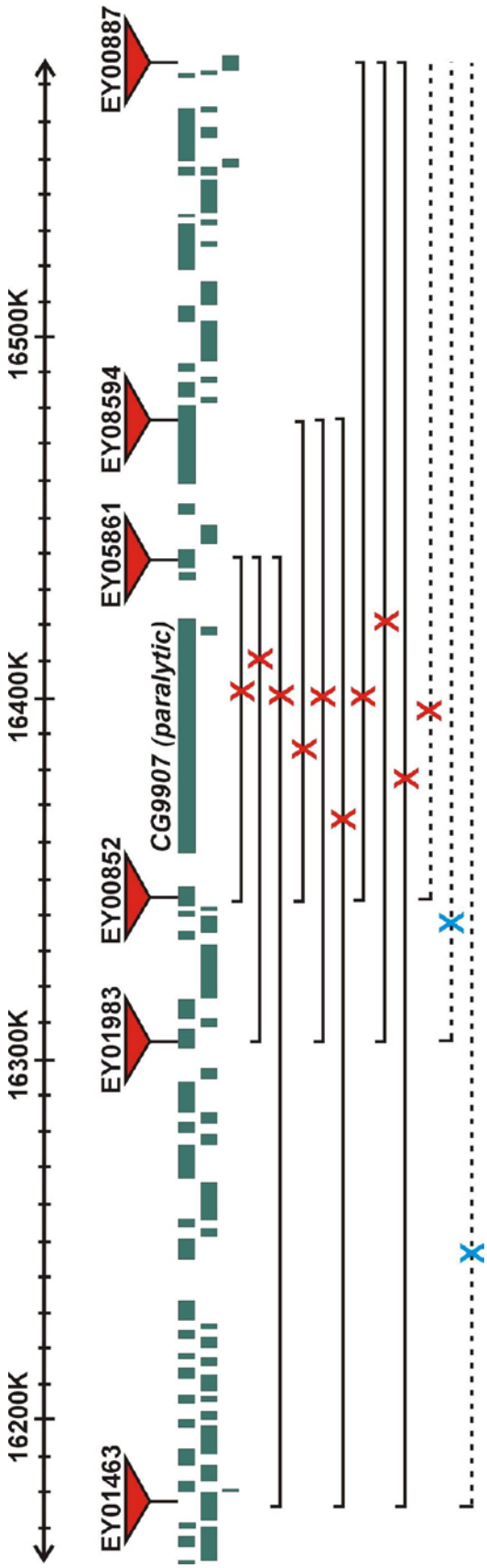
16200K
16300K
16400K
16500K
EY01463
EY01983
EY00852
CG9907 (paralytic)
EY05861
EY08594
EY00887

Table 1. Recombination rates between *Shu* and P-element markers

P-element (inserted in/near)	total flies	parental genotype	recombinant genotype	recombination rate
EY15418 (CG13003)	4214	4007	207	4.91
EY00887 (Axs)	12881	12780	101	0.78
EY0859 (CanA-14F)	6763	6730	33	0.49
EY05861 (CG9902)	6723	6711	12	0.18
paralytic (CG9907)	-	-	-	-
EY00852 (rbp2)	8626	8607	19	0.22
EY01983 (CG4239)	4923	4888	35	0.71
EY01463 (eas)	7866	7798	68	0.86

Figure 13. *Shu* mutant phenotypes are improved when placed in a *para* hypomorphic mutant background. (A) Percentage of 1 day old transheterozygous mutant flies displaying morphological defects (e.g. indented thorax, wings-down or both). The total numbers of observed flies are indicated by parentheses. (B) Climbing ability of 5 day old transheterozygous mutant flies. Data are average ± SEM of 5 groups of 20 flies. $p<0.001$, One Way ANOVA; $^{**}p<0.01$, $^{***}p<0.001$, Bonferroni t-test *post hoc* compared to *Shu.* (C) Turning angle of 5 day old transheterozygous mutant flies. n = 24 flies. $p< 0.001$, Kruskal-Wallis One Way ANOVA, $^{*}p<0.05$, Dunn's method *post hoc* compared to *Shu.* (D) Velocity of 5 day old transheterozygous mutant flies. n = 24 flies. $p<0.001$, Kruskal-Wallis One Way ANOVA; $^{*}p<0.05$, Dunn's method *post hoc* compared to *Shu.* (E) Velocity of ether-induced head movement in transheterozygous mutant flies. $p = 0.049$, Kruskal-Wallis One Way ANOVA. (F) Velocity of either-induced hind leg movement in transheterozygous mutant flies. For E and F, *Shu*; *n* = 10, *Shu/para*^{ST76}; *n* = 13, *Shu/para*^{ts1}; *n* =12, *Shu/*^{parats115}; n =14.

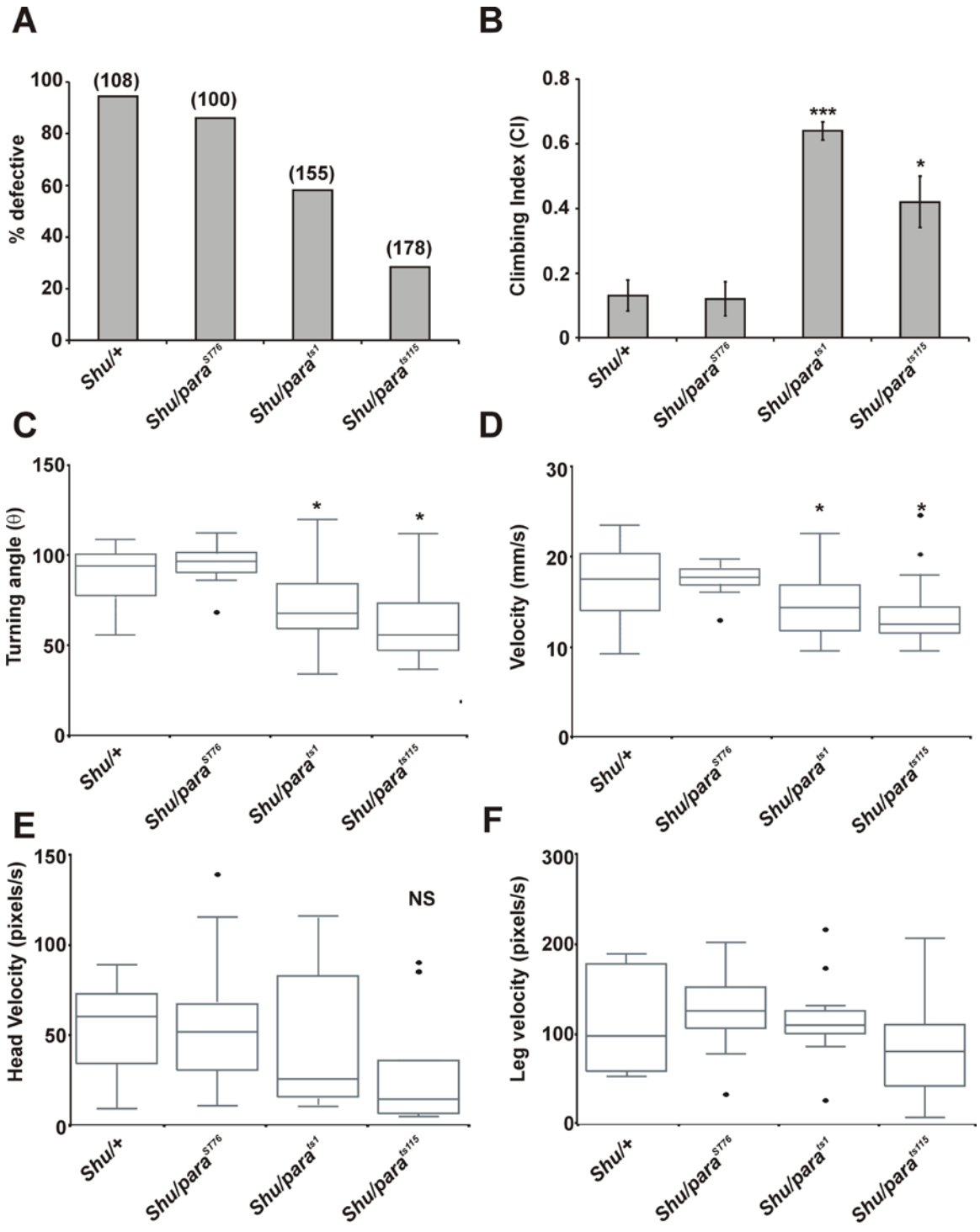
A
% defective
(108)
(100)
(155)
(178)
Shu/+
Shu/para ST76
Shu/para ts1
Shu/para ts115
B
Climbing Index (CI)
***
*
C
Turning angle (θ)
D
Velocity (mm/s)
E
Head Velocity (pixels/s)
NS
F
Leg velocity (pixels/s)

(see methods). With the exception of the transgene *EY15418*, all combinations pairing one insertion distal and one proximal to cytological region 14E resulted in an estimated nucleotide location for the mutation residing in the 64 kb *CG9907* locus (Figure 12). Therefore, our mapping results strongly indicate that the *Shu* mutation must lie in the *CG9907* locus, encoding for the voltage-gated sodium channel *para.*

Shu behavioral and morphological defects are suppressed when in a transheterozygous combination with *para* hypomorphic alleles

To examine the effects of *para* mutations on the phenotypes of *Shu,* the neurological mutant was crossed to three hypomorphic alleles of *para, para*^{ts1}, *para*^{ts115} and *para*^{ST76} (Siddiqi and Benzer, 1976, Ganetzky, 1984*).* All three alleles have been shown previously to be semi-lethal when heterozygous over deletions and inversions that uncover *para* (Ganetzky, 1984). I found similar results as those originally reported by Ganetzky (data not shown). I hypothesized that if *Shu* were a hypomorphic or loss-of-function allele of *para* I would see a reduction in the survival or worsening of its phenotypes in the resulting *Shu para* hypomorphic heteroallelic flies. In contrast, if *Shu* was a hypermorph or gain-of-function allele of *para,* introduction of a poorly functioning *para* sodium channel gene into the lithium-responsive mutant background should improve its morphological and behavioral defects. In agreement with the latter scenario, I found that flies transheterozygous for *Shu* and the hypomorphic alleles showed a decrease in the morphological defects characteristic of *Shu*

females (Figure 13A). Furthermore, the heteroallelic flies not only exhibited improved ability to climb, but a significant reduction in the angle of direction change, indicative of a suppression of mutant behavior (Figures 13B, C). Examination of ether-induced leg-shaking behavior in the transheterozygotes showed only a mild reduction in the velocity of hind leg shaking in *Shu/para*^{ts1} and *Shu/para*^{ts115} mutants, albeit not statistically significant when compared to the mutant alone (Figure 13F). As seen in the other behavioral experiments performed, *Shu/para*^{ST76} flies were indistinguishable with the mutant alone and in some cases worse. However, a significant improvement was observed in ether-induced head movement in *Shu/para*^{ts115} transheterozygotes (Figure 13E). Overall, these data support the mapping findings that *Shu* is likely an allele of *para*. The fact that many of the mutant phenotypes are improved in combination with two of the three *para* hypomorphic alleles tested, suggests that the *Shu* mutant is likely a gain-of-function allele of the voltage-gated sodium channel gene.

RNAi knockdown of *para* transcripts in neurons rescues the *Shu* mutant phenotypes

I investigated further the possibility that the *Shu* mutant may be a gain-of-function allele by employing a GAL4/UAS-RNAi system to knockdown *para* transcript levels in the flies. I crossed two different *UAS-RNAi* lines (GD6131, GD6132, VDRC) carrying a construct targeting the *para* mRNA to *Shu elav-GAL4* to knockdown *para* mRNA levels pan-neuronally. Both *UAS-para-RNAi* lines were found to completely abolish the morphological defects in *Shu* mutant

females and drastically improve phenotypes in *Shu* males, which display a much more severe behavioral and morphological phenotype than females (Figure 14A). I next tested the behavior of *Shu* mutants subjected to *para* RNAi knockdown (KD) and found that their climbing ability (Figure 14B), median turning angle (Figure 14C), median velocity (Figure 14D) as well as the tracking traces (Figure 14G) were significantly improved to near wild-type levels compared to transgenic controls. An investigation of ether-induced leg-shaking behavior revealed that, unlike the *Shu* hypomorphic *para* allelic combinations, both the leg-shaking and head-shaking of *Shu* transgenic RNAi rescues were dramatically suppressed (Figure 14E, F). Expression of the *UAS-para-RNAi* in other tissues, such as muscle (Myosin-heavy-chain-GAL4) or in glial cells (repo-GAL4) showed no improvement in any aspects of the mutant defects examined (data not shown). These data, combined with the allelic experiments confirm that *Shu* must be a gain-of-function allele of *para*, somehow causing increased neuronal activity.

Shu mutants carry a missense mutation in a highly conserved region of *para*

To determine if any potential mutation(s) were present in the *para* locus of the fully isogenized *Shu* mutant, all coding regions were sequenced. I found a novel G to A transition mutation in exon 24 resulting in the substitution of a methionine for isoleucine at the amino acid M1350 of *para (para*-RA, flybase*)* (Figure 15A). To validate that this mutation was not introduced during my extensive backcrossing, I sequenced and identified the same M1350I mutation in the original *Shu/FM6* line I had obtained from Dr. Williamson (data not shown).

An amino acid alignment of Para with its homolog *Sodium channel, voltage-gated, type 2, alpha subunit* (*SCN3A*) from other species demonstrated that the mutated methionine is highly conserved from invertebrates to humans likely owing to its importance in sodium channel function (Figure 15B). The M1350I mutation lies in the transmembrane segment S2 in homology domain III of the sodium channel (Figure 11, yellow star). In addition, a tri-nucleotide insertion in the C-terminal domain of *para* was identified in *Shu*. This GGC insertion results in the addition of an extra alanine residue in a 14 amino acid segment of alanines. This region of the sodium channel protein was not evolutionarily conserved in organisms. Furthermore, it is not even conserved in closely related *Drosophila* species (data not shown). This finding suggests that the addition of an extra alanine in this C-terminus region is not likely to have a deleterious effect on the fly.

Discussion

In this study I employed a straight-forward recombination based mapping strategy to aid in the identification of the *Shu* mutation. Using this technique I screened over 50,000 flies for recombination events between the eye color markers and the dominant, fully penetrant *Shu* phenotypes. Subsequent genetic experiments using *para* hypomorphic alleles and RNAi knockdown of *para* in the *Shu* mutant background strongly indicates the *Shu* is a gain-of-function allele of the voltage-gated sodium channel *para.* Furthermore, a novel mutation resulting in a methionine to isoleucine change in the S2 transmembrane segment of homology domain III has been identified as the likely lesion that alters sodium

Figure 14. RNAi Knockdown of *para* in neurons rescues all aspects of the *Shu* mutant phenotypes. (A) Percentage of 1 day old mutant flies displaying morphological defects (e.g. indented thorax, wings-down or both. Number of flies scored indicated in parentheses (first value, females; second value, males). Line 1 (*UAS-para-RNAi* GD6132, VDRC), Line 2 (*UAS-para-RNAi* GD6131, VDRC). (B) Reactive climbing of 5 day old mutant flies. Data are average CI ± SEM of ≥ 5 groups of 20 flies per genotype tested. $p<0.001$, One Way ANOVA; ***$p<0.001$, Bonferroni t-test *post hoc.* (C) Median turning angle of 5 day old flies. $p<0.001$, Kruskal-Wallis One Way ANOVA on Ranks; *$p<0.05$, Dunn's method *post hoc*. (D) Median velocity of 5 day old mutant flies. n = 24 flies per genotype. $p<0.001$, Kruskal-Wallis One Way ANOVA on Ranks; *$p<0.05$, Dunn's method *post hoc.* (E) Median velocity of ether-induced head movement in mutant flies. n =10 flies. $p<0.001$, Kruskal-Wallis One Way ANOVA on Ranks; *$p<0.05$, Dunn's method *post hoc*. (F) Median velocity of either-induced hind leg movement in transheterozygous mutant flies. n = 10 flies. $p = 0.015$, Kruskal-Wallis One Way ANOVA on Ranks; *$p<0.05$, Dunn's method *post hoc.* (G) Representative 1 min traces of mutant locomotion.

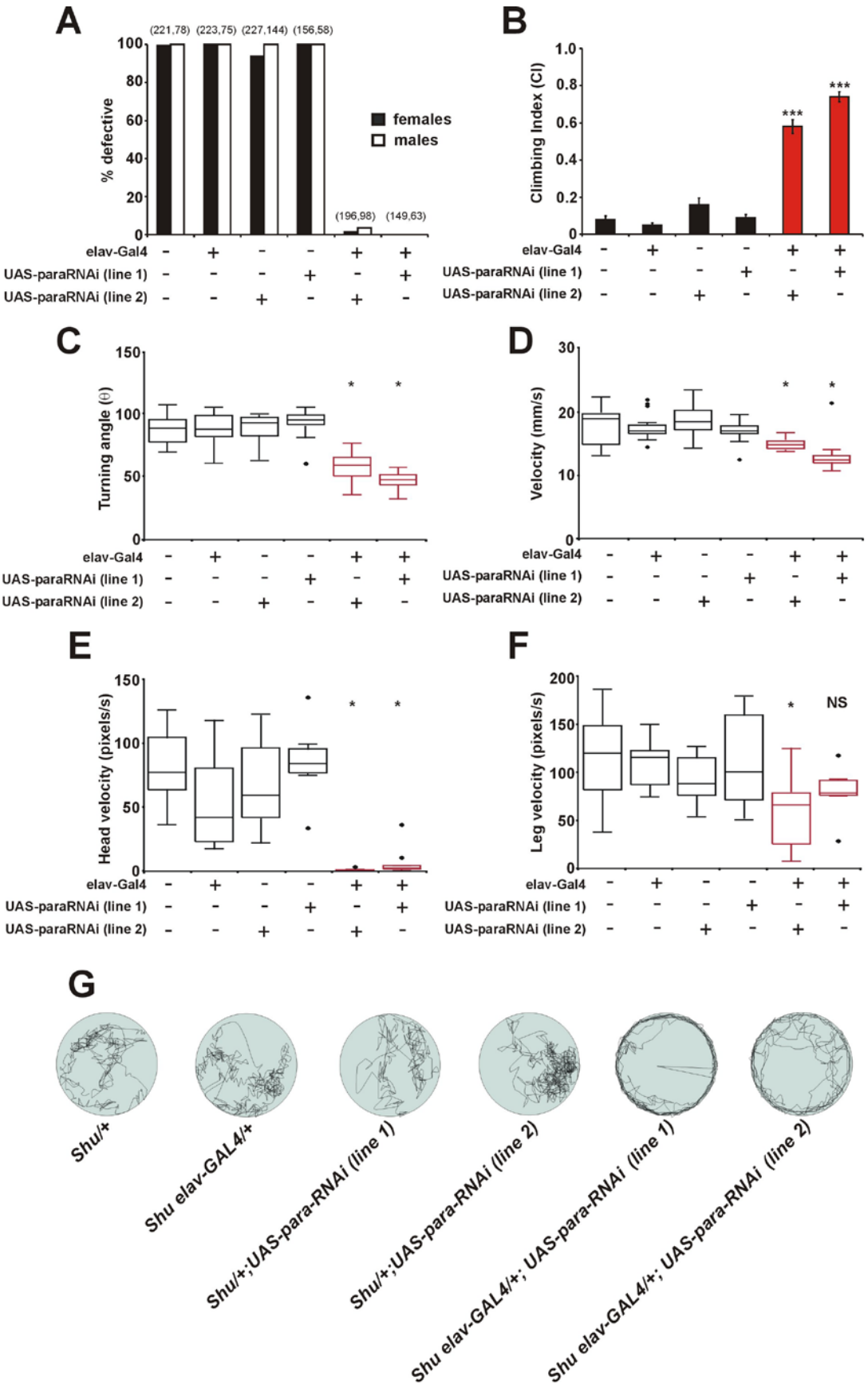
A
(221,78) (223,75) (227,144) (156,58)
(196,98) (149,63)
% defective
females
males
elav-Gal4
UAS-paraRNAi (line 1)
UAS-paraRNAi (line 2)
B
Climbing Index (CI)
***
***
C
Turning angle (θ)
D
Velocity (mm/s)
E
Head velocity (pixels/s)
F
Leg velocity (pixels/s)
NS
G
Shu/+
Shu elav-GAL4/+
Shu/+;UAS-para-RNAi (line 1)
Shu/+;UAS-para-RNAi (line 2)
Shu elav-GAL4/+; UAS-para-RNAi (line 1)
Shu elav-GAL4/+; UAS-para-RNAi (line 2)

Figure 15. Identification of a novel mutation in a highly conserved residue in *Shu* mutants. (A) DNA sequencing chromatogram identifying a G to A transition mutation at nucleotide position 4,050 according to the *paraRA* cDNA transcript. This mutation results in a methionine to isoleucine at M1350I. (B) Protein alignment of Para with the neuronal sodium channel SCN3A in other species.

A

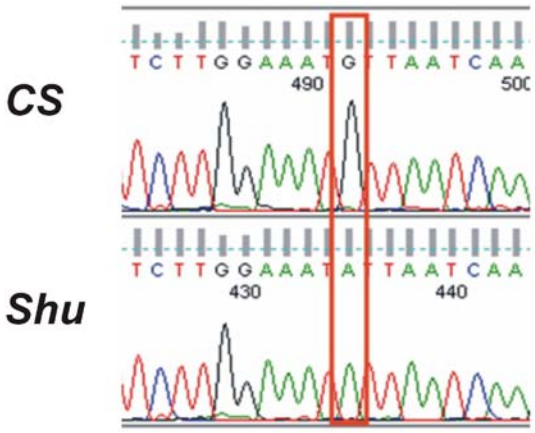

B

Human SCN3A	1217	LLSSGALAFEDIYIEQRKTIKTMLEYADKVFTYIFILEMLLKWVAYGFQT	1266
Chimpanzee SCN3A	1228	LLSSGALAFEDIYIEQRKTIKTMLEYADKVFTYIFILEMLLKWVAYGFQT	1277
Dog SCN3A	1167	LLSSGALAFEDIYIEQRKTIKTMLEYADKVFTYIFILEMLLKWVAYGFQT	1216
Cow SCN3A	1216	LLSSGALAFEDIYIEQRKTIKTMLEYADKVFTYIFILEMLLKWVAYGFQT	1265
Mouse Scn3a	1229	LLSSGALAFEDIYIEQRKTIKTMLEYADKVFTYIFILEMLLKWVAYGFQT	1278
Rat Scn3a	1168	LLSSGALAFEDIYIEQRKTIKTMLEYADKVFTYIFILEMLLKWVAYGFQT	1217
Drosophila para	1312	LMSSLALALEDVHLPQRPILQDILYYMDRIFTVIFFLEMLIKWLALGFKV	1361
Mosquito NaCh	1266	LLSSLALALEDVHLPQRPILQDILYYMDRIFTVIFFLEMLIKWLALGFKV	1315

channel function in the mutant. My mapping of the *Shu* mutation was carried out using a well-established P-element mapping scheme used to successfully map several other mutations in *Drosophila* (Zhai et al., 2003, Lindsay et al., 2008). Utilizing calculations adapted from Zhai *et al.,* every combination of flanking P-element markers tested, with the exception of *EY15418*, resulted in an estimated nucleotide position of the mutation inside of the *para* genomic locus. The transgene *EY15418* is inserted just 3' of *CG13003,* located 349 kb distal of *para.*

In contrast, the second furthest P-element from *para, EY01463* resulted in a recombination rate of 0.86%. *EY01463* is only 217 kb from the center of the *para* locus*.* If one divides the molecular distance of *EY15418* by that of *EY01463*, the difference is a 1.6 fold increase in distance. Thus one would estimate that the recombination rate of *EY15418* should be ~1.38%. However, the actually recombination rate for *EY15418* is 3.5 fold higher.

One explanation is that this particular genomic location maybe a region of increased meiotic recombination. It is well established in other organisms from human to yeast that particular genomic regions coined "hotspots" exhibit large increases in recombination frequency compared with the surrounding genomic landscape (Steinmetz et al., 1986, Grimm et al., 1989, Farah et al., 2002, Yao et al., 2002). However, obvious evidence for such regions in *Drosophila* have been absent, although it is known that certain areas in the genome do exhibit different levels of recombination (Begun and Aquadro, 1992). Another possibility is that the P-element transgenic insertion *EY15418* is not annotated to the correct molecularly-defined position on the chromosome. Testing for this possibility

could be achieved using the well-established technique, inverse PCR using primers specific to this particular transgenic construct. Nevertheless, 10 of the 12 calculations made between flanking P-element pairs resulted in an estimated location of the mutation within *para.*

To test that *Shu* maybe a mutant allele of the voltage-gated sodium channel I combined the mutant with three different hypomorphic *para* alleles, $para^{ST76}$, $para^{ts1}$ and $para^{ts115}$ (Suzuki, 1970, Siddiqi and Benzer, 1976). As previously reported, I found that all mutants became paralyzed at their particular restrictive temperatures (data not shown). Likewise, when I placed these hypomorphic mutants in combination with a *para* recessive lethal allele, there was a stark reduction in the number of heteroallelic female progeny eclosing (data not shown). As previously reported, this indicates that even at permissive temperatures (i.e. <25^{o}C), these temperature-sensitive *para* alleles show hypomorphic function (Ganetzky, 1984).

I found that the many aspects of the *Shu* mutant defects were significantly improved when placed in combination with either $para^{ts1}$ or $para^{ts115}$ (Figure 13). Morphological defects in these two transheterozyous mutant flies were reduced, reactive climbing ability was improved and the turning angle and velocity were reduced compared to *Shu* alone. Though, a significant reduction in the velocity of leg-shaking and head movements upon recovery from ether anesthesia was only observed in *Shu/*$para^{ts115}$ mutants. This finding is reasonable when one considers that these flies exhibited the strongest reduction in morphological defects and decreases in locomotor parameters analyzed using the video

tracking systems. Interestingly, the heteroallelic combination of *Shu* with *para*^{ST76} did not rescue any of the morphological or behavioral phenotypes of the lithium-responsive mutant. In fact, a closer examination of ether-induced leg-shaking behaviors and video tracking locomotor analysis of this mutant combination, indicated that it may actually make the behavioral phenotypes of *Shu* slightly more severe (Figure 13C, D, F).

A careful interpretation of the above results are challenging due to the fact that the exact molecular lesions in *para*^{ST76} *and para*^{ts115} have not been identified. However, a study looking at *para*^{ts1} *and para*^{ST76} neurons from embryonic cultures using electrophysiological techniques showed that only 2% of neurons from *para*^{ST76} embryos expressed a detectable sodium current compared to ~50% for *para*^{ts1} (O'Dowd et al., 1989). This finding may help explain the lack of improvement observed in *Shu/para*^{ST76} flies. If little or no sodium current is produced from the *para*^{ST76} derived sodium channels, then the only functional channels would be those coming from the *Shu para* locus. Much like the situation found in *Shu*/Y males who only carry the *Shu* gain-of-function allele, *Shu/para*^{ST76} mutants would show more severe defects because a larger percentage of the sodium channels expressed would exhibit increased activity. This is exactly what I have observed. Whereas, in *Shu/para*^{ts115} *and Shu/para*^{ts1} a balance between sodium channels with increased sodium current and those with reduced sodium current may result in a net effect of the final neuronal output along the neuronal membrane and at the synapse. However, the relatively good health of the *para*^{ST76} homozygous mutant flies argues against the observation of

a very low percentage of neurons exhibiting sodium channel current in embryonic cultures and complicates the net output model proposed above.

Next, I found that knockdown of *para* transcript levels in *Shu* neurons using the GAL4/UAS system, drastically improved all behavioral and morphological defects observed in the mutant (Figure 14). Importantly, I could also rescue the phenotypes in *Shu* males, who show a much more severe phenotype than females due to the fact that *Shu* is located on the X chromosome and *Shu* males are therefore hemizygous for the *Shu para* locus. It is important to note that a third *UAS-para-RNAi* line (KK104775) was found to be lethal when driven using the pan-neuronal driver *elav* in wild-type flies, indicating a strong reduction in sodium channel expression sufficient to cause lethality (data not shown). In contrast, wild-type flies expressing either GD6131 or GD6132 exhibited delayed eclosion and some lethargy as adults, but otherwise appeared healthy. Examination of *para* transcripts in these flies using qRT-PCR would help to validate these observations. Therefore, the *UAS-para-RNAi* lines GD6131 and GD6132 used in this study likely cause a more mild reduction in *para* levels, causing a similar effect as seen in the transheterozygous *Shu para* temperature-sensitive flies.

Sequencing of all the protein-encoding exons of *para* revealed a G to A transition mutation in exon 24 of the sodium channel α subunit gene. This mutation results in a missense mutation of a conserved methionine to an isoleucine in the S2 transmembrane segment of homology domain III. The potential of this M1350I missense mutation to be deleterious to proper sodium

channel function is strengthened by several lines of evidence. First, this M1350I mutation is at a residue found to be conserved throughout evolution (Figure 15B) and is present in all nine single sodium channel α subunit genes in humans (data not shown). Second, many of the lesions which cause epileptic syndromes like GEFS and SMEI in humans have been found to be concentrated in the transmembrane segments of the protein (Meisler and Kearney, 2005). Lastly, a recent study has shown that oxidation of conserved methionine residues in the α subunit sodium channel protein Nav1.4 resulted in an inhibition of channel inactivation (Kassmann et al., 2008). These data suggest that the M1350I mutation may mimic methionine oxidation and inhibit inactivation, resulting in the increased neuronal excitability observed in *Shu.*

Overall, the data presented in this chapter strongly indicates that the lithium-responsive neurological defects in *Shu* are caused by a gain-of-function mutation in the voltage-gated sodium channel *para*. To best of my knowledge, this is the first sodium channel mutation identified in *Drosophila* which results in increased sodium channel activity. It will be interesting to perform functional studies of this mutated sodium channel to determine the exact electrophysiological properties which are responsible for increased *para* function in the *Shu* mutant.

CHAPTER III

IDENTIFICATION OF GENES FUNCTIONALLY INTERACTING WITH *SHUDDERER*

Introduction

Microarray analyses and lithium

The effect of the mood-stabilizing ion lithium, on gene expression has been extensively studied in humans, mammals and cell culture (Brandish et al., 2005, McQuillin et al., 2007, Seelan et al., 2008, Fatemi et al., 2009). However, as is often the case with microarray expression studies, data between studies has not yielded consistent results, diminishing the validity of the target genes identified.

Drosophila offers a couple of advantages that make it ideal for performing gene expression profiling. First, its quick generation times allows for the ability to extensively backcross flies to isogenize their genomes. Thus, a comparison between different strains, mutants or environmental conditions allows for data not significantly affected by variability in genetic background. Second, mRNAs can be extracted from large sample sizes using hundreds or thousands of flies, reducing problems in variability that may become problematic using vertebrate model organisms due to limited access to an adequate number of biological samples.

Given the advantages that *Drosophila* can provide, I performed gene expression analyses on *Shu* and *CS* after 24 hr of treatment with either standard fly food or food containing 50 mM LiCl. Total RNA was isolated from the heads

of the flies and subjected to microarray analysis consisting of three biological replicates for each genotype using Affymetrix GeneChip® *Drosophila* Genome 2.0 Arrays. Each chip is composed of 18,800 probe sets representing over 18,500 transcripts. The three replicates showed high correlation coefficients ($R>0.93$), indicating that the experimental data were sufficiently reproducible.

To the best of my knowledge, this is the first known gene expression profiling ever performed on *Drosophila* flies after treatment with mood-stabilizing compounds. In addition, many homologues of genes implicated in human disease are present in the fly genome, making this sort of gene expression analysis a worthwhile endeavor (Fortini et al., 2000). Therefore, it is likely that the results presented here and those already published (Kasuya et al., 2009a) will aid in the identification of novel targets of lithium action in the vertebrate system.

Drosophila genetic screens

For over a century, *Drosophila* has been at the forefront of biomedical research from its humble beginnings in the lab of Morgan (Allen, 1978), through sequencing of its entire genome, to the ability to control gene expression both spatially and temporally in the fly. However, its most important attribute as a model organism has been its ability to be utilized as an agent for the identification of mutations causing preselected phenotypes, by way of unbiased forward genetic screening. Early on, many genetic screens were performed using the mutagen ethyl methanesulfonate (EMS) to generate point mutations. Although this method has been valuable, the identification of the point mutation(s)

responsible for the mutant phenotypes can prove difficult and laborious. Another commonly used screening strategy, involves the use of P-element transposons as mutagens, which insert themselves at random throughout the genome. One advantage of this method is that it allows for easier identification of mutated genes using inverse PCR. However, P-element transposon mutations are usually not nulls, as many prefer to insert in non-coding up-stream regions of genes (Kelley et al., 1987). As a result, these insertion mutations are often hypomorphic or have no effects altogether. Therefore, it can be difficult to identify mutated genes which require a severe reduction or alteration in function to observe a phenotype. An alternative screening solution to those mentioned above, called a deficiency screen, can be employed to quickly survey the entire genome looking for genomic regions containing genes functionally interacting with a particular mutant of interest.

A deficiency is a genomic deletion that can cover anywhere from tens of thousands of bases up to several mega bases in length. Over several decades, the collection of deficiencies now available to the fly community now covers more the >92% of the genome (Ryder et al., 2007). Using these large deficiencies, one can quickly screen through the entire genome using a relatively small amount of fly lines, looking for genes that functionally interact with a mutant of interest. The premise for this screen is that if a gene interacts with the mutant examined, than reduction in that gene's expression by 50% will either enhance or suppress the mutant of interest's phenotype, revealing their interaction. Owing the effectiveness and relevance of using deficiencies with regards to genetic

screening, many labs have recently employed deficiency screens to identify genes interacting with their gene of interest (Jattani et al., 2009, Shao et al., 2010, Wright et al., 2010).

In this chapter, I sought to identify novel genes functionally interacting with the gain-of-function sodium channel mutant, *Shu*. Gene expression arrays using mRNA from both *CS* and *Shu* female flies with and without lithium treatment revealed that the calcineurin α-subunit gene, *CanA-14F* and several antimicrobial peptide genes were significantly up-regulated in the mutant. Furthermore, the increased expression levels of these antimicrobial peptide genes were attenuated by administration of a diet containing lithium. Lastly, a rigorous deficiency screen covering most of the autosomes in *Shu* resulted in the identification of cytological region 53D-F on the second chromosome as a region containing a gene or genes that strongly suppresse the *Shu* phenotypes. Subsequent RNAi knockdown of genes in this region revealed that a reduction in the expression level of the glutathione S transferase gene, *GstS1,* significantly improved the *Shu* phenotypes.

Materials and Methods

Fly stocks and culture conditions

Flies were reared at 25°C in a 12 hr light: 12 hr dark cycle, on a conventional cornmeal/glucose/yeast/agar medium supplemented with the mold inhibitor methyl 4-hydroxybenzoate (0.05 %). *UAS-nla*^{t1} and *UAS-nla*^{t2} were kindly provided by Dr. Kyung-Tai Min (Indiana University). The P-element lines *y*^{1} *w*^{67c23} *P{EPgy2}EY09066* and *y** *w** *P{GawB}NP6106 / FM7c* were obtained

from Bloomington Stock Center. The following RNAi lines were obtained from the Vienna Drosophila RNAi Center (VDRC), *UAS-CG8950-RNAi (GD36069), UAS-CG8964-RNAi (KK103485), UAS-CG30460-RNAi (KK105307), UAS-CG6967-RNAi (KK105899), UAS-CG6984-RNAi (KK110411), UAS-CG9850-RNAi (GD46582)* and *UAS-GstS1-RNAi (GD16335).* All Deficiency stocks for the second and third chromosomes for the suppressor screen were obtained from the Bloomington Stock Center

Reactive climbing assay

The reactive climbing assay was performed essentially as previously described (Greene et al., 2003) using a countercurrent apparatus that was originally invented by (Benzer, 1967). Briefly, groups of 20 flies were placed into one tube (tube #0), tapped to the bottom and allowed 15 sec to climb, at which point the flies that had climbed were transferred to the next tube. This process was repeated a total of 5 times. After the fifth trial, the flies in each tube (#0 ~ #5) were counted. The climbing index (CI) was calculated using the following formula: $CI = \Sigma(Ni \times i)/(5 \times \Sigma Ni)$, where i and Ni represent the tube number (0-5) and the number of flies in the tube, respectively. At least 5 groups were tested for each genotype or treatment.

Analysis of "wing-down and indented thorax"

Male and female collected shortly after eclosion and scored 24 hr later as either *defective* (i.e. wing down and/or indented thorax) or *normal* (wild-type wing posture/thorax).

Microarray and RT-PCR analyses

One day-old CS females were kept in a vial containing the regular cornmeal-based food with or without 50mM LiCl for 24 hr. Their heads were cut on dry ice block and stored at -80°C until use. Total RNA was extracted from 75~100 fly heads using the TRIzol Reagent (Invitrogen, Carlsbad, CA) followed by an RNeasy (Qiagen, Valencia, CA) cleanup step and DNase I digestion. The RNA was resuspended in DEPC-treated water and subjected to microarray analysis. Three independent RNA samples were prepared and analyzed for each treatment group. Microarray experiments were carried out at the Translational Genomics Research Institute (Phoenix, Arizona) using the Affymetrix *Drosophila* Genome 2.0 Arrays (Affymetrix, Santa Clara, CA). Image data were quantified by using the genechip-operating software Affymetrix GCOS v1.4. Gene expression data were analyzed using GeneSpring software. The comparisons were made between signals for CS and *Shu*/+ with or without lithium treatment using Welch's t-test. Three independent samples were prepared for each genotype.

For semi-quantitative RT-PCR, RNA was extracted using the same methods as described above and single-strand cDNA libraries were synthesized with DNase I-treated RNA using Superscript III reverse transcriptase kit (Invitrogen, Carlsbad, CA). 5'-TTCGCTAAGCAGTAGCTGCGAC-3' and 5'-GTTAACACGCAGGCGACGGAA-3' for *rp49* as a control. Transcript levels were quantified by running the PCR products on an agarose gel and analyzing the pixel intensity of the bands using Image J software (NIH).

Quantitative real-time polymerase chain reactions (qPCR) were performed using the TaqMan MicroRNA Assay kit with primers specific to *CanA-14F* (Dm02542296_s1)(Applied Biosystems Inc., Foster City, CA, USA)) following the manufacturer's instructions. Each qPCR assay was conducted in triplicate using cDNA derived from 10 ng total RNA from a biological replicate. Differences in the expression level of *CanA-14F* in different genotypes were calculated using the ΔΔCt method (Livak and Schmittgen, 2001). Samples were normalized using the *ribosomal protein 49 (rp49)* RNA as an endogenous control (Dm02151827_g1). Dilution curves were generated for both the *CanA-14F* and *rp49* primer sets to ensure the amplification efficiencies for both were similar to allow for an accurate comparison using the ΔΔCt method.

Whole-mount RNA *in situ* hybridization

Both adult and larval brains were dissected in PBS and tissues were fixed with 4% paraformaldehyde in PBS for 30 min at room temperature. Samples were washed three times in PBS containing 0.3% Tween 20 and then incubated in hybridization buffer (5X SSC, 50% formamide, 150mM Tris-HCl pH 7.5, 1.5mM EDTA) for 2 hr at 50^{o}C. Samples were then incubated in hybridization buffer containing 0.1 µg/ml sense or antisense RNA probe overnight at 52^{o}C. The brains were washed two times using wash buffer (1X SSC, 50% formamide, 10mM Tris-HCl pH 7.5, 50mM EDTA) for 1 hr at 52^{o}C. Signals were detected immunohistochemically with anti-digoxigenin antibodies conjugated with alkaline phosphatase (Roche, Nutley, NJ) using NBT/BCIP (Roche, Nutley, NJ) as substrates. Digoxigenin-labeled RNA probes for *CanA-14F* were generated

using the MAXIscript SP6/T7 in vitro transcription kit (Applied Biosystems, Carlsbad, CA) according to the manufacturer instructions. The primers, 5CCG9819F; 5'-GGAGGAGGGCCAGAAATCACTGT-3' and 3CCG9819R; 5'-CTGGACCAACCGGATCCCTAGA-3' were used to generate a *CanA-14F* specific DNA template (based on Affimetrix probe set) for Digoxigenein (DIG)-labeling reactions.

Deficiency screen for suppressors of *Shudderer*

Shu/FM7 females were crossed to males harboring deficiency chromosomes covering the second and third chromosomes. The resulting F1 *Shu/+; Df(2)/+ or Shu/+; Df(3)/+* females were scored using two separate parameters. The first parameter involved scoring the females for any morphological defects. Flies were considered to be defective if they exhibited: down-turned wings, an indentation of the dorsal thorax, or both. The second parameter for screening involved subjecting the *Shu/+; Df/+* females to a reactive climbing assay as described in Materials and Methods. Those genomic deletions that resulted in a suppression of morphological defects, improvement in climbing ability or both, were re-crossed to *Shu/FM7* to confirm the initial findings. Once established as a potential suppressor region, smaller, molecularly-defined deficiencies covering the original genomic regions were obtained from the Bloomington Stock Center and were again screened for morphological defects and climbing ability. When the region of interest was reduced to a manageable size, RNAi lines were obtained from the Vienna *Drosophila* RNAi Center, specific for genes in the suppressor region.

Statistical analysis

The gene expression data were analyzed using GeneSpring software. The comparisons were made between two genotypes. Lists were filtered for the genes that were present in all three independent samples of at least one of the two genotypes. Genes that had a fold change > 2 with *P*-value < 0.05 (Welch t-test) were discussed in this study. For behavioral experiments, statistical comparisons between two groups were performed using a two-tailed Student's t-test assuming unequal variance. Statistical significance between multiple groups was determined using One Way ANOVA with Holm-Sidak comparisons between control and treatment groups *post hoc.* Specifically for the shuddering assays, One Way ANOVA on Ranks and Dunn's method comparisons were performed *post hoc,* due to non-normal distribution of the data. Statistical analyses were performed using SigmaStat for Windows Version 3.11 (Systat Software, Inc., Point Richmond, CA).

Results

Microarray analysis of *Shu* mutant gene expression reveals the up-regulation of *CanA-14F* and immune response genes

To gain insights into the molecular mechanisms that underlie the lithium-responsive neurological phenotypes of *Shu*, we investigated the effect of the *Shu* mutation on genome-wide gene expression by performing microarray-based gene profiling. We used the *Shu* stock outcrossed to the *CS* strain 18 times to identify alterations in transcript levels caused by the *Shu* mutation. Three

biological replicates were tested for each genotype using Affymetrix GeneChip® *Drosophila* Genome 2.0 Arrays. Each chip is composed of 18,800 probe sets representing over 18,500 transcripts. The three replicates showed high correlation coefficients (R>0.93), indicating that the experimental data were sufficiently reproducible.

In this study, we analyzed the gene expression data using the GeneSpring software and focused on genes that were detected in all three replicates for either wild-type or *Shu* mutant flies, excluding genes expressed only at a very low level in both genotypes. Among those consistently expressed genes, 17 genes displayed a significant difference (p<0.05) in transcript levels with a fold change greater than 2 between the wild-type and *Shu* mutant flies (Table 2). Fourteen and three genes were up and down-regulated, respectively, in *Shu* mutants compared to *CS* flies.

One of the 14 genes that were significantly up-regulated in *Shu* mutants was *Calcineurin A-14F (CanA-14F),* which encodes a catalytic subunit of calcineurin, Ca^{2+}/calmodulin-activated Ser/Thr protein phosphatase. The *CanA-14F* transcript is up-regulated in *Shu* 2.2-fold with a *P*-value of 0.0109. Calcineurin is composed of a catalytic A subunit (M_r ~60 kDa) and a regulatory B subunit (M_r ~19kDa). The *Drosophila melanogaster* genome has three genes that encode calcineurin A catalytic subunits; *Calcineurin A1 (CanA1)*, *Protein phosphatase 2B-14D (Pp2B-14D)*, and *CanA-14F*. In addition, *Calcineurin B (CanB) and Calcineurin B2 (CanB2)* encode for the regulatory B subunit. Of these 5 calcineurin genes, only *CanA-14F* was differentially regulated in *Shu*

mutants compared to wild-type flies. The microarray data showed that fold differences between *Shu* and *CS* in mRNA levels of *CanA1*, *Pp2B-14D*, *CanB* and *CanB2* are 0.97, 0.87, 0.96 and 1.03, respectively (Table 3). Based on the analysis of the *Drosophila melanogaster* genome (http://flybase.org/), *CanA-14F* is localized to the region 14F (sequence coordinates: 16,459,506-16,481,160) on the X-chromosome near the predicted site of the *Shu* mutation. When comparing *Shu* mutants and *CS* flies, the transcript levels of genes localized between *para* and *r* were either not significantly different (fold change greater than 2 and $p < 0.05$) or below the detection limit.

As presented in Chapter 2, *Shu* is a gain-of-function allele of the voltage-gated sodium channel *para,* whose expression is mainly restricted to the nervous system. Therefore, genes functionally interacting with *para* will also likely be present in neurons. To determine if *CanA-14F* is expressed in the fly CNS, I performed whole mount RNA *in situ* hybridizations for *CanA-14F* on both adult and third instar larval brains. With an antisense RNA probe for *CanA-14F*, widespread signals were detected in the third instar larval brain (Figure 16A). In the adult brain, *CanA-14F* mRNA was detected in those regions containing neuronal cell bodies, with relatively stronger signals in the lateral regions of the central brain (Figure 16C). No *CanA-14F in situ* hybridization signal was observed in the adult optic lobe (Figure 16C). Under the same staining conditions, a sense RNA probe did not show positive signals either in the larval or adult brains (Figure 16B and 16D), demonstrating the specificity of the signals generated with the antisense probe.

Table 2. Genes differentially* expressed in *Shu* compared to *CS*

gene symbol	fold change	p-value	function
DptB	↑12.2	0.0343	defense response (AMP)
AttC	↑8.94	0.0471	defense response (AMP)
CecC	↑8.22	0.0423	defense response (AMP)
AttB	↑7.99	0.017	defense response (AMP)
CG31809	↑6.57	0.00089	steroid dehydrogenase activity
AttA	↑6.31	0.0172	defense response (AMP)
Ste12DOR	↑3.33	0.0342	protein kinase CK2 activity
CecB	↑3.17	0.0159	defense response (AMP)
PGRP-SB1	↑2.78	0.03	defense response
CG13335	↑2.31	0.0246	unknown
CanA-14F	↑2.21	0.0109	serine/threonine phosphatase
CG32368	↑2.20	0.00278	unknown
Ccp84Aa	↑2.13	0.000836	chitin structural component
CG31272	↑2.04	0.0283	transporter/lipase actvity
CG9377	↓14.3	0.0488	serine-type endopeptidase activity
CG31116	↓3.57	0.0163	voltage-gated chloride channel
Nox	↓2.28	0.0174	oxidoreductase activity

*Genes listed correspond to >2 fold change in mRNA level, signal present on all three chips for either wild-type or *Shu* RNA samples and had a p-value of <0.05. Gene ranking is based on amount of fold change, p-value was determined by Welch's t test.

Table 3. Expression levels of calcineurin subunit genes in *Shu*

calcineurin subunit gene	cytological location	fold change
CanA1	100B1	0.97
Pp2B-14D	14E1-14E3	0.86
CanA-14F	14E3-14F1	2.21
CanB	4F5	0.96
CanB2	43E16	1.03

These results were consistent with the data reported in FlyAtlas, an online microarray-based atlas of gene expression in multiple tissues of adult *Drosophila* (http://www.flyatlas.org/) (Chintapalli et al., 2007). FlyAtlas shows that C*anA-14F* is present and relatively enriched in the adult CNS. Although my microarray analysis and RT-PCR experiment clearly indicated up-regulation of *CanA-14F* in the head of *Shu* mutants compared to *CS* flies, the *in situ* hybridization analysis was not able to detect either quantitative or qualitative differences in *CanA-14F* mRNA expression in the brains from *Shu* mutants and wild-type flies (data not shown). This is probably due to the less quantitative nature of *in situ* hybridization techniques compared to microarray and RT-PCR analyses.

Overexpression of an inhibitor of calcineurin reduces the severity of the *Shu* phenotypes

The *Drosophila* gene *sarah* (*sra*), also known as *nebula* (*nla)*, is an ortholog of the human *Down's syndrome critical region 1* gene (*DSCR1*) and encodes an endogenous inhibitor of calcineurin (Fuentes et al., 2000, Ejima et al., 2004). I hypothesized that if increased *CanA-14F* expression was involved in the manifestations of the *Shu* mutant phenotypes, that overexpression of *nebula* would decrease calcineurin activity, thus rescuing the mutant defects. To test this hypothesis, I generated a double transgenic fly with two independent insertions of a *UAS-nebula* construct (designated *UAS-nla^{t1} and UAS-nla^{t2}*). These transgenic lines have been shown to be sufficient to drive increased expression of *nebula* in flies (Chang et al., 2003). I found that expression of these *UAS-nla* lines in *Shu,* driven ubiquitously or in neurons, was sufficient to

significantly lower that percentage of female flies displaying morphological defects (Figure 17A). When *nla* was expressed in muscle, glia or adipose tissues, no significant improvement in morphological defects were observed (Figure 17). These data suggest that a reduction of calcineurin activity is sufficient to improve *Shu* morphology. Furthermore, although other calcineurin subunit genes are expressed in the non-neural tissues, inhibiting their enzymatic activity in glia or muscles didn't rescue the morphological defects observed in *Shu*. This suggests that the inhibition may be specific to *CanA-14F*, whose expression is restricted to the nervous system (http://www.flyatlas.org/). Interestingly, expression of *nla* was not sufficient to rescue the reactive climbing defects in *Shu*, despite the strong improvements in anatomical defects (Figure 17B). Overall, these results suggest that calcineurin activity may play a role in the manifestations of the *Shu* phenotypes.

Hypomorphic mutant alleles of *CanA-14F*

improve the *Shu* phenotypes

To achieve a more specific reduction in *CanA-14F* levels than attained with the *UAS-nla* experiments, I crossed two P-element transgenic lines, *NP6106* and *EY9066,* inserted near the 5' start site of *CanA-14F* (Figure 18A) into the *Shu* mutant background. I was able to confirm that both transgenic insertion lines in the *CanA-14F* 5' region caused reduced mRNA levels compared to controls (Figure 18B). One copy of the mutated *CanA-14F* transcript was sufficient to reduce the frequency of *Shu* flies exhibiting morphological defects (Figure 18C). In addition, the heteroallelic *Shu/EY09066* and *Shu/NP6106* flies showed a

Figure 16. *CanA-14F* is expressed in both larval and adult CNS. (A and B) 3rd instar larval CNS and (C and D) adult brain. A *CanA-14F* digoxigenin-labeled anti-sense strand RNA was used as a probe (B and C), and a digoxigenin-labeled sense strand RNA was used as the control. The expression pattern in both the larval and adult brains suggests that the *CanA-14F* transcript is present in areas of high concentrations of neuronal cell bodies.

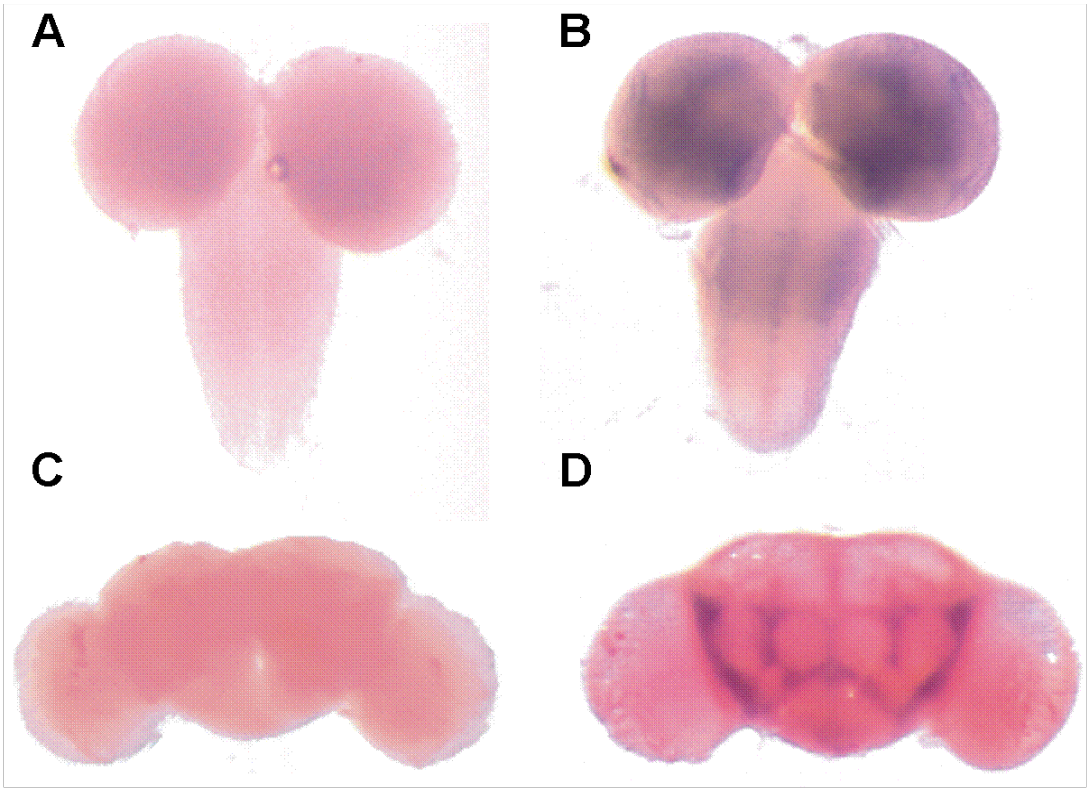
A
B
C
D

Figure 17. Overexpression of *nebula* suppresses *Shu* mutant morphological defects. (A) The percentage of morphological defects in all the *Shu* controls lines were > 80% defective (black bars). Expression of *nebula* ubiquitously in the fly, pan-neuronally or in cholinergic neurons resulted in a dramatic reduction in the percentage of defects in the mutants (red bars). No such reduction was observed when *nebula* was expressed in glia, muscle or fat body tissues, respectively. n > 250 per genotype. (B) Reactive climbing ability of *Shu* transgenic lines tested. Data are average CI ± SEM, n ≥ 5 groups of 20 flies.

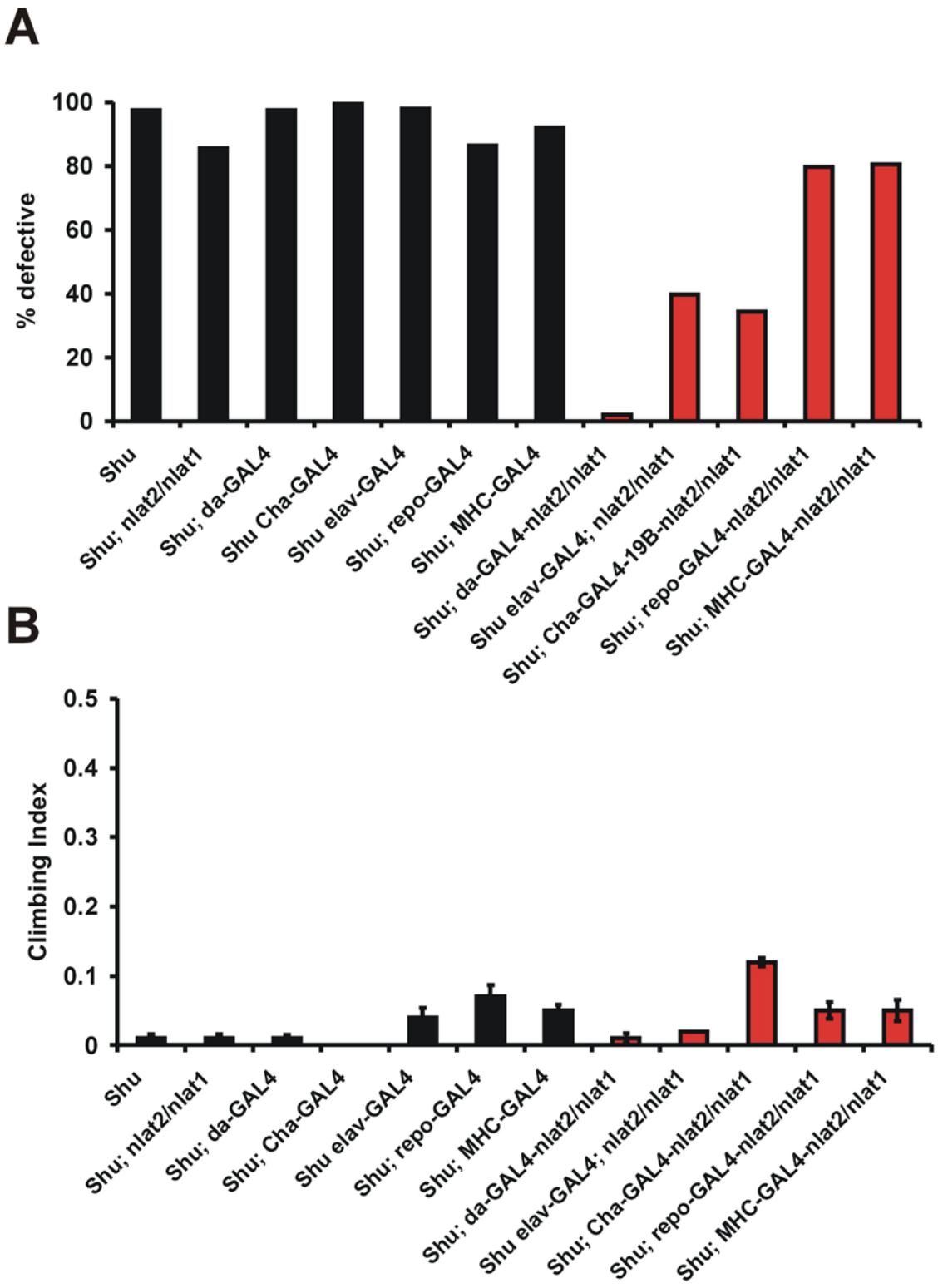
A
% defective
100
80
60
40
20
0
Shu
Shu; nlat2/nlat1
Shu; da-GAL4
Shu Cha-GAL4
Shu elav-GAL4
Shu; repo-GAL4
Shu; MHC-GAL4
Shu; da-GAL4-nlat2/nlat1
Shu elav-GAL4; nlat2/nlat1
Shu; Cha-GAL4-19B-nlat2/nlat1
Shu; repo-GAL4-nlat2/nlat1
Shu; MHC-GAL4-nlat2/nlat1
B
Climbing Index
0.5
0.4
0.3
0.2
0.1
0
Shu
Shu; nlat2/nlat1
Shu; da-GAL4
Shu; Cha-GAL4
Shu elav-GAL4
Shu; repo-GAL4
Shu; MHC-GAL4
Shu; da-GAL4-nlat2/nlat1
Shu elav-GAL4; nlat2/nlat1
Shu; Cha-GAL4-nlat2/nlat1
Shu; repo-GAL4-nlat2/nlat1
Shu; MHC-GAL4-nlat2/nlat1

Figure 18. P-element insertion mutants near the 5' start site of *CanA-14F*, improve *Shu* phenotypes. (A) *P{Epgy2}EY09066* is inserted 72bp upstream of the putative transcription start site of *CanA-14F*. The transposon also contains a UAS binding site for forced expression using the GAL4/UAS system. *P{GawB}NP6106* is inserted 103bp upstream from the 5' end of *CanA-14F* exon 1 and contains an enhancer-trap motif. (B) *CanA-14F* transcript levels determined by quantitative real-time RT-PCR in homozygous P-element mutant females whose insertion sites are illustrated in A. Fold-change was determined using ΔΔCt method by comparing levels of *CanA-14F* mRNA in the mutant lines to the w^{2202U}, a control line used to isogenize both mutant strains. (C) Morphological defects observed in *Shu* females trans-heterozygous over hypomorphic P-element mutant alleles of *CanA-14F.* (B) Reactive climbing ability in *Shu* females trans-heterozygous over hypomorphic P-element mutant alleles of *CanA-14F* females. Data are mean ± SEM of 3-5 groups of 20 flies. $p < 0.001$, One Way ANOVA, *$p < 0.05$,**$p < 0.005$, ***$p < 0.001$, Bonferonni t-test.

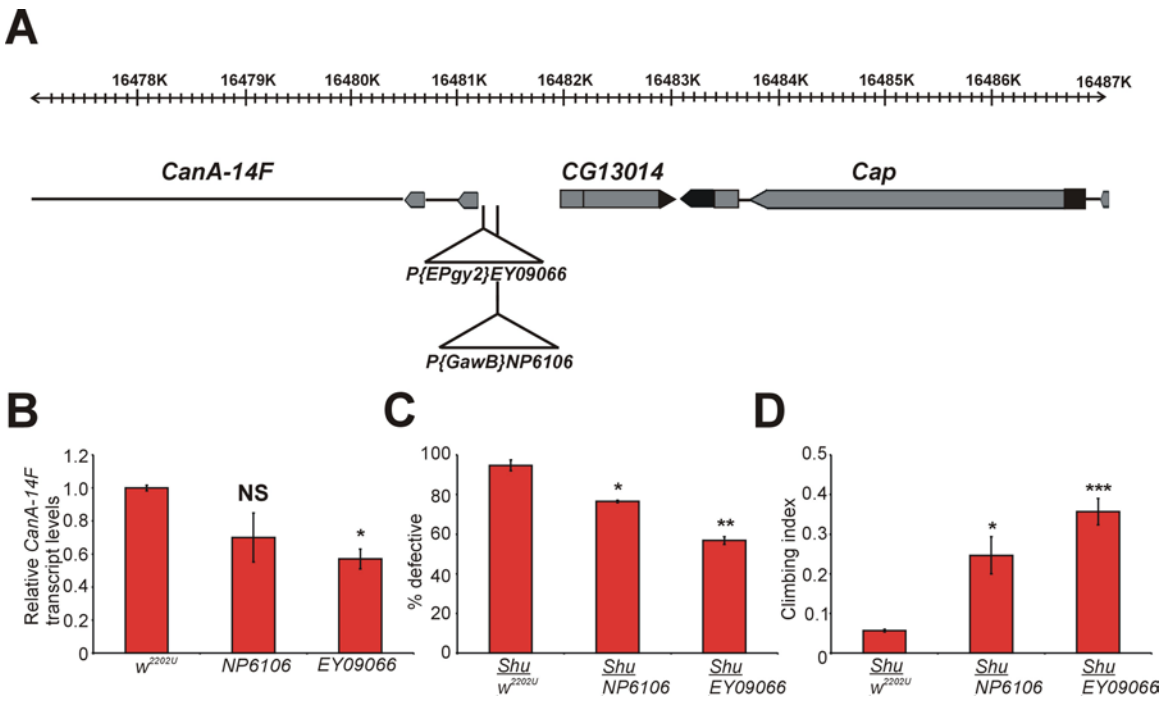
A
16478K
16479K
16480K
16481K
16482K
16483K
16484K
16485K
16486K
16487K
CanA-14F
CG13014
Cap
P{EPgy2}EY09066
P{GawB}NP6106
B
Relative CanA-14F transcript levels
1.2
1.0
0.8
0.6
0.4
0.2
0
NS
*
w2202U
NP6106
EY09066
C
% defective
100
80
60
40
20
0
*
**
Shu w2202U
Shu NP6106
Shu EY09066
D
Climbing index
0.5
0.4
0.3
0.2
0.1
0
*
***
Shu w2202U
Shu NP6106
Shu EY09066

significant improvement in reactive climbing ability (Figure 18D). These data suggest that increased *CanA-14F* levels are involved in the *Shu* mutant phenotypes. However, subsequent experiments which included both over-expression and RNAi knockdown of *CanA-14F* using the GAL4/UAS system resulted in ambiguous data that did not support the earlier findings (data not shown). Therefore, it appears that increased *CanA-14F* may be important for manifesting the *Shu* phenotypes, but is not the primary cause (see Chapter II).

Genes involved in innate immune responses are up-regulated in *Shu*

An intriguing finding from our microarray analysis is that seven of the 14 genes significantly up-regulated in *Shu* mutants are involved in the innate immune response (Table 2). These genes include *Diptericin B* (*DptB*), *Attacin A* (*AttA)*, *Attacin B* (*AttB*), *Attacin C* (*AttC*), *Cecropin B* (*CecB*), and *Cecropin C* (*CecC*), all of which encode for antimicrobial peptides against gram-negative bacteria (Lemaitre and Hoffmann, 2007). Additionally, *PGRP-SB1* encoding for a peptidoglycan recognition protein (Lemaitre and Hoffmann, 2007) is up-regulated in *Shu*. A more rigorous analysis of the microarray data using the web-accessible program DAVID (the Database for Annotation, Visualization and Integrated Discovery: http://david.abcc.ncifcrf.gov/) (Dennis et al., 2003) also revealed that a group of genes involved in the innate immunity are the most significantly enriched among those in the list of differentially regulated genes ($p<0.05$) in *Shu* mutants compared to the *CS* flies. The enrichment score and

median p-value (EASE score) for the innate immune response genes were 5.96 and of 2.4×10^{-7}, respectively.

The effects of lithium treatment on gene expression profiles were investigated in *Shu*. When the normalized microarray data from *Shu* mutants with or without lithium treatment were compared to those from the *CS* flies without lithium treatment, it was found that treatment of *Shu* mutants with lithium had a general propensity to normalize the levels of immune system genes that were up-regulated in *Shu* mutants (Figure 19A). *CanA-14F* transcript levels in *Shu* mutants were still significantly higher than those in the control wild-type flies even after lithium treatment (Figure 19A). RT-PCR analysis performed by Dr. Junko Kasuya, a research scientist in the lab, also revealed that innate immune response genes were down-regulated by lithium treatment in *Shu* mutants but not in the wild-type flies, confirming the suppressing effects of lithium on the innate immune response genes in *Shu* mutants (Figure 19B and C).

An unbiased forward genetic screen reveals several regions on the second and third chromosomes that suppress the *Shu* mutant phenotypes

To elucidate the molecular and cellular mechanisms underlying the "therapeutic" action of lithium in the *Shu* mutant, it was necessary to identify other components of the biological pathway where the *Shu* gene functions. I hypothesized that the neurological phenotypes of *Shu* could be enhanced or suppressed when the activity of the genes functionally interacting with *Shu* were reduced by 50%. To test this hypothesis, deficiencies spanning most of the second and third chromosomes were introduced into the *Shu* mutant background

Figure 19. **Lithium suppresses the increased expression of innate immune response genes in *Shu* mutants.** (A) Expression levels of innate immune response genes and *CanA-14F* in wild-type females were compared with those in *Shu* mutants with or without 50 mM lithium treatment for 24 hr. Microarray data are presented as normalized average signal intensities of three biological replicates for each condition. *$p < 0.05$, **$p < 0.01$, NS, not significant, Welch's t-test (B) Effects of lithium treatment on expression levels of innate immune response genes and *CanA-14F* were examined by RT-PCR.

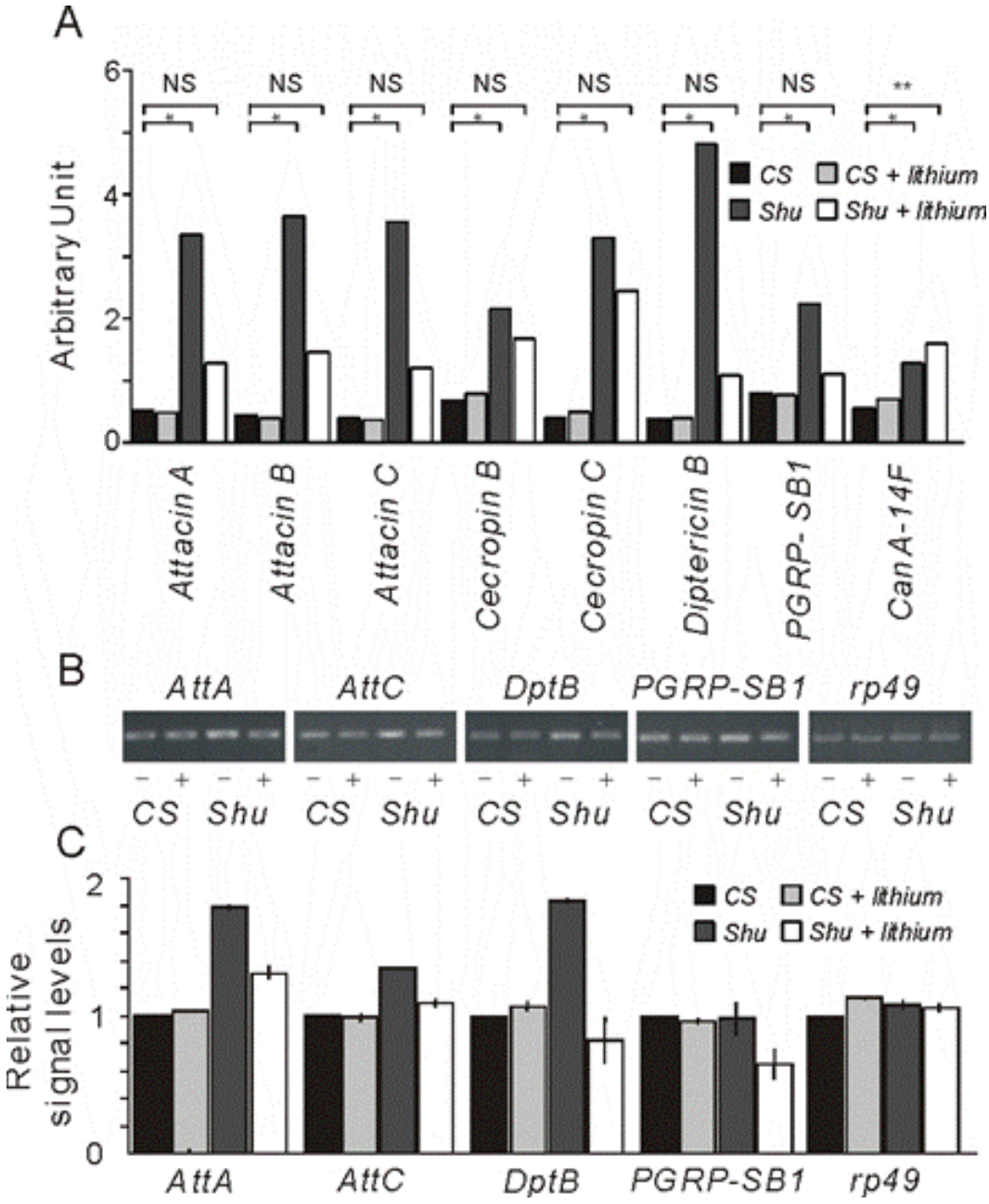
A
Arbitrary Unit
6
4
2
0
NS
NS
NS
NS
NS
NS
NS
**
CS
CS + lithium
Shu
Shu + lithium
Attacin A
Attacin B
Attacin C
Cecropin B
Cecropin C
Diptericin B
PGRP- SB1
CanA-14F
B
AttA
AttC
DptB
PGRP-SB1
rp49
CS
Shu
C
Relative signal levels
2
1
0
AttA
AttC
DptB
PGRP-SB1
rp49

and examined if it resulted in a modification of the *Shu* phenotype. Out of the 176 deficiency lines covering both autosomes, eight deficiencies showed a dramatic effect on the *Shu* behavior; both greatly improving the climbing ability and/or reducing the frequency of morphological defects of the mutant (Table 4). They also significantly mitigated other neurological phenotypes of *Shu* mutants such as spontaneous jerking and abnormal wing posture. Specifically, the cytological region 53D-53F on the second chromosome provided one of the strongest suppressions observed. In fact, the improvement provided by the introduction of deletions covering this region was so robust that *Shu* males, which are functionally sterile, were now able to mate and produce progeny (data not shown). To date, this level of suppression has not been observed by deficiencies in other genomic regions.

Using a number of deficiencies that cover cytological region 53, I and Dr. Junko Kasuya were able to narrow down the suppressor region to only six genes from the initial suppressor region (Figure 20A). The genes present in this small region included: *CG8950, CG6967* and *CG30460*, each encoding for an enoyl-CoA hydratase, *Sphingosine-1-phosphate lyase (Sply)* and *Glutathione S transferase S1 (GstS1)*, respectively. Other genes in this region included: *CG8950, CG6967* and *CG30460*, each encoding for proteins of unknown function. Thus, based on the deficiency data, one or more of these six genes should be responsible for suppression of the *Shu* phenotypes.

Table 4. Deficiencies that significantly improve the *Shu* phenotypes

Deficiency	Chromosome	Cytological location	Climbing Index	% defective
Shu + (Df)1567	2L	23C3-23D2	0.40	22.1
Shu + (Df)6404	2R	53E-53F11	0.49	n/a*
Shu + (Df)3906	3L	64C-65C	0.06	0
Shu + (Df)997	3L	67A2-67D13	0.28	40
Shu + (Df)1518	3R	81F3-82F7	0.33	30.3
Shu + (Df)6756	3R	85C4-85D14	0.35	25
Shu + (Df)1920	3R	89B5-89C7	0.43	40
Shu + (Df)8583	3R	94E1-94F2	0.26	33.3

*n/a-morphology was not scored for this mutant

RNAi knockdown of genes covered by the deletion *Df(2R)BSC433* reveals that *GstS1* is the gene responsible for suppression of the *Shu* phenotypes

I chose to try and identify the *Shu* suppressor gene(s) by employing *UAS-RNAi* lines to knockdown expression levels of each of the six remaining genes expression of each individual gene, it was my hope that I could phenocopy the suppression observed by *Df(2R)BSC433*. These *UAS-RNAi* lines were crossed to *Shu/FM7; da-GAL4* (ubiquitous, strong expression) females and the resulting F1 females specific for each gene (*Shu da-GAL4-UAS-RNAi*) were scored for morphological defects. *Shu* controls containing just the *UAS-RNAi* transgene or *da-GAL4* were also scored. *Shu da*-GAL4 flies driving expression of RNAi for both *CG6967* and *CG8964* proved lethal. (data not shown). This effect was not due to the transgene itself as all controls remained viable. The other three RNAi lines displayed only mild improvements in the *Shu* morphology. However, when the *RNAi* transgene targeting *GstS1* was driven in the *Shu* background, it provided a strong suppression of the mutant phenotypes, very similar to that seen by *Df(2R)BSC433* (Figure 20B). I also found that the knockdown of *GstS1* also improved male defects enough to allow for the production of progeny when crossed to *CS* females. These data prove that a reduction in the expression level of *GstS1* significantly suppresses the *Shu* phenotypes through a yet to be determined mechanism.

Discussion

In this chapter, using both gene expression arrays and a deficiency screen in *Shu*, I have been able to identify novel genes that appear to interact with the gain-of-function mutant sodium channel gene. First, gene expression profiling of *CS* has already provided novel data on lithium's effect on gene expression in the adult fly nervous system and aided in the identification of the *List*, a gene important for protection from lithium toxicity (Kasuya et al., 2009a, Kasuya et al., 2009b).

Here, I show that the Ca^{2+}/calmodulin-dependent serine/threonine phosphatase alpha subunit gene, *CanA-14F* is overexpressed in the *Shu* mutant. Calcineurin plays an essential role in the mammalian immune system. In particular, calcineurin activates T-cells by dephosphorylation of the transcription factors NFATs (nuclear factors of activated T cells) and by enhancing their nuclear translocation (Hogan et al., 2003). It has recently been demonstrated that calcineurin is also involved in the self-defense system in *Drosophila* larvae by activating the evolutionarily conserved innate immune response pathway (Dijkers and O'Farrell, 2007). One of the calcineurin catalytic subunit genes, *CanA1*, is expressed in the larval hemocytes and promotes induction of innate immune responses in the fat body in response to gram-negative bacteria or nitric oxide (Dijkers and O'Farrell, 2007). Although the involvement of *CanA-14F* in innate immune responses has never been shown, it is possible that increased transcript levels of innate immune response genes in the adult *Shu* heads are a

Figure 20. Downregulation of *GstS1* strongly suppresses the *Shu* phenotypes. (A) Six of seven deletions covering cytological region 53D-F on the second chromosome rescue the *Shu* phenotypes. Deletions that rescued (red) and did not rescue (black) the *Shu* phenotypes. Dashed bars indicate that the deletion extends beyond 53D-F. Df(2R)BSC433 has allowed for the candidate suppressor region to be reduced to an area only containing 6 genes. They are represented (blue squares) between the two thin black dashed lines. (B) Percentage of *Shu* female flies displaying morphological defects after specific RNAi knockdown of the six candidate genes. Note that driving expression of RNAi for *CG6967* and *CG8950* ubiquitously in the fly resulted in adult lethality or semi-lethality, respectively. n>20 flies.

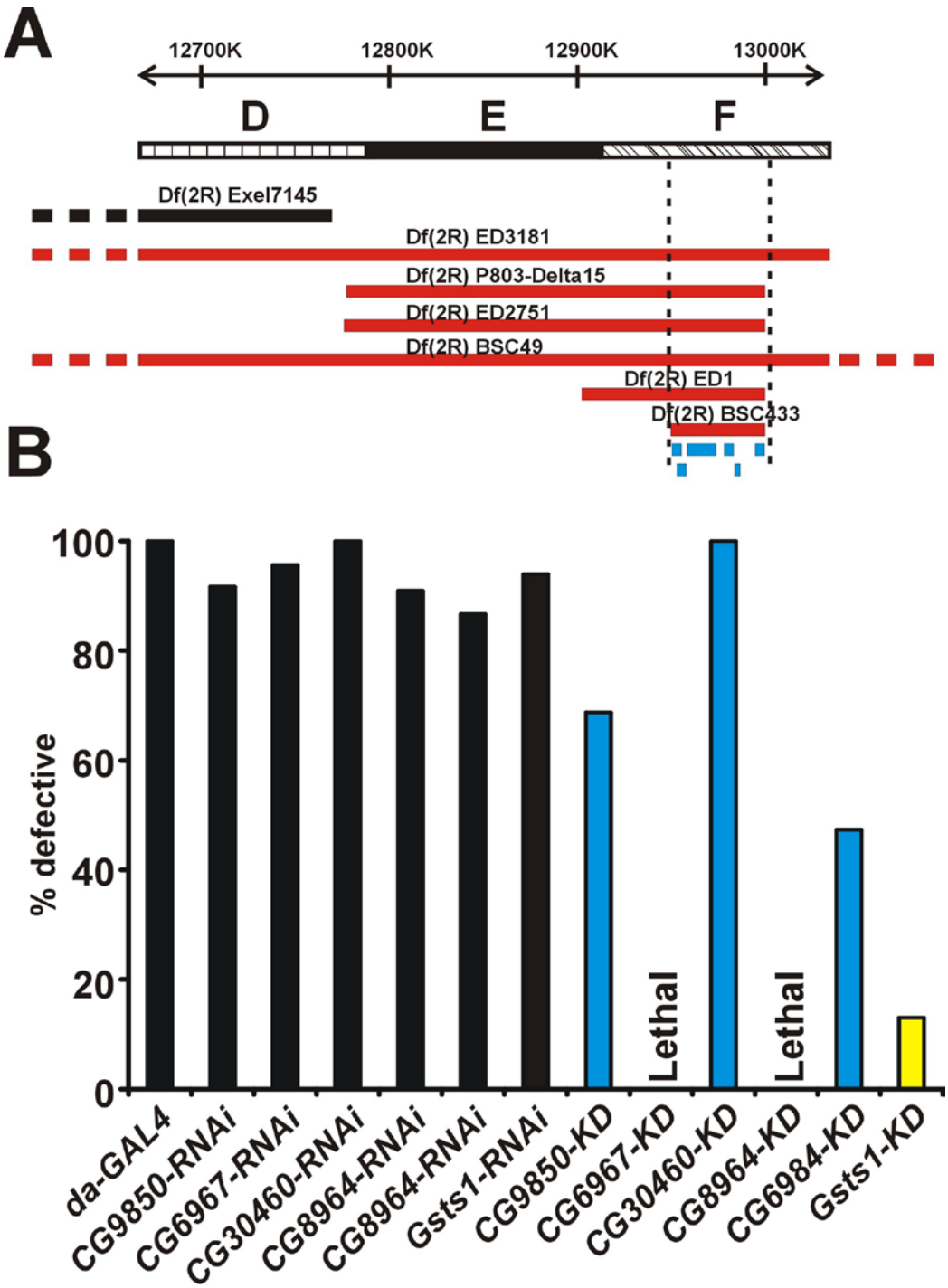
A
12700K
12800K
12900K
13000K
D
E
F
Df(2R) Exel7145
Df(2R) ED3181
Df(2R) P803-Delta15
Df(2R) ED2751
Df(2R) BSC49
Df(2R) ED1
Df(2R) BSC433
B
% defective
100
80
60
40
20
0
Lethal
Lethal
da-GAL4
CG9850-RNAi
CG6967-RNAi
CG30460-RNAi
CG8964-RNAi
CG8964-RNAi
Gsts1-RNAi
CG9850-KD
CG6967-KD
CG30460-KD
CG8964-KD
CG6984-KD
Gsts1-KD

direct consequence of up-regulation of *CanA-14F* caused by the *Shu* mutation.

Importantly, *CanA-14F* is expressed in both the larval and adult nervous system based on *in situ* hybridization (Figure 16). Furthermore, overexpression of *nla*, an endogenous inhibitor protein of calcineurin activity, significantly rescued the morphological defects in *Shu* when driven in neurons (Figure 17). In addition, introduction of *CanA-14F* hypomorphic alleles into the *Shu* mutant background significantly improved both and behavioral defects in the mutant (Figure 18). These data suggest that *CanA-14F* plays some role in the nervous system that counteracts the deleterious effects of the mutant *para* allele, either directly or indirectly.

How exactly *CanA-14F* is involved in alterations of the *Shu* mutant phenotypes remains unknown. However, there are several reasonable possibilities. The phosphatase calcineurin has been shown to influence many aspects of neuronal function through dephosphorylation of its many substrates. It is known that calcineurin targets are intimately involved in neurotransmitter synthesis, endocytosis, exocytosis and transport of ions across the plasma membrane (Groth et al., 2003). It is also possible that *CanA-14F* modulates nuclear translocation and/or activities of particular transcription factors such as NFAT, which modulate expression of neuronal genes critical for the physiological properties of neurons (Graef et al., 2003). Calcineurin's influence on plasticity is highlighted by its important role in the regulation of learning and memory, a hallmark of neuronal modulation (Baumgartel et al., 2008). Therefore,

calcineurin could affect neuronal function independent of the mutated sodium channel to modulate the *Shu* phenotypes by altering neuronal plasticity.

Another, more direct role for calcineurin in modifying the *Shu* phenotypes could be through dephosphorylation of the sodium channel α subunit protein. It has been well established that PKA and other kinases phosphorylate sodium channels at multiple sites leading to modulation of sodium channel function (see Chapter II introduction) (Berendt et al., 2010). Although overwhelming support for this interaction has not been generated, several studies in insects and mammals suggest that calcineurin can influence sodium channel function through removal of phosphate groups (Chen et al., 1995, Lavialle-Defaix et al., 2010). In particular, administration of the calcineurin inhibitor cyclosporine A, was sufficient to inhibit a specific form of sodium current in the cockroach, indicating that a reduction in calcineiurin activity can shut off sodium channel function in certain neuronal sub-groups (Lavialle-Defaix et al., 2010).

Finally, recent GWAS studies of schizophrenia and BPD patients have revealed that the immune system may play an important role in the pathophysiology of these psychiatric diseases (Purcell et al., 2009, Shi et al., 2009). Likewise, calcineurin plays an essential role in the mammalian immune system. In particular, calcineurin activates T-cells by dephosphorylation of the transcription factors NFATs (nuclear factors of activated T cells) and by enhancing their nuclear translocation (Hogan et al., 2003). It has recently been demonstrated that calcineurin is also involved in the innate immune system in *Drosophila* larvae by activating the evolutionarily conserved innate immune

response pathway (Dijkers and O'Farrell, 2007). One of the calcineurin catalytic subunit genes, *CanA1*, is expressed in the larval hemocytes and promotes induction of innate immune responses in the fat body in response to gram-negative bacteria or nitric oxide (Dijkers and O'Farrell, 2007). Although the involvement of *CanA-14F* in innate immune responses has never been shown, it is possible that increased transcript levels of innate immune response genes in the adult *Shu* heads are a direct consequence of up-regulation of *CanA-14F* caused by the *Shu* mutation. Intriguingly, a recent report has shown that the antimicrobial peptide, *Drosomycin* can physically bind to *para* and influence gating properties of the channel (Cohen et al., 2009).

It is important to note that not only were a whole host of AMP genes significantly up-regulated in *Shu,* but also that lithium treatment for 24 hr was sufficient to reduce their expression back to levels seen in *CS* flies. This reduction in AMP gene expression upon lithium treatment was not observed in the controls, suggesting lithium's effect is specific to the mutant (Figure 19B, C). Several studies have now indicated that the mood-stabilizing drug can modulate the innate immune response, possibly through inhibition of its well known target GSK-3β (Fatemi et al., 2009, Beurel et al., 2010).

In addition to those potential genes identified from the expression arrays, I identified several genomic regions containing genes that when introduced into the *Shu* background, significantly improve both the morphological and behavioral phenotypes of the mutant (Table 4). From here, I focused on cytological region 53 on the second chromosome, which provided some of the strongest

suppression of the mutant phenotypes. Using a number of smaller, molecularly defined deletion lines, I narrowed the region of interest down to only six genes. Next, I knocked down expression of each of the six transcripts and revealed the gene *GstS1* was responsible for the observed suppression (Figure 20B).

The gene *GstS1* is a glutathione S transferase expressed broadly throughout the fly (http://flyatlas.org). It has been shown that over-expression of this gene is protective against dopaminergic cell loss in a Parkinson's disease model fly (Whitworth et al., 2005). However, in *Shu* the role of *GstS1* is likely through a different mechanism than those found in the Parkinson's study, as a reduction and not increase in expression leads to an observable improvement in the mutant phenotypes. In addition, a recent study in flies has shown that *GstS1* mutants have increases in neuronal excitability at the larval NMJ and that adults exhibit increased aggression (Ueda and Wu, 2009). This alteration in excitability been shown to be mediated through reactive oxygen species (ROS) effecting the NMJ, thus by reducing *GstS1*, a known player in ROS clearance, it mimics increased ROS and drives increases in membrane excitability (Ueda and Wu, 2008). Because the *Shu* mutant is caused by extreme increases in neuronal excitability, it is hard to explain how a reduction in *GstS1,* which also increases neuronal excitability, could suppress the phenotypes of the lithium-responsive mutant. One possible explanation could be that some sort of feedback loop resulting from a reduction of *GstS1* gene activity may dampen neuronal excitability in *Shu*, indirectly counteracting the effects of the *para* gain-of-function allele.

Finally, a recent study in *Drosophila* investigating the effects of Copy Number Variations (CNV) on halothane has led to the finding that the introduction of *Df(2R)ED1* into a wild-type background results in resistance to the anesthetic (Alone et al., 2009). This deletion was also able to strongly suppress the *Shu* mutant phenotypes, when placed in the mutant background (Figure 20A). This finding is interesting, considering that anesthetics target ion channels (Yamakura et al., 2001). Furthermore, many leg-shaking mutants respond violently to the anesthetic diethyl ether and even some *para* alleles exhibit resistant to its effects (Gamo et al., 1998). Therefore, it is highly possible that the gene responsible for this halothane resistance is *GstS1.*

Here, using two different methods I have identified a number of genes and genomic regions that may functionally interact with *Shu.* These experiments will aid in future projects in the lab and may lead to the identification of novel targets for lithium as well as new proteins involved in the regulation of neuronal function.

CHAPTER IV

SUMMARY AND FUTURE DIRECTIONS

This thesis project had three main goals. The first goal was to fully characterize the phenotypic defects in the lithium-responsive neurological mutant, *Shu*. I began this project by extensively backcrossing the original *Shu/FM6* line from Mr. Rodney Williamson to eliminate potential modifiers in the mutant background. Next, I confirmed the original findings from over 25 years ago that the mutant exhibited severe locomotor defects and that these defects could be significantly improved by administration of a diet containing lithium. I also employed a novel video tracking analysis system, in collaboration with Dr. Hiroshi Ishimoto (Kitamoto lab), to more accurately quantify the general locomotion of the mutant its ether-induced leg-shaking behaviors. Importantly, these locomotor parameters were also improved by lithium treatments. Furthermore, I and Dr. Hiroshi Ishimoto discovered that the *Shu* mutant displays abnormalities in sleep architecture, of which has never been observed or reported in any other hyperexcitable mutants.

Second, to understand how *Shu* exhibits the striking neurological phenotypes and how they are improved by lithium, it was essential that I identify the mutated gene and determine the nature of the mutation. To achieve this goal I performed an extensive recombination-based, mapping technique using molecularly-defined P-element insertions as dominant markers. The results of the mutation mapping strongly indicated that the mutated gene causing the *Shu* neurological defects lay within the voltage-gated sodium channel gene *para*. To

provide evidence to support the mapping results, I crossed *Shu* mutants to several hypomorphic *para* alleles and showed that two of the three *Shu/para* heteroallelic mutants were strongly rescued both morphologically as well as behaviorally. These data supported the mapping results and suggested that *Shu* maybe a gain-of-function mutant allele of *para.* To further strength these findings, I employed the UAS/GAL4 binary system to knockdown *para* transcript levels in *Shu* neurons using RNAi technology. In line with my earlier observations above, knockdown of *para* in *Shu* resulted in a robust rescue of all aspects of the mutant defects. In fact, the rescue was so complete that the flies were nearly indistinguishable with the wild-type strains based on both appearance and all behaviors examined. Lastly, sequencing of all *para* exons in *Shu* revealed the presence of a novel missense mutation resulting in the change of a highly conserved methionine residue to an isoleucine in the S2 transmembrane segment of homology domain III of the sodium channel.

The third challenge was to indentify genes functionally interacting with the *Shu* mutant using both a gene expression array and an unbiased, forward genetic screen. These studies identified the calcineurin α subunit gene *CanA-14F*, a whole host of immune response genes and *GstS1* as promising targets of future investigation. Furthermore, a number of genomic regions, yet to be fully explored, have been shown to significantly suppress the mutant phenotypes of *Shu*. Indicating several other genes await to be identified that somehow affect sodium channel function in *Shu*.

Taken together, I have satisfactorily completed the initial goals set forth for this thesis project. I have extensively characterized the many interesting behaviors and morphological defect in *Shu* mutants. Furthermore, I have discovered that the *Shu* mutant is a gain-of-function allele of the voltage-gated sodium channel *para.* To date, this is the first identification of a sodium channel mutation in *Drosophila* causing increased channel activity.

To confirm that the mutation identified in *Shu* is actually responsible for the manifestations of its neurological phenotypes, two separate experimental techniques must be employed. The first will involve the use of the well-established *Xenopus* ooctye heterologous system to investigate the electrophysiological properties of the mutated sodium channel. With this well-established system one can express functional sodium channels in the oocyte and analyze a whole host of gating properties including activation, inactivation, persistent current and many others (Warmke et al., 1997). This experiment will not only confirm if the M1350I mutation is the cause of the *Shu* phenotypes, but help to shed light on how alterations in the sodium channel may result in increased neuronal excitability in the mutant. The second experiment will consist of the generation of a *UAS-para*^{M1350I} transgenic fly to attempt to overexpress a sodium channel harboring the *Shu* mutation in an otherwise wild-type fly, in an attempt to phenocopy the neurological phenotypes of the mutant. It is my belief that this strategy will work successfully due to the very strong dominant nature of the *Shu* mutation.

The second major question remaining is how the mood-stabilizing drug lithium elicits its positive impact on the behavioral phenotypes of *Shu*. Given that I am confident that *Shu* is caused by improper sodium channel function, several lines of evidence suggest that the drug could have a direct effect on sodium channel function in this fly. Interestingly, it has been reported in neuronal cell cultures that the mood-stabilizing drug can inhibit Na^+ influx in sodium channels independent of the its well-stabilized target, GSK-3β (Yanagita et al., 2007). In addition, the drug lamotrigine, commonly used to treat patients with BPD, acts through alterations in sodium channel function (Rogawski and Loscher, 2004). Importantly, this drug has not been shown to exhibit deleterious effects on wild-type flies when administered chronically, until very late in adulthood (Avanesian et al., 2010) Furthermore, the sodium channel α subunit gene *SCN8A* has been found to be a risk factor for BPD in a Chinese Han population (Wang et al., 2008). Lastly, ANK3 () was found to be associated with BPD patients in one of the largest GWAS ever conducted (Ferreira et al., 2008). ANK3 has been shown to play an essential role in the proper localization of sodium channels along the membranes of neurons (Lemaillet et al., 2003).

Therefore future experiments include; investigating the effect of lamotrigine on *Shu* behaviors, continuing to prove or disprove the roles of either GSK-3β or the inositol processing enzymes IPPase and IMPase in lithium's effect on the mutant. Additionally, the effect of the mood-stabilizing drug on sleep behaviors in *Shu* and wild-type must be investigated.

Taken together, many exciting avenues of scientific investigations remain for this interesting lithium-responsive neurological mutant. It will be interesting to determine not only the exact sodium-channel dependent mechanism responsible for the *Shu* mutant phenotype. Likewise, identification of the effect of lithium on *Shu* may lead to the discovery of novel targets and lithium-dependent mechanisms on nervous system function towards future drug development to aid patients suffering from BPD. Finally, both the gene expression array and the deficiency screen have uncovered a number of genes which appear to functionally interact with the *Shu* mutant, fueling future studies in the lab for years to come.

REFERENCES

Aberle H, Bauer A, Stappert J, Kispert A, Kemler R (beta-catenin is a target for the ubiquitin-proteasome pathway. Embo J 16:3797-3804.1997).

Abou-Khalil B, Ge Q, Desai R, Ryther R, Bazyk A, Bailey R, Haines JL, Sutcliffe JS, George AL, Jr. (Partial and generalized epilepsy with febrile seizures plus and a novel SCN1A mutation. Neurology 57:2265-2272.2001).

Acquas E, Fibiger HC (Chronic lithium attenuates dopamine D1-receptor mediated increases in acetylcholine release in rat frontal cortex. Psychopharmacology (Berl) 125:162-167.1996).

Allen GE (1978) Thomas Hunt Morgan : the man and his science. Princeton, N.J.: Princeton University Press.

Allison JH, Stewart MA (Reduced brain inositol in lithium-treated rats. Nat New Biol 233:267-268.1971).

Alone DP, Rodriguez JC, Noland CL, Nash HA (Impact of gene copy number variation on anesthesia in Drosophila melanogaster. Anesthesiology 111:15-24.2009).

Atack JR (Inositol monophosphatase inhibitors: a novel treatment for bipolar disorder? Biol Psychiatry 37:761-763.1995).

Attwood PV, Ducep JB, Chanal MC (Purification and properties of myo-inositol-1-phosphatase from bovine brain. Biochem J 253:387-394.1988).

Avanesian A, Khodayari B, Felgner JS, Jafari M (Lamotrigine extends lifespan but compromises health span in Drosophila melanogaster. Biogerontology 11:45-52.2010).

Baastrup PC, Schou M (Lithium as a prophylactic agents. Its effect against recurrent depressions and manic-depressive psychosis. Arch Gen Psychiatry 16:162-172.1967).

Baraban JM (Toward a crystal-clear view of lithium's site of action. Proc Natl Acad Sci U S A 91:5738-5739.1994).

Baumann P, Nil R, Souche A, Montaldi S, Baettig D, Lambert S, Uehlinger C, Kasas A, Amey M, Jonzier-Perey M (A double-blind, placebo-controlled study of citalopram with and without lithium in the treatment of therapy-resistant depressive patients: a clinical, pharmacokinetic, and pharmacogenetic investigation. J Clin Psychopharmacol 16:307-314.1996).

Baumgartel K, Genoux D, Welzl H, Tweedie-Cullen RY, Koshibu K, Livingstone-Zatchej M, Mamie C, Mansuy IM (Control of the establishment of aversive memory by calcineurin and Zif268. Nat Neurosci 11:572-578.2008).

Beaulieu JM, Marion S, Rodriguiz RM, Medvedev IO, Sotnikova TD, Ghisi V, Wetsel WC, Lefkowitz RJ, Gainetdinov RR, Caron MG (A beta-arrestin 2

signaling complex mediates lithium action on behavior. Cell 132:125-136.2008).

Beaulieu JM, Sotnikova TD, Yao WD, Kockeritz L, Woodgett JR, Gainetdinov RR, Caron MG (Lithium antagonizes dopamine-dependent behaviors mediated by an AKT/glycogen synthase kinase 3 signaling cascade. Proc Natl Acad Sci U S A 101:5099-5104.2004).

Begun DJ, Aquadro CF (Levels of naturally occurring DNA polymorphism correlate with recombination rates in D. melanogaster. Nature 356:519-520.1992).

Benzer S (BEHAVIORAL MUTANTS OF Drosophila ISOLATED BY COUNTERCURRENT DISTRIBUTION. Proc Natl Acad Sci U S A 58:1112-1119.1967).

Berendt FJ, Park KS, Trimmer JS (Multisite phosphorylation of voltage-gated sodium channel alpha subunits from rat brain. J Proteome Res 9:1976-1984.2010).

Berger Z, Ttofi EK, Michel CH, Pasco MY, Tenant S, Rubinsztein DC, O'Kane CJ (Lithium rescues toxicity of aggregate-prone proteins in Drosophila by perturbing Wnt pathway. Hum Mol Genet 14:3003-3011.2005).

Bernards A, Hariharan IK (Of flies and men--studying human disease in Drosophila. Curr Opin Genet Dev 11:274-278.2001).

Berridge MJ, Downes CP, Hanley MR (Lithium amplifies agonist-dependent phosphatidylinositol responses in brain and salivary glands. Biochem J 206:587-595.1982).

Berridge MJ, Downes CP, Hanley MR (Neural and developmental actions of lithium: a unifying hypothesis. Cell 59:411-419.1989).

Berry GT, Wu S, Buccafusca R, Ren J, Gonzales LW, Ballard PL, Golden JA, Stevens MJ, Greer JJ (Loss of murine Na+/myo-inositol cotransporter leads to brain myo-inositol depletion and central apnea. J Biol Chem 278:18297-18302.2003).

Besson M, Martin JR (Centrophobism/thigmotaxis, a new role for the mushroom bodies in Drosophila. J Neurobiol 62:386-396.2005).

Beurel E, Michalek SM, Jope RS (Innate and adaptive immune responses regulated by glycogen synthase kinase-3 (GSK3). Trends Immunol 31:24-31.2010).

Bier E (Drosophila, the golden bug, emerges as a tool for human genetics. Nat Rev Genet 6:9-23.2005).

Bilen J, Bonini NM (Drosophila as a model for human neurodegenerative disease. Annu Rev Genet 39:153-171.2005).

Boggs DR, Joyce RA (The hematopoietic effects of lithium. Semin Hematol 20:129-138.1983).

Bowden CL, Brugger AM, Swann AC, Calabrese JR, Janicak PG, Petty F, Dilsaver SC, Davis JM, Rush AJ, Small JG, et al. (Efficacy of divalproex vs lithium and placebo in the treatment of mania. The Depakote Mania Study Group. JAMA 271:918-924.1994).

Brand AH, Perrimon N (Targeted gene expression as a means of altering cell fates and generating dominant phenotypes. Development 118:401-415.1993).

Brandish PE, Su M, Holder DJ, Hodor P, Szumiloski J, Kleinhanz RR, Forbes JE, McWhorter ME, Duenwald SJ, Parrish ML, Na S, Liu Y, Phillips RL, Renger JJ, Sankaranarayanan S, Simon AJ, Scolnick EM (Regulation of gene expression by lithium and depletion of inositol in slices of adult rat cortex. Neuron 45:861-872.2005).

Brumby AM, Richardson HE (Using Drosophila melanogaster to map human cancer pathways. Nat Rev Cancer 5:626-639.2005).

Bushey D, Huber R, Tononi G, Cirelli C (Drosophila Hyperkinetic mutants have reduced sleep and impaired memory. J Neurosci 27:5384-5393.2007).

Bushey D, Hughes KA, Tononi G, Cirelli C (Sleep, aging, and lifespan in Drosophila. BMC Neurosci 11:56.2010).

Cade J (Lithium salts in the treatment of psychotic excitement. Med J Aust 2:349-352.1949).

Cadigan KM, Nusse R (Wnt signaling: a common theme in animal development. Genes Dev 11:3286-3305.1997).

Camins A, Verdaguer E, Junyent F, Yeste-Velasco M, Pelegri C, Vilaplana J, Pallas M (Potential mechanisms involved in the prevention of neurodegenerative diseases by lithium. CNS Neurosci Ther 15:333-344.2009).

Carmichael J, Sugars KL, Bao YP, Rubinsztein DC (Glycogen synthase kinase-3beta inhibitors prevent cellular polyglutamine toxicity caused by the Huntington's disease mutation. J Biol Chem 277:33791-33798.2002).

Catterall WA (From ionic currents to molecular mechanisms: the structure and function of voltage-gated sodium channels. Neuron 26:13-25.2000).

Celniker SE (The Drosophila genome. Curr Opin Genet Dev 10:612-616.2000).

Chalecka-Franaszek E, Chuang DM (Lithium activates the serine/threonine kinase Akt-1 and suppresses glutamate-induced inhibition of Akt-1 activity in neurons. Proc Natl Acad Sci U S A 96:8745-8750.1999).

Chang KT, Shi YJ, Min KT (The Drosophila homolog of Down's syndrome critical region 1 gene regulates learning: implications for mental retardation. Proc Natl Acad Sci U S A 100:15794-15799.2003).

Chen TC, Law B, Kondratyuk T, Rossie S (Identification of soluble protein phosphatases that dephosphorylate voltage-sensitive sodium channels in rat brain. J Biol Chem 270:7750-7756.1995).

Chiaroni P, Azorin JM, Dassa D, Henry JM, Giudicelli S, Malthiery Y, Planells R (Possible involvement of the dopamine D3 receptor locus in subtypes of bipolar affective disorder. Psychiatr Genet 10:43-49.2000).

Chintapalli VR, Wang J, Dow JA (Using FlyAtlas to identify better Drosophila melanogaster models of human disease. Nature genetics 39:715-720.2007).

Choi WS, Sung CK (Effects of lithium and insulin on glycogen synthesis in L6 myocytes: additive effects on inactivation of glycogen synthase kinase-3. Biochim Biophys Acta 1475:225-230.2000).

Cirelli C, Bushey D, Hill S, Huber R, Kreber R, Ganetzky B, Tononi G (Reduced sleep in Drosophila Shaker mutants. Nature 434:1087-1092.2005).

Cohen L, Moran Y, Sharon A, Segal D, Gordon D, Gurevitz M (Drosomycin, an innate immunity peptide of Drosophila melanogaster, interacts with the fly voltage-gated sodium channel. J Biol Chem 284:23558-23563.2009).

Cohen LS, Friedman JM, Jefferson JW, Johnson EM, Weiner ML (A reevaluation of risk of in utero exposure to lithium. JAMA 271:146-150.1994).

Coppen A, Noguera R, Bailey J, Burns BH, Swani MS, Hare EH, Gardner R, Maggs R (Prophylactic lithium in affective disorders. Controlled trial. Lancet 2:275-279.1971).

Cryns K, Shamir A, Van Acker N, Levi I, Daneels G, Goris I, Bouwknecht JA, Andries L, Kass S, Agam G, Belmaker H, Bersudsky Y, Steckler T, Moechars D (IMPA1 is essential for embryonic development and lithium-like pilocarpine sensitivity. Neuropsychopharmacology 33:674-684.2008).

Cundall RL, Brooks PW, Murray LG (A controlled evaluation of lithium prophylaxis in affective disorders. Psychol Med 2:308-311.1972).

Dascal N, Lotan I (Activation of protein kinase C alters voltage dependence of a Na+ channel. Neuron 6:165-175.1991).

Davis RL (Olfactory memory formation in Drosophila: from molecular to systems neuroscience. Annu Rev Neurosci 28:275-302.2005).

De Sarno P, Li X, Jope RS (Regulation of Akt and glycogen synthase kinase-3 beta phosphorylation by sodium valproate and lithium. Neuropharmacology 43:1158-1164.2002).

Dennis G, Jr., Sherman BT, Hosack DA, Yang J, Gao W, Lane HC, Lempicki RA (DAVID: Database for Annotation, Visualization, and Integrated Discovery. Genome biology 4:P3.2003).

Derst C, Walther C, Veh RW, Wicher D, Heinemann SH (Four novel sequences in Drosophila melanogaster homologous to the auxiliary Para sodium

channel subunit TipE. Biochem Biophys Res Commun 339:939-948.2006).

Dijkers PF, O'Farrell PH (Drosophila calcineurin promotes induction of innate immune responses. Curr Biol 17:2087-2093.2007).

Dmitrzak-Weglarz M, Rybakowski JK, Slopien A, Czerski PM, Leszczynska-Rodziewicz A, Kapelski P, Kaczmarkiewicz-Fass M, Hauser J (Dopamine receptor D1 gene -48A/G polymorphism is associated with bipolar illness but not with schizophrenia in a Polish population. Neuropsychobiology 53:46-50.2006).

Dokucu ME, Yu L, Taghert PH (Lithium- and valproate-induced alterations in circadian locomotor behavior in Drosophila. Neuropsychopharmacology 30:2216-2224.2005).

Einat H, Yuan P, Szabo ST, Dogra S, Manji HK (Protein kinase C inhibition by tamoxifen antagonizes manic-like behavior in rats: implications for the development of novel therapeutics for bipolar disorder. Neuropsychobiology 55:123-131.2007).

Ejima A, Tsuda M, Takeo S, Ishii K, Matsuo T, Aigaki T (Expression level of sarah, a homolog of DSCR1, is critical for ovulation and female courtship behavior in Drosophila melanogaster. Genetics 168:2077-2087.2004).

el-Mallakh RS (Acute lithium neurotoxicity. Psychiatr Dev 4:311-328.1986).

Embi N, Rylatt DB, Cohen P (Glycogen synthase kinase-3 from rabbit skeletal muscle. Separation from cyclic-AMP-dependent protein kinase and phosphorylase kinase. Eur J Biochem 107:519-527.1980).

Escayg A, MacDonald BT, Meisler MH, Baulac S, Huberfeld G, An-Gourfinkel I, Brice A, LeGuern E, Moulard B, Chaigne D, Buresi C, Malafosse A (Mutations of SCN1A, encoding a neuronal sodium channel, in two families with GEFS+2. Nat Genet 24:343-345.2000).

Fahmy OG, Fahmy MJ (Cytogenetic Analysis of the Action of Carcinogens and Tumor Inhibitors in Drosophila Melanogaster. VII. Differential Induction of Visible to Lethal Mutations by Related Nitrogen Mustards. Genetics 45:419-438.1960).

Farah JA, Hartsuiker E, Mizuno K, Ohta K, Smith GR (A 160-bp palindrome is a Rad50.Rad32-dependent mitotic recombination hotspot in Schizosaccharomyces pombe. Genetics 161:461-468.2002).

Fatemi SH, Reutiman TJ, Folsom TD (The role of lithium in modulation of brain genes: relevance for aetiology and treatment of bipolar disorder. Biochem Soc Trans 37:1090-1095.2009).

Feng G, Deak P, Chopra M, Hall LM (Cloning and functional analysis of TipE, a novel membrane protein that enhances Drosophila para sodium channel function. Cell 82:1001-1011.1995).

Fergestad T, Ganetzky B, Palladino MJ (Neuropathology in Drosophila membrane excitability mutants. Genetics 172:1031-1042.2006).

Ferreira MA, O'Donovan MC, Meng YA, Jones IR, Ruderfer DM, Jones L, Fan J, Kirov G, Perlis RH, Green EK, Smoller JW, Grozeva D, Stone J, Nikolov I, Chambert K, Hamshere ML, Nimgaonkar VL, Moskvina V, Thase ME, Caesar S, Sachs GS, Franklin J, Gordon-Smith K, Ardlie KG, Gabriel SB, Fraser C, Blumenstiel B, Defelice M, Breen G, Gill M, Morris DW, Elkin A, Muir WJ, McGhee KA, Williamson R, MacIntyre DJ, MacLean AW, St CD, Robinson M, Van Beck M, Pereira AC, Kandaswamy R, McQuillin A, Collier DA, Bass NJ, Young AH, Lawrence J, Ferrier IN, Anjorin A, Farmer A, Curtis D, Scolnick EM, McGuffin P, Daly MJ, Corvin AP, Holmans PA, Blackwood DH, Gurling HM, Owen MJ, Purcell SM, Sklar P, Craddock N (Collaborative genome-wide association analysis supports a role for ANK3 and CACNA1C in bipolar disorder. Nat Genet 40:1056-1058.2008).

Ferrie LJ, Gartside SE, Martin KM, Young AH, McQuade R (Effect of chronic lithium treatment on D2/3 autoreceptor regulation of dopaminergic function in the rat. Pharmacol Biochem Behav 90:218-225.2008).

Fornai F, Longone P, Cafaro L, Kastsiuchenka O, Ferrucci M, Manca ML, Lazzeri G, Spalloni A, Bellio N, Lenzi P, Modugno N, Siciliano G, Isidoro C, Murri L, Ruggieri S, Paparelli A (Lithium delays progression of amyotrophic lateral sclerosis. Proc Natl Acad Sci U S A 105:2052-2057.2008).

Fortini ME, Skupski MP, Boguski MS, Hariharan IK (A survey of human disease gene counterparts in the Drosophila genome. J Cell Biol 150:F23-30.2000).

Friedman E, Gershon S (Effect of lithium on brain dopamine. Nature 243:520-521.1973).

Fuentes JJ, Genesca L, Kingsbury TJ, Cunningham KW, Perez-Riba M, Estivill X, de la Luna S (DSCR1, overexpressed in Down syndrome, is an inhibitor of calcineurin-mediated signaling pathways. Hum Mol Genet 9:1681-1690.2000).

Gamo S, Dodo K, Matakatsu H, Tanaka Y (Molecular genetical analysis of Drosophila ether sensitive mutants. Toxicol Lett 100-101:329-337.1998).

Ganetzky B (Genetic studies of membrane excitability in Drosophila: lethal interaction between two temperature-sensitive paralytic mutations. Genetics 108:897-911.1984).

Ganetzky B, Wu C-F (Genes and membrane excitability in Drosophila. Trends in Neurosciences 8:322-326.1985).

Ganzhorn AJ, Chanal MC (Kinetic studies with myo-inositol monophosphatase from bovine brain. Biochemistry 29:6065-6071.1990).

George AL, Jr. (Inherited disorders of voltage-gated sodium channels. J Clin Invest 115:1990-1999.2005).

Gilestro GF, Cirelli C (pySolo: a complete suite for sleep analysis in Drosophila. Bioinformatics 25:1466-1467.2009).

Goldin AL, Barchi RL, Caldwell JH, Hofmann F, Howe JR, Hunter JC, Kallen RG, Mandel G, Meisler MH, Netter YB, Noda M, Tamkun MM, Waxman SG, Wood JN, Catterall WA (Nomenclature of voltage-gated sodium channels. Neuron 28:365-368.2000).

Gould TD, Einat H, Bhat R, Manji HK (AR-A014418, a selective GSK-3 inhibitor, produces antidepressant-like effects in the forced swim test. Int J Neuropsychopharmacol 7:387-390.2004).

Gould TD, Manji HK (Glycogen synthase kinase-3: a putative molecular target for lithium mimetic drugs. Neuropsychopharmacology 30:1223-1237.2005).

Graef IA, Wang F, Charron F, Chen L, Neilson J, Tessier-Lavigne M, Crabtree GR (Neurotrophins and netrins require calcineurin/NFAT signaling to stimulate outgrowth of embryonic axons. Cell 113:657-670.2003).

Grahame-Smith DG (Serotonin in affective disorders. Int Clin Psychopharmacol 6 Suppl 4:5-13.1992).

Greasley PJ, Gore MG (Bovine inositol monophosphatase. Studies on the binding interactions with magnesium, lithium and phosphate ions. FEBS Lett 331:114-118.1993).

Greene JC, Whitworth AJ, Kuo I, Andrews LA, Feany MB, Pallanck LJ (Mitochondrial pathology and apoptotic muscle degeneration in Drosophila parkin mutants. Proc Natl Acad Sci U S A 100:4078-4083.2003).

Grigliatti T, Suzuki DT (Temperature-sensitive mutations in Drosophila melanogaster. V. A mutation affecting concentrations of pteridines. Proc Natl Acad Sci U S A 67:1101-1108.1970).

Grimes CA, Jope RS (The multifaceted roles of glycogen synthase kinase 3beta in cellular signaling. Prog Neurobiol 65:391-426.2001).

Grimm T, Muller B, Dreier M, Kind E, Bettecken T, Meng G, Muller CR (Hot spot of recombination within DXS164 in the Duchenne muscular dystrophy gene. Am J Hum Genet 45:368-372.1989).

Groth RD, Dunbar RL, Mermelstein PG (Calcineurin regulation of neuronal plasticity. Biochem Biophys Res Commun 311:1159-1171.2003).

Gurvich N, Klein PS (Lithium and valproic acid: parallels and contrasts in diverse signaling contexts. Pharmacol Ther 96:45-66.2002).

Hart DA (Augmentation of zinc ion stimulation of lymphoid cells by calcium and lithium. Exp Cell Res 121:419-425.1979).

Hendricks JC, Lu S, Kume K, Yin JC, Yang Z, Sehgal A (Gender dimorphism in the role of cycle (BMAL1) in rest, rest regulation, and longevity in Drosophila melanogaster. J Biol Rhythms 18:12-25.2003).

Hesketh JE, Nicolaou NM, Arbuthnott GW, Wright AK (The effect of chronic lithium administration on dopamine metabolism in rat striatum. Psychopharmacology (Berl) 56:163-166.1978).

Hogan PG, Chen L, Nardone J, Rao A (Transcriptional regulation by calcium, calcineurin, and NFAT. Genes & development 17:2205-2232.2003).

Huang Y, Stern M (In vivo properties of the Drosophila inebriated-encoded neurotransmitter transporter. J Neurosci 22:1698-1708.2002).

Inhorn RC, Majerus PW (Properties of inositol polyphosphate 1-phosphatase. J Biol Chem 263:14559-14565.1988).

Isom LL, De Jongh KS, Patton DE, Reber BF, Offord J, Charbonneau H, Walsh K, Goldin AL, Catterall WA (Primary structure and functional expression of the beta 1 subunit of the rat brain sodium channel. Science 256:839-842.1992).

Isom LL, Ragsdale DS, De Jongh KS, Westenbroek RE, Reber BF, Scheuer T, Catterall WA (Structure and function of the beta 2 subunit of brain sodium channels, a transmembrane glycoprotein with a CAM motif. Cell 83:433-442.1995).

Jacobson SJ, Jones K, Johnson K, Ceolin L, Kaur P, Sahn D, Donnenfeld AE, Rieder M, Santelli R, Smythe J, et al. (Prospective multicentre study of pregnancy outcome after lithium exposure during first trimester. Lancet 339:530-533.1992).

Jattani R, Patel U, Kerman B, Myat MM (Deficiency screen identifies a novel role for beta 2 tubulin in salivary gland and myoblast migration in the Drosophila embryo. Dev Dyn 238:853-863.2009).

Jope RS, Williams MB (Lithium and brain signal transduction systems. Biochem Pharmacol 47:429-441.1994).

Kaidanovich-Beilin O, Milman A, Weizman A, Pick CG, Eldar-Finkelman H (Rapid antidepressive-like activity of specific glycogen synthase kinase-3 inhibitor and its effect on beta-catenin in mouse hippocampus. Biol Psychiatry 55:781-784.2004).

Kamiya K, Kaneda M, Sugawara T, Mazaki E, Okamura N, Montal M, Makita N, Tanaka M, Fukushima K, Fujiwara T, Inoue Y, Yamakawa K (A nonsense mutation of the sodium channel gene SCN2A in a patient with intractable epilepsy and mental decline. J Neurosci 24:2690-2698.2004).

Kaplan WD, Trout WE, 3rd (The behavior of four neurological mutants of Drosophila. Genetics 61:399-409.1969).

Kassmann M, Hansel A, Leipold E, Birkenbeil J, Lu SQ, Hoshi T, Heinemann SH (Oxidation of multiple methionine residues impairs rapid sodium channel inactivation. Pflugers Arch 456:1085-1095.2008).

Kasuya J, Kaas G, Kitamoto T (Effects of lithium chloride on the gene expression profiles in Drosophila heads. Neurosci Res 64:413-420.2009a).

Kasuya J, Kaas GA, Kitamoto T (A putative amino acid transporter of the solute carrier 6 family is upregulated by lithium and is required for resistance to lithium toxicity in Drosophila. Neuroscience 163:825-837.2009b).

Kelley MR, Kidd S, Berg RL, Young MW (Restriction of P-element insertions at the Notch locus of Drosophila melanogaster. Mol Cell Biol 7:1545-1548.1987).

Kim YT, Shin SM, Lee WY, Kim GM, Jin DK (Expression of expanded polyglutamine protein induces behavioral changes in Drosophila (polyglutamine-induced changes in Drosophila). Cell Mol Neurobiol 24:109-122.2004).

Klein PS, Melton DA (A molecular mechanism for the effect of lithium on development. Proc Natl Acad Sci U S A 93:8455-8459.1996).

Koh K, Joiner WJ, Wu MN, Yue Z, Smith CJ, Sehgal A (Identification of SLEEPLESS, a sleep-promoting factor. Science 321:372-376.2008).

Koh YH, Rehfeld K, Ganetzky B (A Drosophila model of early onset torsion dystonia suggests impairment in TGF-beta signaling. Hum Mol Genet 13:2019-2030.2004).

Kume K, Kume S, Park SK, Hirsh J, Jackson FR (Dopamine is a regulator of arousal in the fruit fly. J Neurosci 25:7377-7384.2005).

Kwon Y, Shen WL, Shim HS, Montell C (Fine thermotactic discrimination between the optimal and slightly cooler temperatures via a TRPV channel in chordotonal neurons. J Neurosci 30:10465-10471.2010).

Lange C (1886) Bidrag til Urinsyrediatesens Klinik. In: Hostpitalstidende, vol. 5, pp 1-15, Also pp. 21-38, 45-63,69-83.

Lavialle-Defaix C, Moignot B, Legros C, Lapied B (How does calcium-dependent intracellular regulation of voltage-dependent sodium current increase the sensitivity to the oxadiazine insecticide indoxacarb metabolite decarbomethoxylated JW062 (DCJW) in insect pacemaker neurons? J Pharmacol Exp Ther 333:264-272.2010).

Lee CH, Dixon JF, Reichman M, Moummi C, Los G, Hokin LE (Li+ increases accumulation of inositol 1,4,5-trisphosphate and inositol 1,3,4,5-tetrakisphosphate in cholinergically stimulated brain cortex slices in guinea pig, mouse and rat. The increases require inositol supplementation in mouse and rat but not in guinea pig. Biochem J 282 (Pt 2):377-385.1992).

Leech AP, Baker GR, Shute JK, Cohen MA, Gani D (Chemical and kinetic mechanism of the inositol monophosphatase reaction and its inhibition by Li+. Eur J Biochem 212:693-704.1993).

Lemaillet G, Walker B, Lambert S (Identification of a conserved ankyrin-binding motif in the family of sodium channel alpha subunits. J Biol Chem 278:27333-27339.2003).

Lemaitre B, Hoffmann J (The host defense of Drosophila melanogaster. Annu Rev Immunol 25:697-743.2007).

Lenox RH (Role of receptor coupling to phosphoinositide metabolism in the therapeutic action of lithium. Adv Exp Med Biol 221:515-530.1987).

Lenox RH, McNamara RK, Papke RL, Manji HK (Neurobiology of lithium: an update. J Clin Psychiatry 59 Suppl 6:37-47.1998).

Lenox RH, Wang L (Molecular basis of lithium action: integration of lithium-responsive signaling and gene expression networks. Mol Psychiatry 8:135-144.2003).

Li M, West JW, Lai Y, Scheuer T, Catterall WA (Functional modulation of brain sodium channels by cAMP-dependent phosphorylation. Neuron 8:1151-1159.1992).

Lin WH, Wright DE, Muraro NI, Baines RA (Alternative splicing in the voltage-gated sodium channel DmNav regulates activation, inactivation, and persistent current. J Neurophysiol 102:1994-2006.2009).

Lindsay HA, Baines R, ffrench-Constant R, Lilley K, Jacobs HT, O'Dell KM (The dominant cold-sensitive Out-cold mutants of Drosophila melanogaster have novel missense mutations in the voltage-gated sodium channel gene paralytic. Genetics 180:873-884.2008).

Loughney K, Kreber R, Ganetzky B (Molecular analysis of the para locus, a sodium channel gene in Drosophila. Cell 58:1143-1154.1989).

Luykx JJ, Boks MP, Terwindt AP, Bakker S, Kahn RS, Ophoff RA (The involvement of GSK3beta in bipolar disorder: integrating evidence from multiple types of genetic studies. Eur Neuropsychopharmacol 20:357-368.2010).

Mamiya K, Sadanaga T, Sekita A, Nabeyama Y, Yao H, Yukawa E (Lithium concentration correlates with QTc in patients with psychosis. J Electrocardiol 38:148-151.2005).

Manji HK, Bersudsky Y, Chen G, Belmaker RH, Potter WZ (Modulation of protein kinase C isozymes and substrates by lithium: the role of myo-inositol. Neuropsychopharmacology 15:370-381.1996).

Manji HK, Etcheberrigaray R, Chen G, Olds JL (Lithium decreases membrane-associated protein kinase C in hippocampus: selectivity for the alpha isozyme. J Neurochem 61:2303-2310.1993).

Manji HK, Lenox RH (Long-term action of lithium: a role for transcriptional and posttranscriptional factors regulated by protein kinase C. Synapse 16:11-28.1994).

Manji HK, Lenox RH (Lithium: a molecular transducer of mood-stabilization in the treatment of bipolar disorder. Neuropsychopharmacology 19:161-166.1998).

Manji HK, Moore GJ, Chen G (Lithium at 50: have the neuroprotective effects of this unique cation been overlooked? Biol Psychiatry 46:929-940.1999).

Manji HK, Moore GJ, Rajkowska G, Chen G (Neuroplasticity and cellular resilience in mood disorders. Molecular Psychiatry 578-593.2000).

Manji HK, Potter WZ (1997) Monoaminergic mechanisms in bipolar disorder. . New York: Marcel Dekker.

Manji HK, Potter WZ, Lenox RH (Signal transduction pathways. Molecular targets for lithium's actions. Arch Gen Psychiatry 52:531-543.1995).

Marmol F (Lithium: bipolar disorder and neurodegenerative diseases Possible cellular mechanisms of the therapeutic effects of lithium. Prog Neuropsychopharmacol Biol Psychiatry 32:1761-1771.2008).

Massot O, Rousselle JC, Fillion MP, Januel D, Plantefol M, Fillion G (5-HT1B receptors: a novel target for lithium. Possible involvement in mood disorders. Neuropsychopharmacology 21:530-541.1999).

McBride SM, Choi CH, Wang Y, Liebelt D, Braunstein E, Ferreiro D, Sehgal A, Siwicki KK, Dockendorff TC, Nguyen HT, McDonald TV, Jongens TA (Pharmacological rescue of synaptic plasticity, courtship behavior, and mushroom body defects in a Drosophila model of fragile X syndrome. Neuron 45:753-764.2005).

McGuire SE, Roman G, Davis RL (Gene expression systems in Drosophila: a synthesis of time and space. Trends Genet 20:384-391.2004).

McQuillin A, Rizig M, Gurling HM (A microarray gene expression study of the molecular pharmacology of lithium carbonate on mouse brain mRNA to understand the neurobiology of mood stabilization and treatment of bipolar affective disorder. Pharmacogenet Genomics 17:605-617.2007).

Meisler MH, Kearney J, Escayg A, MacDonald BT, Sprunger LK (Sodium channels and neurological disease: insights from Scn8a mutations in the mouse. Neuroscientist 7:136-145.2001).

Meisler MH, Kearney JA (Sodium channel mutations in epilepsy and other neurological disorders. J Clin Invest 115:2010-2017.2005).

Miklos GL, Rubin GM (The role of the genome project in determining gene function: insights from model organisms. Cell 86:521-529.1996).

Miklowitz DJ, Johnson SL (The psychopathology and treatment of bipolar disorder. Annu Rev Clin Psychol 2:199-235.2006).

Montezinho LP, Castro MM, Duarte CB, Penschuck S, Geraldes CF, Mork A (The interaction between dopamine D2-like and beta-adrenergic receptors in the prefrontal cortex is altered by mood-stabilizing agents. J Neurochem 96:1336-1348.2006).

Mora A, Sabio G, Risco AM, Cuenda A, Alonso JC, Soler G, Centeno F (Lithium blocks the PKB and GSK3 dephosphorylation induced by ceramide through protein phosphatase-2A. Cell Signal 14:557-562.2002).

Mudher A, Shepherd D, Newman TA, Mildren P, Jukes JP, Squire A, Mears A, Drummond JA, Berg S, MacKay D, Asuni AA, Bhat R, Lovestone S (GSK-3beta inhibition reverses axonal transport defects and behavioural phenotypes in Drosophila. Mol Psychiatry 9:522-530.2004).

Numann R, Catterall WA, Scheuer T (Functional modulation of brain sodium channels by protein kinase C phosphorylation. Science 254:115-118.1991).

O'Brien WT, Harper AD, Jove F, Woodgett JR, Maretto S, Piccolo S, Klein PS (Glycogen synthase kinase-3beta haploinsufficiency mimics the behavioral and molecular effects of lithium. J Neurosci 24:6791-6798.2004).

O'Dowd DK, Germeraad SE, Aldrich RW (Alterations in the expression and gating of Drosophila sodium channels by mutations in the para gene. Neuron 2:1301-1311.1989).

Ohmori I, Ouchida M, Ohtsuka Y, Oka E, Shimizu K (Significant correlation of the SCN1A mutations and severe myoclonic epilepsy in infancy. Biochem Biophys Res Commun 295:17-23.2002).

Okusa MD, Crystal LJ (Clinical manifestations and management of acute lithium intoxication. Am J Med 97:383-389.1994).

Olson RO, Liu Z, Nomura Y, Song W, Dong K (Molecular and functional characterization of voltage-gated sodium channel variants from Drosophila melanogaster. Insect Biochem Mol Biol 38:604-610.2008).

Osterwalder T, Yoon KS, White BH, Keshishian H (A conditional tissue-specific transgene expression system using inducible GAL4. Proc Natl Acad Sci U S A 98:12596-12601.2001).

Padiath QS, Paranjpe D, Jain S, Sharma VK (Glycogen synthase kinase 3beta as a likely target for the action of lithium on circadian clocks. Chronobiol Int 21:43-55.2004).

Palladino MJ, Keegan LP, O'Connell MA, Reenan RA (dADAR, a Drosophila double-stranded RNA-specific adenosine deaminase is highly developmentally regulated and is itself a target for RNA editing. RNA 6:1004-1018.2000a).

Palladino MJ, Keegan LP, O'Connell MA, Reenan RA (A-to-I pre-mRNA editing in Drosophila is primarily involved in adult nervous system function and integrity. Cell 102:437-449.2000b).

Papale LA, Paul KN, Sawyer NT, Manns JR, Tufik S, Escayg A (Dysfunction of the Scn8a voltage-gated sodium channel alters sleep architecture, reduces diurnal corticosterone levels, and enhances spatial memory. J Biol Chem 285:16553-16561.2010).

Park J, Lee SB, Lee S, Kim Y, Song S, Kim S, Bae E, Kim J, Shong M, Kim JM, Chung J (Mitochondrial dysfunction in Drosophila PINK1 mutants is complemented by parkin. Nature 441:1157-1161.2006).

Pasquali L, Busceti CL, Fulceri F, Paparelli A, Fornai F (Intracellular pathways underlying the effects of lithium. Behav Pharmacol 21:473-492.2010).

Perez-Cruet J, Tagliamonte A, Tagliamonte P, Gessa GL (Stimulation of serotonin synthesis by lithium. J Pharmacol Exp Ther 178:325-330.1971).

Phiel CJ, Klein PS (Molecular targets of lithium action. Annu Rev Pharmacol Toxicol 41:789-813.2001).

Pineda-Trujillo N, Carrizosa J, Cornejo W, Arias W, Franco C, Cabrera D, Bedoya G, Ruiz-Linares A (A novel SCN1A mutation associated with severe GEFS+ in a large South American pedigree. Seizure 14:123-128.2005).

Price LH, Charney DS, Delgado PL, Heninger GR (Lithium and serotonin function: implications for the serotonin hypothesis of depression. Psychopharmacology (Berl) 100:3-12.1990).

Purcell SM, Wray NR, Stone JL, Visscher PM, O'Donovan MC, Sullivan PF, Sklar P (Common polygenic variation contributes to risk of schizophrenia and bipolar disorder. Nature 460:748-752.2009).

Ren M, Senatorov VV, Chen RW, Chuang DM (Postinsult treatment with lithium reduces brain damage and facilitates neurological recovery in a rat ischemia/reperfusion model. Proc Natl Acad Sci U S A 100:6210-6215.2003).

Repnikova E, Koles K, Nakamura M, Pitts J, Li H, Ambavane A, Zoran MJ, Panin VM (Sialyltransferase regulates nervous system function in Drosophila. J Neurosci 30:6466-6476.2010).

Rogawski MA, Loscher W (The neurobiology of antiepileptic drugs. Nat Rev Neurosci 5:553-564.2004).

Rowe MK, Chuang DM (Lithium neuroprotection: molecular mechanisms and clinical implications. Expert Rev Mol Med 6:1-18.2004).

Ryder E, Ashburner M, Bautista-Llacer R, Drummond J, Webster J, Johnson G, Morley T, Chan YS, Blows F, Coulson D, Reuter G, Baisch H, Apelt C, Kauk A, Rudolph T, Kube M, Klimm M, Nickel C, Szidonya J, Maroy P, Pal M, Rasmuson-Lestander A, Ekstrom K, Stocker H, Hugentobler C, Hafen E, Gubb D, Pflugfelder G, Dorner C, Mechler B, Schenkel H, Marhold J, Serras F, Corominas M, Punset A, Roote J, Russell S (The DrosDel deletion collection: a Drosophila genomewide chromosomal deficiency resource. Genetics 177:615-629.2007).

Scheffer IE, Harkin LA, Grinton BE, Dibbens LM, Turner SJ, Zielinski MA, Xu R, Jackson G, Adams J, Connellan M, Petrou S, Wellard RM, Briellmann RS, Wallace RH, Mulley JC, Berkovic SF (Temporal lobe epilepsy and GEFS+ phenotypes associated with SCN1B mutations. Brain 130:100-109.2007).

Schlief T, Schonherr R, Imoto K, Heinemann SH (Pore properties of rat brain II sodium channels mutated in the selectivity filter domain. Eur Biophys J 25:75-91.1996).

Schneider D (Using Drosophila as a model insect. Nat Rev Genet 1:218-226.2000).

Schou M (Lithium treatment at 52. J Affect Disord 67:21-32.2001).

Schreibmayer W, Wallner M, Lotan I (Mechanism of modulation of single sodium channels from skeletal muscle by the beta 1-subunit from rat brain. Pflugers Arch 426:360-362.1994).

Seelan RS, Khalyfa A, Lakshmanan J, Casanova MF, Parthasarathy RN (Deciphering the lithium transcriptome: microarray profiling of lithium-modulated gene expression in human neuronal cells. Neuroscience 151:1184-1197.2008).

Shaldubina A, Johanson RA, O'Brien WT, Buccafusca R, Agam G, Belmaker RH, Klein PS, Bersudsky Y, Berry GT (SMIT1 haploinsufficiency causes brain inositol deficiency without affecting lithium-sensitive behavior. Mol Genet Metab 88:384-388.2006).

Shaltiel G, Shamir A, Nemanov L, Yaroslavsky Y, Nemets B, Ebstein RP, Belmaker RH, Agam G (Inositol monophosphatase activity in brain and lymphocyte-derived cell lines of bipolar patients. World J Biol Psychiatry 2:95-98.2001).

Shao W, Wu J, Chen J, Lee DM, Tishkina A, Harris TJ (A modifier screen for Bazooka/PAR-3 interacting genes in the Drosophila embryo epithelium. PLoS One 5:e9938.2010).

Shi J, Levinson DF, Duan J, Sanders AR, Zheng Y, Pe'er I, Dudbridge F, Holmans PA, Whittemore AS, Mowry BJ, Olincy A, Amin F, Cloninger CR, Silverman JM, Buccola NG, Byerley WF, Black DW, Crowe RR, Oksenberg JR, Mirel DB, Kendler KS, Freedman R, Gejman PV (Common variants on chromosome 6p22.1 are associated with schizophrenia. Nature 460:753-757.2009).

Siddiqi O, Benzer S (Neurophysiological defects in temperature-sensitive paralytic mutants of Drosophila melanogaster. Proc Natl Acad Sci U S A 73:3253-3257.1976).

Silverstone PH, McGrath BM, Kim H (Bipolar disorder and myo-inositol: a review of the magnetic resonance spectroscopy findings. Bipolar Disord 7:1-10.2005).

Sofola O, Kerr F, Rogers I, Killick R, Augustin H, Gandy C, Allen MJ, Hardy J, Lovestone S, Partridge L (Inhibition of GSK-3 ameliorates Abeta pathology in an adult-onset Drosophila model of Alzheimer's disease. PLoS Genet 6.2010).

Song J, Tanouye M (Role for para sodium channel gene 3' UTR in the modification of Drosophila seizure susceptibility. Dev Neurobiol 67:1944-1956.2007).

Song W, Liu Z, Tan J, Nomura Y, Dong K (RNA editing generates tissue-specific sodium channels with distinct gating properties. J Biol Chem 279:32554-32561.2004).

Srinivasan J, Schachner M, Catterall WA (Interaction of voltage-gated sodium channels with the extracellular matrix molecules tenascin-C and tenascin-R. Proc Natl Acad Sci U S A 95:15753-15757.1998).

Stachel SE, Grunwald DJ, Myers PZ (Lithium perturbation and goosecoid expression identify a dorsal specification pathway in the pregastrula zebrafish. Development 117:1261-1274.1993).

Stallone F, Shelley E, Mendlewicz J, Fieve RR (The use of lithium in affective disorders. 3. A double-blind study of prophylaxis in bipolar illness. Am J Psychiatry 130:1006-1010.1973).

Steinmetz M, Stephan D, Fischer Lindahl K (Gene organization and recombinational hotspots in the murine major histocompatibility complex. Cell 44:895-904.1986).

Stern M, Ganetzky B (Identification and characterization of inebriated, a gene affecting neuronal excitability in Drosophila. J Neurogenet 8:157-172.1992).

Stern M, Kreber R, Ganetzky B (Dosage effects of a Drosophila sodium channel gene on behavior and axonal excitability. Genetics 124:133-143.1990).

Sugawara T, Mazaki-Miyazaki E, Fukushima K, Shimomura J, Fujiwara T, Hamano S, Inoue Y, Yamakawa K (Frequent mutations of SCN1A in severe myoclonic epilepsy in infancy. Neurology 58:1122-1124.2002).

Sun YM, Favre I, Schild L, Moczydlowski E (On the structural basis for size-selective permeation of organic cations through the voltage-gated sodium channel. Effect of alanine mutations at the DEKA locus on selectivity, inhibition by Ca2+ and H+, and molecular sieving. J Gen Physiol 110:693-715.1997).

Suzuki DT (Temperature-sensitive mutations in Drosophila melanogaster. Science 170:695-706.1970).

Sysko R, Walsh BT (A systematic review of placebo response in studies of bipolar mania. J Clin Psychiatry 68:1213-1217.2007).

Szczepankiewicz A, Skibinska M, Hauser J, Slopien A, Leszczynska-Rodziewicz A, Kapelski P, Dmitrzak-Weglarz M, Czerski PM, Rybakowski JK (Association analysis of the GSK-3beta T-50C gene polymorphism with schizophrenia and bipolar disorder. Neuropsychobiology 53:51-56.2006).

Trout WE, Kaplan WD (Mosaic mapping of foci associated with longevity in the neurological mutants Hk1 and Sh5 of Drosophila melanogaster. Exp Gerontol 16:461-474.1981).

Trudeau MM, Dalton JD, Day JW, Ranum LPW, Meisler MH (Heterozygosity for a truncation allele of sodium channel SCN8A in a family with ataxia and cognitive impairment. 205 presented at the 54th Annual Meeting of the American Society of Human Genetics Bethesda, Maryland, USa.2004).

Ueda A, Wu CF (Effects of hyperkinetic, a beta subunit of Shaker voltage-dependent K+ channels, on the oxidation state of presynaptic nerve terminals. J Neurogenet 22:1-13.2008).

Ueda A, Wu CF (Effects of social isolation on neuromuscular excitability and aggressive behaviors in Drosophila: altered responses by Hk and gsts1, two mutations implicated in redox regulation. J Neurogenet 23:378-394.2009).

Van Lookeren Campagne MM, Wang M, Spek W, Peters D, Schaap P (Lithium respecifies cyclic AMP-induced cell-type specific gene expression in Dictyostelium. Dev Genet 9:589-596.1988).

Wada A, Yokoo H, Yanagita T, Kobayashi H (Lithium: potential therapeutics against acute brain injuries and chronic neurodegenerative diseases. J Pharmacol Sci 99:307-321.2005).

Wallace RH, Scheffer IE, Barnett S, Richards M, Dibbens L, Desai RR, Lerman-Sagie T, Lev D, Mazarib A, Brand N, Ben-Zeev B, Goikhman I, Singh R, Kremmidiotis G, Gardner A, Sutherland GR, George AL, Jr., Mulley JC, Berkovic SF (Neuronal sodium-channel alpha1-subunit mutations in generalized epilepsy with febrile seizures plus. Am J Hum Genet 68:859-865.2001).

Wang H, Friedman E (Increased association of brain protein kinase C with the receptor for activated C kinase-1 (RACK1) in bipolar affective disorder. Biol Psychiatry 50:364-370.2001).

Wang JW, Humphreys JM, Phillips JP, Hilliker AJ, Wu CF (A novel leg-shaking Drosophila mutant defective in a voltage-gated K(+)current and hypersensitive to reactive oxygen species. J Neurosci 20:5958-5964.2000).

Wang Y, Zhang J, Li X, Ji J, Yang F, Wan C, Feng G, Wan P, He L, He G (SCN8A as a novel candidate gene associated with bipolar disorder in the Han Chinese population. Prog Neuropsychopharmacol Biol Psychiatry 32:1902-1904.2008).

Warmke JW, Reenan RA, Wang P, Qian S, Arena JP, Wang J, Wunderler D, Liu K, Kaczorowski GJ, Van der Ploeg LH, Ganetzky B, Cohen CJ (Functional expression of Drosophila para sodium channels. Modulation by the membrane protein TipE and toxin pharmacology. J Gen Physiol 110:119-133.1997).

West JW, Patton DE, Scheuer T, Wang Y, Goldin AL, Catterall WA (A cluster of hydrophobic amino acid residues required for fast Na(+)-channel inactivation. Proc Natl Acad Sci U S A 89:10910-10914.1992).

Whitworth AJ, Theodore DA, Greene JC, Benes H, Wes PD, Pallanck LJ (Increased glutathione S-transferase activity rescues dopaminergic neuron loss in a Drosophila model of Parkinson's disease. Proc Natl Acad Sci U S A 102:8024-8029.2005).

Williams RS, Cheng L, Mudge AW, Harwood AJ (A common mechanism of action for three mood-stabilizing drugs. Nature 417:292-295.2002).

Williamson RL (Lithium stops hereditary shuddering in Drosophila melanogaster. Psychopharmacology (Berl) 76:265-268.1982).

Wright AP, Fox AN, Johnson KG, Zinn K (Systematic screening of Drosophila deficiency mutations for embryonic phenotypes and orphan receptor ligands. PLoS One 5:e12288.2010).

Wu CF, Ganetzky B (Genetic alteration of nerve membrane excitability in temperature-sensitive paralytic mutants of Drosophila melanogaster. Nature 286:814-816.1980).

Xu J, Culman J, Blume A, Brecht S, Gohlke P (Chronic treatment with a low dose of lithium protects the brain against ischemic injury by reducing apoptotic death. Stroke 34:1287-1292.2003).

Yamakura T, Bertaccini E, Trudell JR, Harris RA (Anesthetics and ion channels: molecular models and sites of action. Annu Rev Pharmacol Toxicol 41:23-51.2001).

Yanagita T, Maruta T, Uezono Y, Satoh S, Yoshikawa N, Nemoto T, Kobayashi H, Wada A (Lithium inhibits function of voltage-dependent sodium channels and catecholamine secretion independent of glycogen synthase kinase-3 in adrenal chromaffin cells. Neuropharmacology 53:881-889.2007).

Yang Y, Wang Y, Li S, Xu Z, Li H, Ma L, Fan J, Bu D, Liu B, Fan Z, Wu G, Jin J, Ding B, Zhu X, Shen Y (Mutations in SCN9A, encoding a sodium channel alpha subunit, in patients with primary erythermalgia. J Med Genet 41:171-174.2004).

Yao H, Zhou Q, Li J, Smith H, Yandeau M, Nikolau BJ, Schnable PS (Molecular characterization of meiotic recombination across the 140-kb multigenic a1-sh2 interval of maize. Proc Natl Acad Sci U S A 99:6157-6162.2002).

Yeh PA, Chien JY, Chou CC, Huang YF, Tang CY, Wang HY, Su MT (Drosophila notal bristle as a novel assessment tool for pathogenic study of Tau toxicity and screening of therapeutic compounds. Biochem Biophys Res Commun 391:510-516.2010).

York JD, Ponder JW, Majerus PW (Definition of a metal-dependent/Li(+)-inhibited phosphomonoesterase protein family based upon a conserved three-

dimensional core structure. Proc Natl Acad Sci U S A 92:5149-5153.1995).

Yu FH, Catterall WA (Overview of the voltage-gated sodium channel family. Genome Biol 4:207.2003).

Zhai RG, Hiesinger PR, Koh TW, Verstreken P, Schulze KL, Cao Y, Jafar-Nejad H, Norga KK, Pan H, Bayat V, Greenbaum MP, Bellen HJ (Mapping Drosophila mutations with molecularly defined P element insertions. Proc Natl Acad Sci U S A 100:10860-10865.2003).